AN ABSTRACT OF THE THESIS OF

Menno Gustaaf Dinkelman (Name) for the Doctor of Philosophy (Degree)

in Oceanography (Major) presented on July 20, 1973 (Date)

Title: LATE QUATERNARY RADIOLARIAN PALEO-OCEANOGRAPHY OF THE PANAMA BASIN, EASTERN EQUATORIAL PACIFIC

Abstract approved: Redacted for Privacy

A total of 57 core top samples from the Panama Basin were used in a quantitative study of complete radiolarian thanatocoenoses to determine whether surface oceanographic conditions are reflected in the microplankton faunas deposited onto and buried in the sea floor. Information obtained from this study was used to resolve the sequence of temporal fluctuations in oceanographic and climatologic conditions in the eastern equatorial Pacific. Four piston cores from within the basin were sampled on the basis of carbonate stratigraphies to levels no older than 130,000 years B. P. Although the sample intervals are irregular and samples are not closely spaced, this procedure allowed reasonably good stratigraphic resolution. Because of high diversity at low latitudes, the 131 radiolarian taxa recognized in this study accounted for only 37-61% of the individuals encountered in counts of >1000 specimens.

Q-mode factor analysis of the surface sediment samples yielded three end member samples, which allowed recognition of three different assemblages. The dominant assemblage can be identified with a tropical fauna and the least important assemblage is considered to be associated with the Peru Current fauna. The distribution of the tropical assemblage does not reflect surface oceanographic conditions whereas the distribution of the Peru Current assemblage shows a weak association with surface conditions. The other assemblage shows no coherent distribution pattern. The nature of this assemblage is best explained by considering it to be a residual of the tropical fauna resulting from chemical and mechanical modification in the water column and at the sea floor. All evidence suggests that solution, winnowing and lateral transport are major processes in determining the distribution of the faunal assemblages in the sediments of the Panama Basin.

The signal of the Peru Current assemblage in the surface study was used for a quantitative analysis of the subsurface samples. This analysis yielded the following results: 1) During most of the last glacial, assemblages associated with the Peru Current were deposited in the Panama Basin, indicating a northward shift of current boundaries. This has important climatological implications since such a shift must be associated with a shift of the major wind belts and of the South Pacific high pressure cell towards the

equator. 2) At least once during the last glacial, from approximately 50,000 to 40,000 years B. P., warmer conditions are indicated by a re-appearance of tropical assemblages. 3) The previous interglacial appears to have been slightly cooler than present interglacial conditions. 4) The warming trend towards present conditions began between 15,000 and 20,000 years B. P. This is earlier than observed in the North Atlantic.

These results are correlative with records of oceanographic and climatic changes in the southeast Pacific, northwestern South America and the Galapagos Islands.

Late Quaternary Radiolarian Paleo-Oceanography Of the Panama Basin, Eastern Equatorial Pacific

by

Menno Gustaaf Dinkelman

A THESIS

submitted to

Oregon State University

in partial fulfillment of
the requirements for the
degree of

Doctor of Philosophy

June 1974

APPROVED:

Redacted for Privacy

Professor in Oceanography
in charge of major

Redacted for Privacy

Associate Professor in Oceanography
in charge of major

Redacted for Privacy

Dean of the School of Oceanography

Redacted for Privacy

Dean of Graduate School

Date thesis is presented July 20, 1973

Typed by Linda Wille for Menno Gustaaf Dinkelman

ACKNOWLEDGEMENTS

> "Numberless in short are the ways, and sometimes imperceptable, in which the affections (emotions) colour and infect the understanding".
>
> Francis Bacon
> Novum Organum (1620)

My deepest thanks are due to Dr. Tjeerd H. van Andel for his continuing guidance and patience throughout all phases of my long career as a graduate student. His words of advice and encouragement at times when success seemed beyond my grasp are warmly appreciated. Sincere thanks are extended to Dr. Ted C. Moore, Jr. for many stimulating discussions about a wide range of topics related to this study and his valuable criticism of the manuscript. I thank Drs. Cyrus W. Field and Wayne V. Burt for their assistance as members of my committee.

A special note of thanks is due Nicklas G. Pisias for his unselfish assistance in helping me to understand the mysteries and idiosyncrasies of computer language. His own research also provided some tangible support for some of my conclusions. Throughout my student years I have profited greatly from discussions, at times heated, with Dr. G. Ross Heath, Dr. William H. Quinn, Dr. J. Ron Zaneveld, Bruce T. Malfait, J. Paul Dauphin, Tim R. Baumgartner, Renato O. Kowsmann, Gordon Ness, David K. Rea and Victor J. Rosato. Too violent disagreements were best quenched at some of

the downtown annexes. I am also grateful to Mrs. Carla Rathbun for calcium carbonate determinations using the LECO analyzer, to Miss Natasa Sotiropoulos for drafting of the figures, to David Reinert for his quick delivery of the photographs in spite of sometimes short notice, and to Mrs. Linda Wille for her excellent typing and the many evening hours she sacrificed to enable me to meet certain deadlines, and to Mrs. Frances Shabica and Ms. Sallie Hee for a sunny smile on rainy mornings.

Above all, I wish to thank my wife, Hanny, for her help, patience and understanding over the entire course of my study. She was left alone for many an evening hour and weekend day while I was pursuing my scientific interests at the University. To my parents, whose sacrifices made my education possible, I am ever grateful.

This research was supported through grants of the Office of Naval Research (Contract No. N00014-67-A-0369-007) and of the National Science Foundation (Contract No. GX 28673) under the CLIMAP project. A research assistantship and, during the last seven months, a hard-working wife provided much needed financial support.

TABLE OF CONTENTS

LIST OF TABLES

LIST OF FIGURES

LATE QUATERNARY RADIOLARIAN PALEO-OCEANOGRAPHY THE PANAMA BASIN, EASTERN EQUATORIAL PACIFIC

INTRODUCTION

In his study of eastern tropical Pacific cores Arrhenius (1952) observed that below the waters of the equatorial current system calcium carbonate (coccoliths and foraminifers) accumulated at a higher rate during glacial periods than during interglacials. He explained this phenomenon as the result of increased upwelling along the equator, which in turn increased primary productivity. He suggested that the stronger upwelling indicates an increase in the intensity of atmospheric circulation during Glacial Ages. Earlier, Schott (1935) and Correns (1937) noticed that the abundances of various major components of deep-sea sediments, especially calcareous plankton, are useful and sensitive indicators of climatic fluctuations. Pratje (1951) was among the first to recognize that siliceous microfossils can be useful measures of cool water conditions in marine sediments. Since then Riedel (1958), Hays (1965), Nigrini (1967, 1968, 1970), Bandy et al., (1971), and Goll and Bjørklund (1971) have shown that certain radiolarian species as well as whole radiolarian assemblages (Sachs, 1973b, c) are sensitive to changing oceanographic conditions. Recent work by Moore (1973a) and Sachs (1973c) has demonstrated the usefulness of complete radiolarian

thanatocoenoses for the interpretation of the late Pleistocene and Holocene oceanographic history of the North Pacific.

The present study was initiated simultaneously with these two. Sachs (1973a) examined the feasibility of quantitative analysis of entire radiolarian faunas and Moore built on the framework provided by that study. For the present study, it was assumed that quantitative analysis of complete radiolarian assemblages is a practical approach to the examination of the ecological response of radiolaria to changing oceanographic conditions.

In the easternmost equatorial Pacific the cool, fertile waters of the Peru Current merge with the warm waters of the equatorial current system, probably exerting a strong influence on the faunal assemblages of the Panama Basin. Fluctuations in the Peru Current and its associated upwelling are generally considered to be dependent on the strength of the southeasterly and southerly winds along the South American coast and the westerlies in the eastern South Pacific. This strong coupling between atmospheric circulation and a major ocean current is of particular interest not only with regard to present day oceanographic variations, but also to the scholar interested in the past climatic and oceanographic history of our planet. Thus, micropaleontological studies might contribute significantly to the solution of important paleo-climatologic problems.

The following questions were posed at the outset:

1) Can the distribution of radiolarian species and of total radiolarian faunas in the surface sediments be related to present-day patterns of upwelling, primary productivity and surface water circulation?

2) How important are processes operating in the water column and at the ocean floor in determining the radiolarian assemblage in the sediment?

3) Is it possible to relate historic climatic and oceanographic changes in this region, as indicated by variations in the composition of radiolarian assemblages in deep-sea cores, to the more thoroughly documented changes in the northern hemisphere?

In order to answer these questions, the study proceeded in two steps:

1) Analyses of surface sediments

   a) From published literature and initial investigation of several surface samples, 131 radiolarian taxa were recognized as potential carriers of specific water mass information. Because of the high diversity of the tropical-subtropical faunas these comprise only about 50% of the fauna.

   b) In 57 surface samples, the proportions of these taxa

were determined. Due to unexpected problems with poor to moderate preservation, and because of reworking, winnowing and lateral transport, the observed faunal distribution could not be related definitively to surface circulation.

2) Stratigraphic Analyses

a) Similarly, the radiolarian compositions were determined of sample suites taken from several piston cores on the basis of carbonate stratigraphies and sedimentation rates calculated from several radiocarbon dates. These sample suites span an interval of approximately 130,000 years. Q-mode factor analysis was used to determine the nature of the changes that occurred in the oceanographic regime of the eastern equatorial Pacific during the late Pleistocene and Holocene.

b) The results were then correlated with climatic records from land and ocean-based sequences elsewhere to give information on how closely coupled glacial conditions were on both hemispheres in the atmospheric and oceanographic realms.

THE PANAMA BASIN

Regional Setting

The Panama Basin in the eastern equatorial Pacific is bordered by the Carnegie and Cocos Ridges to the south and west respectively, and by central and northwestern South America to the north and east. The Galapagos Islands lie at the western extreme of the Carnegie Ridge. The Basin itself is divided by the Malpelo and Coiba Ridges into a deep eastern basin and a shallower western basin. No trenches extend into the Basin. The Peru Trench shoals where the Carnegie Ridge abutts against the continental margin of Ecuador and the Middle America Trench terminates against the western flank of the Cocos Ridge where this ridge joins with the continental margin of Costa Rica. The physiography, structure and tectonic history of the Basin have been described in detail by van Andel, et al., (1971).

Oceanography

The principal features of the surface circulation of the eastern equatorial Pacific and the Panama Bight have been summarized by Wooster and Cromwell (1958), Wyrtki (1965, 1966), Forsbergh (1969) and Stevenson (1970). The surface circulation in the Panama Basin is complex (Figures 3, 4) and the biologic productivity is generally high. The warm Equatorial Countercurrent flows through the

northern part of the basin, whereas the southern part of the basin lies within the influence of the cool, highly productive waters of the Peru Current. The water of the Equatorial Countercurrent is characterized by high surface temperature (>25°C, with little seasonal variation), low salinity (<34‰ due to an excess of rainfall over evaporation) and in general low dissolved oxygen, phosphate and silicate, whereas the waters of the Peru Current have relatively low surface temperatures, high salinities and are rich in nutrients due to continuous upwelling along its course. The eastern, northward-flowing branch of a generally counter-clockwise circulation cell of elliptical shape in the Panama Bight is the Colombia Current. The water of this current is the product of mixing of continental runoff, of the Equatorial Countercurrent and of that part of the Peru Current which hugs the coast of Ecuador.

Wyrtki (1966, Figure 7), in his discussion of eastern equatorial Pacific oceanography, recognizes two water masses in the Panama Basin, the tropical surface water in the north and the equatorial surface water in the south (Figure 1). The water of the Equatorial Countercurrent as well as the water which is carried west in the southern parts of the North Equatorial Current is tropical surface water. The equatorial surface water has properties intermediate between those of the tropical surface water (high tempera-

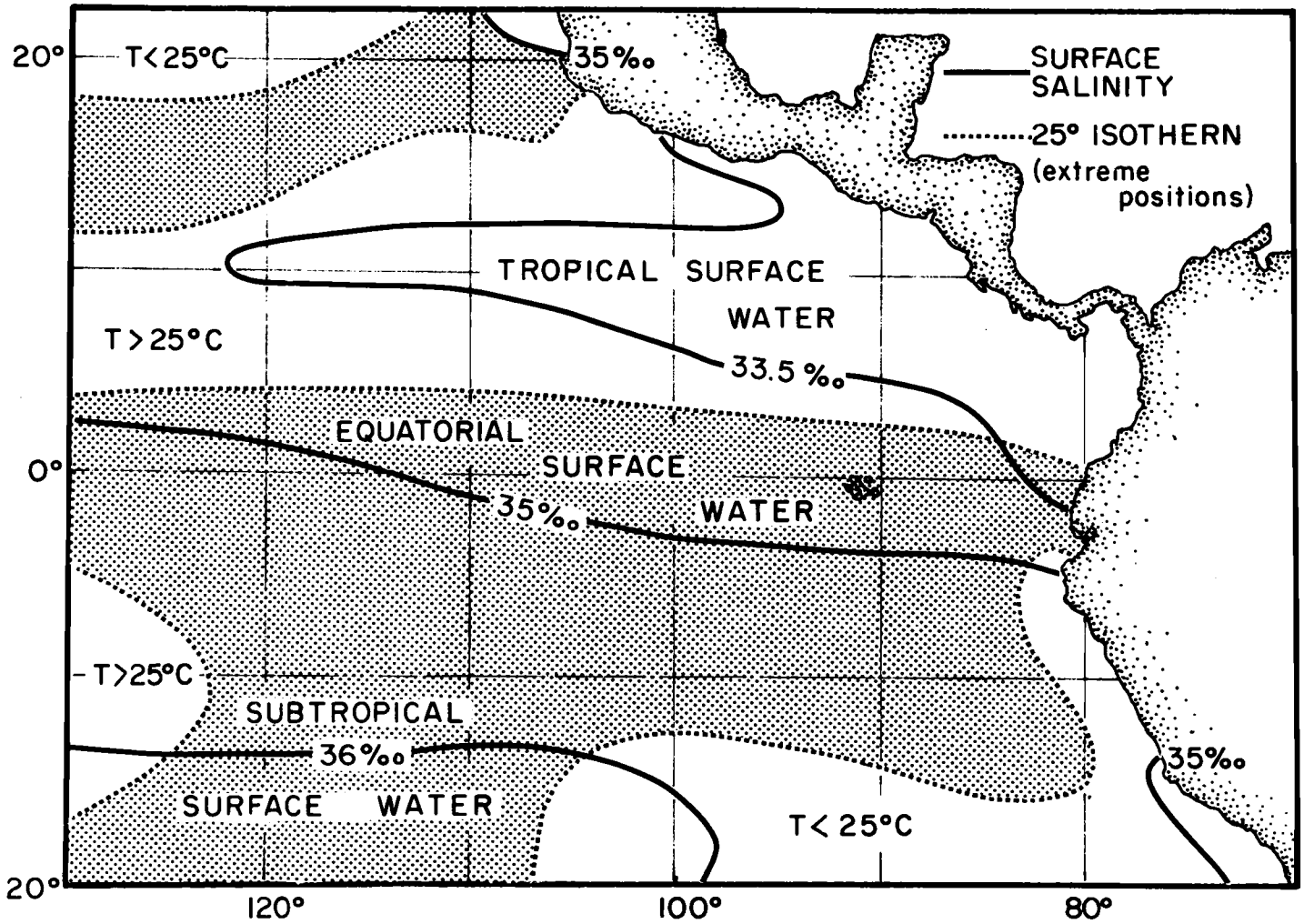

Figure 1 Distribution of the main surface water masses in the eastern equatorial Pacific Ocean (from Wyrtki, 1966).

ture and low salinity) and the sub-tropical surface water (high salinity, generally warm but temperature highly variable from 15° to 28° C). The northern boundary of the sub-tropical surface water approximates the 35% isohaline, whereas its eastern boundary cannot be precisely identified. Off Peru, this water is usually separated from the coast by only a narrow belt of upwelling water of lower salinity and temperature which is associated with the Peru Current. According to Wyrtki, the equatorial surface water is not a direct result of mixing of the two other water masses, but its properties are partially determined by seasonal advection of the cooler Peru Current water and by upwelling. Those parts of the South Equatorial Current which are situated at and north of the equator are typical for the equatorial surface water.

Changes in the surface circulation pattern are clearly related to changes of the intensity and direction of the major wind systems. The Panama Basin is located within the path of north-south seasonal movement of the tradewind-calm belt (Doldrums) system (Figure 2). Thus, during the year, the Basin is successively influenced by the northeast trade winds, the equatorial calm belt and the southeast trade winds. The Doldrums form a zone of light, variable winds between the northeast and southeast trade wind systems. Within the Doldrums the region of actual convergence of the trades is called the Inter-tropical Convergence (I. T. C.). This convergence zone is

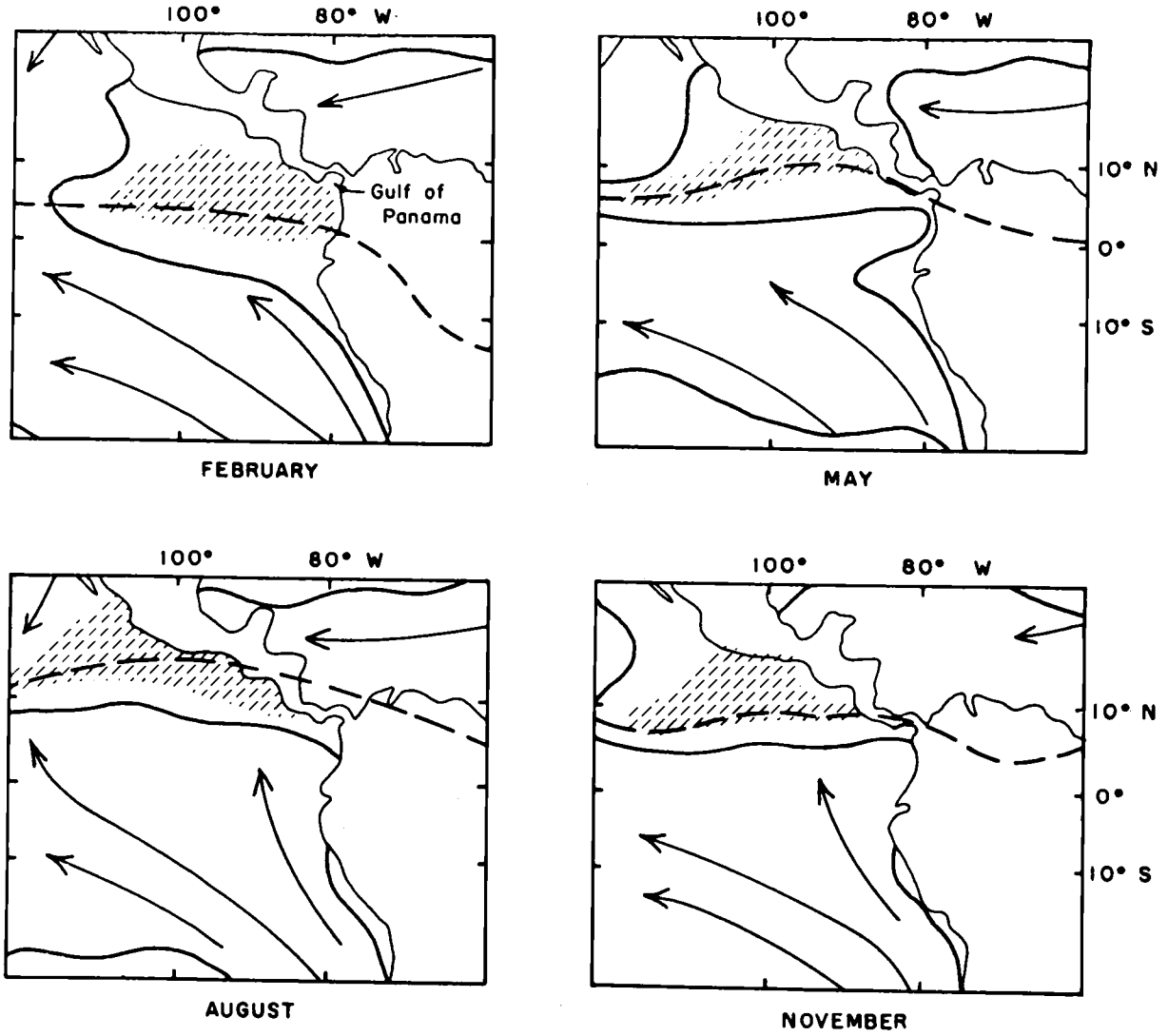

Figure 2. Average positions of the limits of tradewind circulation (heavy solid lines), doldrums (shaded) and the Intertropical Convergence (heavy dashed lines). Arrows indicate average direction of air flow (from Wooster, 1959).

characterized by heavy rains. It lies farthest south during southern summer and it is at its most northerly position during southern winter. The I. T. C. coincides approximately with the northern boundary of the Equatorial Countercurrent (Wyrtki, 1965). The seasonal shift of the I. T. C. has a strong influence on the development of the Equatorial Countercurrent in the region. As long as the I. T. C. is located north of approximately 7°N, the Countercurrent is well developed, but when the I. T. C. shifts towards the equator during southern summer the Countercurrent disappears from the area. Comparing periods with the same general circulation pattern Wyrtki (1965, 1966) recognized three basically different circulation patterns for the eastern equatorial Pacific. Two of these suffice to explain most of the differences between summer and winter situations for the Panama Basin. The third pattern is more significant to the north where it affects the California Current and the North Equatorial Current.

The first typical circulation pattern, which seems to be most stable, governs the area from June to December when the Equatorial Countercurrent is well developed and the South Equatorial Current is quite strong (Figure 3). Most of the Countercurrent water flows around the Costa Rica Dome and eventually enters the North Equatorial Current. During this period the Peru Current is strong and most of its water passes into the South Equatorial Current. The

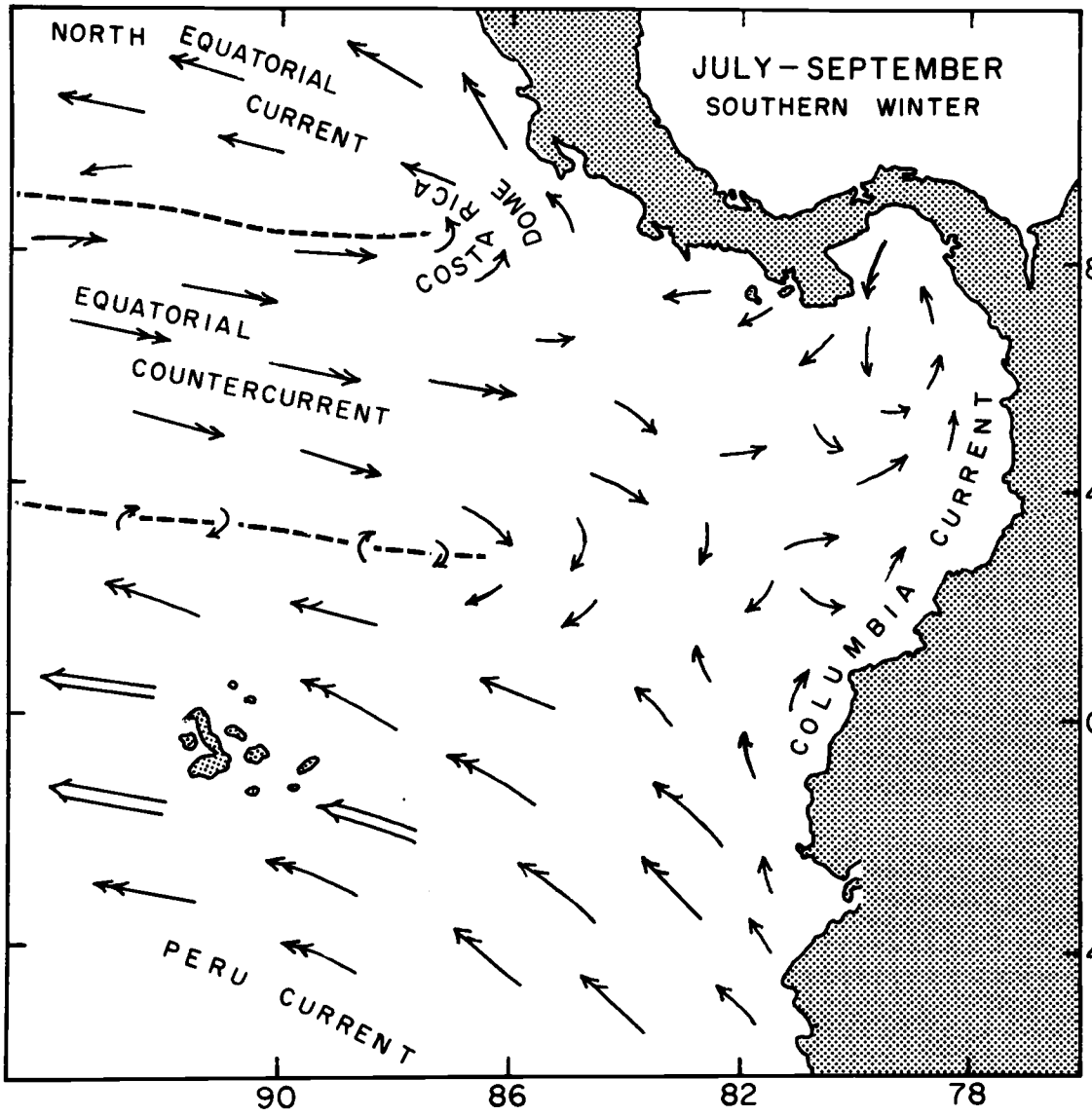

Figure 3 Surface circulation in the Panama Basin, eastern equatorial Pacific, for the southern winter (after Wyrtki, 1965).

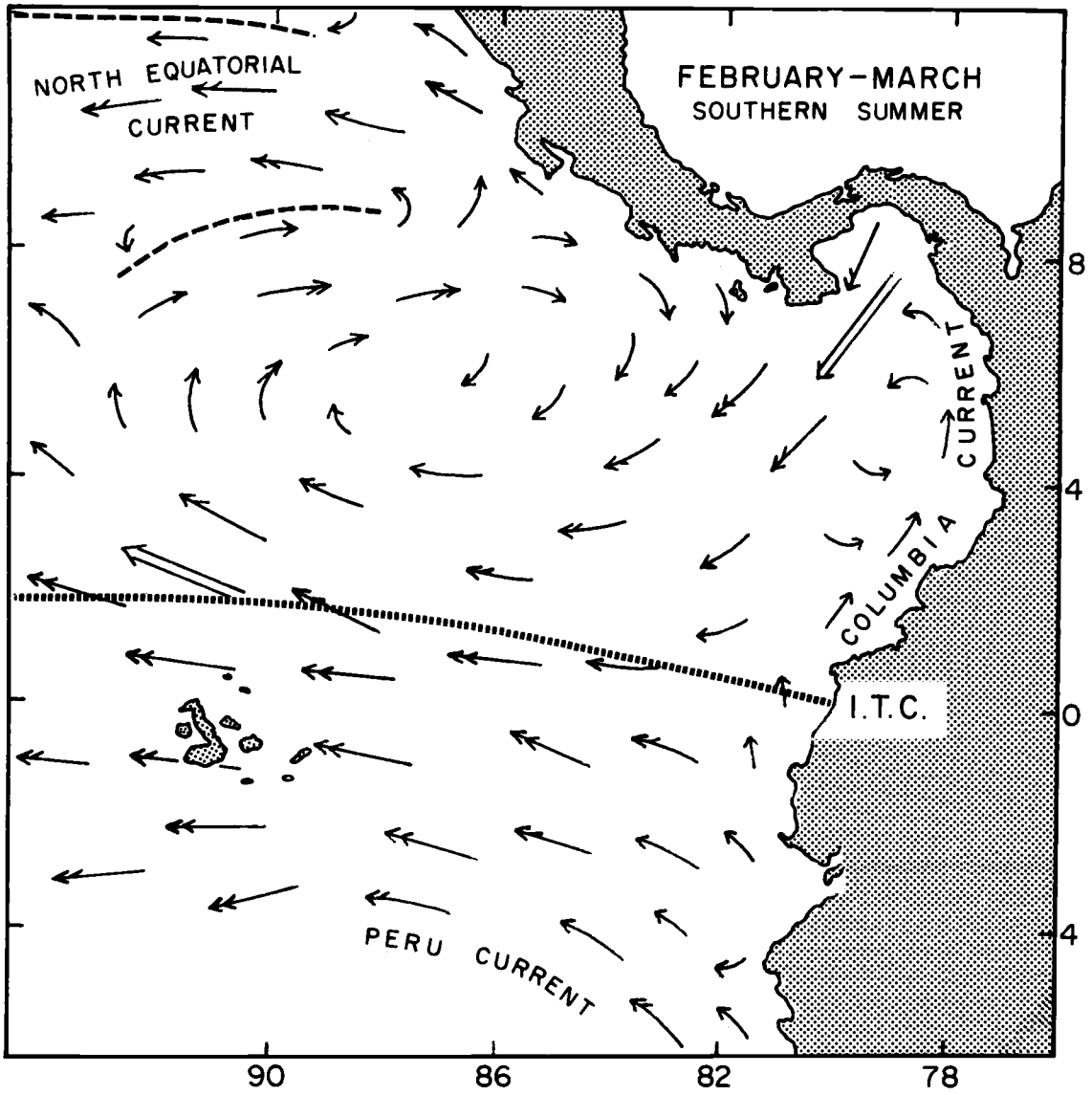

Figure 4 Surface circulation in the Panama Basin, eastern equatorial Pacific, and during southern summer (after Wyrtki, 1965).

Colombia Current, which is wide and slow during May and June, gradually increases both in width and speed and is strongest from August to November.

The second typical circulation pattern is developed from February to April (Figure 4). During this time the Inter-tropical Convergence is in its most southerly position (near 2°N) and consequently the Equatorial Countercurrent has disappeared from the area. The Peru Current is relatively weak and circulation in the central Basin is sluggish, forming a huge anticyclonic eddy, centered near 5°N, 88°W. The Colombia Current is confined to a narrow band of coastal water moving at high speeds and the eddy in the Panama Bight is well developed. The western branch of this eddy is a strong current which leaves the Gulf of Panama in a southwesterly direction and joins the anticyclonic circulation at 5°N, 88°W.

Little is known about the subsurface circulation in the Basin. In the western Basin the subsurface circulation is a complicated pattern of eddies and closed cells with flow in both east and west direction. It is believed to be the result of an intense mixing between surface water and the eastward flowing Equatorial Undercurrent (Pak and Zaneveld, 1973; Stevenson and Taft, 1971). Subsurface southward flow along the coast of Colombia (Stevenson, 1970) probably merges into the Peru-Chile Undercurrent described by Wooster and Gilmartin (1961).

The deep-water circulation of the Basin (Laird, 1971) is affected by the Carnegie and Cocos Ridges which are effective barriers for penetration of Pacific Deep Water into the Basin. Deep water can enter the Basin only across the 2600 m deep sill between the Carnegie Ridge and the continental margin of Ecuador. The main flow is northward into the eastern basin. Although some bottom water enters the western basin through the Malpelo Gap, south of the Malpelo Ridge, the main flow is northward into the deep eastern basin. From there the bottom flow continues through the deep passage between the Coiba and Malpelo Ridges into the western basin.

Biological Productivity

Long-standing commercial and scientific interests in the oceanography of the eastern equatorial Pacific have contributed greatly to an understanding of the area. This research has yielded a large number of primary productivity determinations, usually measured by the radio-carbon method of Steeman Nielsen (1952). The productivity map of Figure 5 (Moore et al., 1973), represents an average of all available productivity measurements (Owen and Zeitschell, 1969; Forsbergh, 1969; Love, 1970, 1971), taken over several seasons. Thus yearly and seasonal variations have been smoothed. The surface samples used in this study represent the

net accumulation of planktonic organisms over several hundreds or even thousands of years. Thus valid comparisons can only be made with long-term average productivity patterns.

As shown in Figure 5, areas with high primary productivity coincide with the region of Peru Current water penetration. A band of high productivity extends from the southern boundary of the map to approximately 2°N. In its southerly confines this band is clearly associated with the Peru Current and with the zone of equatorial upwelling at its northern edge. High productivity, associated with the Colombia Current and with the upwelling in the Panama Bight, is also found in the coastal waters. The southeastern margin of the highly productive Costa Rica Dome can be seen in the northwestern part of the map. Compared with the high productivity values of these areas, the central part of the Basin as well as the waters above the Cocos Ridge have relatively low productivity, although one must bear in mind that even here the values are high and comparable to many areas generally considered to have high primary productivity (e. g. the Equatorial Pacific, 500 mg C/m^2/day, or the Equatorial Indian Ocean, 250 mg C/m^2/day, (Steeman Nielsen and Jensen, 1957).

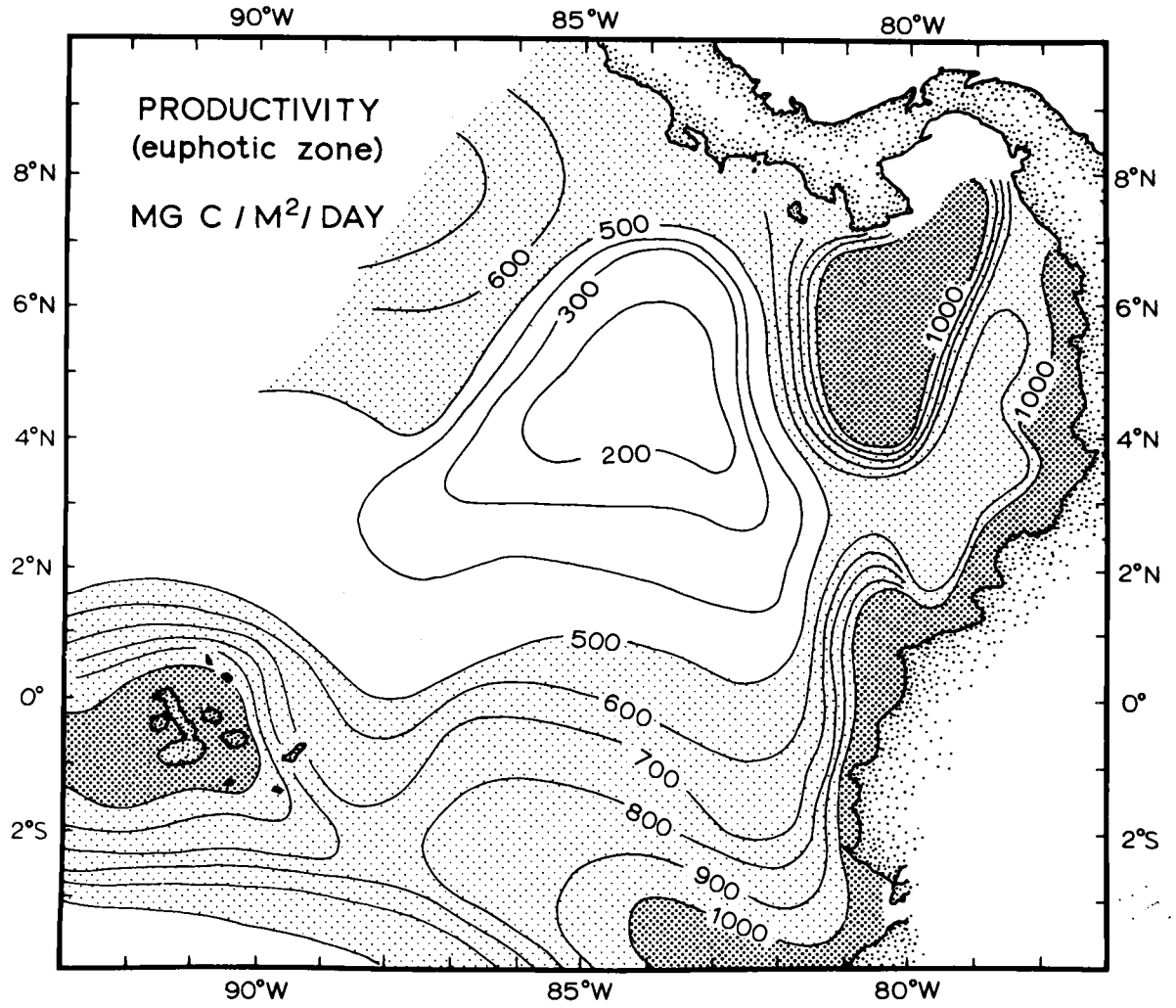

Figure 5. Primary productivity in the Panama Basin, integrated over the euphotic zone (data from Owen and Zeitschell, 1969; Forsbergh, 1969; Love, 1970, 1971 and other unpublished data, combined and averaged over one degree squares) (from Moore et al., 1973).

METHODS

Sampling: The surface samples were taken from tops of piston and gravity cores from the core collections of the Scripps Institution of Oceanography, the Lamont-Doherty Geological Observatory and Oregon State University. Although the surface samples come from levels as deep as 49 cm below the top of the core, they are thought to represent the post-glacial interval and thus to reflect long-term average Recent conditions. This assumption is based on the observation that radio-carbon dates from piston core samples indicate generally high Holocene sedimentation rates (>6 cm/1000 yrs.) in the Panama Basin. The locations of the 61 surface samples were selected in order to provide the best possible representation of surface water mass properties.

For the stratigraphic studies, six cores, taken during the Yaloc '69 cruise of Oregon State University, were selected. The $CaCO_3$ content was determined and plotted as a function of depth in the cores. Sampling of these cores was done on the basis of these carbonate stratigraphies. Fluctuations of $CaCO_3$ content are considered to be primarily a result of temporal variations in the net accumulation rate of biogenic calcium carbonate (Arrhenius, 1952). Time control was provided by radiocarbon dates. The samples studied represent sediments no older than 130,000 years B. P.

Sample intervals in the cores are irregular and samples are not closely spaced, which has imposed some severe restraints on the degree of stratigraphic resolution.

Sample preparation

Initially, in order to recover the Radiolaria from the sediment, a random-strewn slide technique, improved from Nigrini (1967), was used. This method obtained a representative sub-sample from a liquid suspension, but did not allow this subsample to be mounted in such a way that all grains are randomly distributed. Transfer of the subsample to the slide was done with a pipette and settling of the heavier tests in the pipette and surface tension effects of the meniscus prevented a true random distribution on the slide, even when attempting to reduce non-randomness by stirring the slurry with a biological needle. Consequently, it was necessary to count the whole subsample. Since this is very time-consuming, for most of the surface and all of the down-core samples, a random settling technique developed by Moore (1973b) was used.

Sample Counts

The aim of this study is to extract from the paleontological data of a set of deep-sea samples objective and quantitative information concerning the physical state of the natural environment which formed and shaped the planktonic assemblage. One may assume that

analysis of entire assemblages from samples will yield a maximum amount of ecological and depositional information compared to analysis of only a small number of species, which may be affected selectively by special conditions to which they are sensitive. Critical to this assumption is the determination of the optimum number of specimens required to account for most of the variability. The diversity of a fauna is a critical factor in this respect, especially if we do not know if all species in the fauna carry equally important ecological information or if some species are more diagnostic carriers, regardless of what their relative abundance in that fauna is.

Sachs (1973a), after a series of tests, empirically determined that a count of 500 specimens belonging to 120 categories would be sufficient, although he usually encountered only 40-50 species in a single sample count. Of the 120 species, 60 never constituted more than 2% of the population. These were not included in his subsequent quantitative analysis.

As has been pointed out, (Benson, 1966; Nigrini, 1968; Renz, 1973) the diversity of the radiolarian fauna in the Eastern Equatorial Pacific is very high and very few species can be considered to be really common. Rather arbitrarily an initial cutoff value of 2000 specimens was set for the first phase of the surface study. For the majority of the surface samples this was later reduced to 1500 specimens and for all down-core samples to

>1000 specimens per slide. Throughout the study 131 species (categories) were used.

Data Evaluation

The past fifteen years have seen an increased use of mathematical techniques in the geological sciences. The methods most frequently used in micropaleontological studies are recurrent group analysis (Kanaya and Koizumi, 1966; Nigrini, 1970), cluster anslysis (Valentine and Peddicord, 1967; Parker and Berger, 1971) and factor analysis (Imbrie and Kipp, 1971; Lynts, 1971; Sachs, 1973a, b). Recurrent group analysis (Fager, 1957; Fager and McGowan, 1963) is based on the presence or absence of taxa and thus is insensitive to stochastic fluctuations of species abundances. The results are usually presented in a series of maps showing the regions where various assemblages or recurrent groups occur. Cluster analysis (Krumbein and Graybill, 1965; Harbaugh and Merriam, 1968), a simple form of correlation analysis, is a method of searching for relationships in a large symmetrical matrix. It is a logical, pair-by-pair comparison between samples or variables which can be presented in a two-dimensional hierarchical diagram on which the natural breaks between groups are obvious. The clusters do not overlap and at any level of similarity or dissimilarity groups can be picked off by the observer.

Factor analysis (Imbrie and van Andel, 1964; Manson and Imbrie, 1964) is a multivariate, linear mathematical model which apportions each sample (variable) in a data set (usually percentage or absolute abundance data) into contributions from a number of end members or reference samples (variables). The objective of factor analysis is to account for the variance in the data matrix in terms of mixtures of a simple set of extreme compositions. In geological problems these multivariate, linear relationships are usually analyzed for samples in terms of their components (variables; Q-mode analysis). It may then be assumed that samples which cluster together have similar responses to a causal scheme. Such an analysis can be presented in the form of series of maps depicting proportional contributions of each factor to each sample.

In this study two different factor analysis programs were used, the *FAST and *CABFAC programs. A more detailed discussion concerning the Q-mode factor analyses model is given by Imbrie and van Andel (1964), Imbrie and Kipp (1971), Klovan and Imbrie (1971), and Sachs (1973a).

ANALYSIS OF SURFACE SEDIMENTS

The purpose of the surface sediment study was to determine if distribution of radiolarian species and of total radiolarian faunas in surface sediment samples (presumed Holocene deposits) can be related to present-day patterns of upwelling, primary productivity and surface water circulation.

Investigation of radiolarian faunas in surface samples as well as an examination of existing and available information concerning the occurrence of radiolarian species was made to identify useful and important taxa. Eventually, 131 taxa were selected as potentially the most useful. From 45 to 89 species could be observed in any slide count of up to 1500 specimens. Of the 131 species selected, only 45 species were observed to contribute to more than 1% of the total population in any one sample. The other 86 species are rare.

A total of 61 surface samples were selected in order to obtain a good areal coverage of the basin and its immediate surroundings (Figure 6). After these samples were counted, but before processing the raw data, four surface samples (PL 00017, PL00031, PL 00037, and PO 00198), which contained too few radiolaria (<400 per sample), most of them fragmented or severely corroded, were eliminated from the data set.

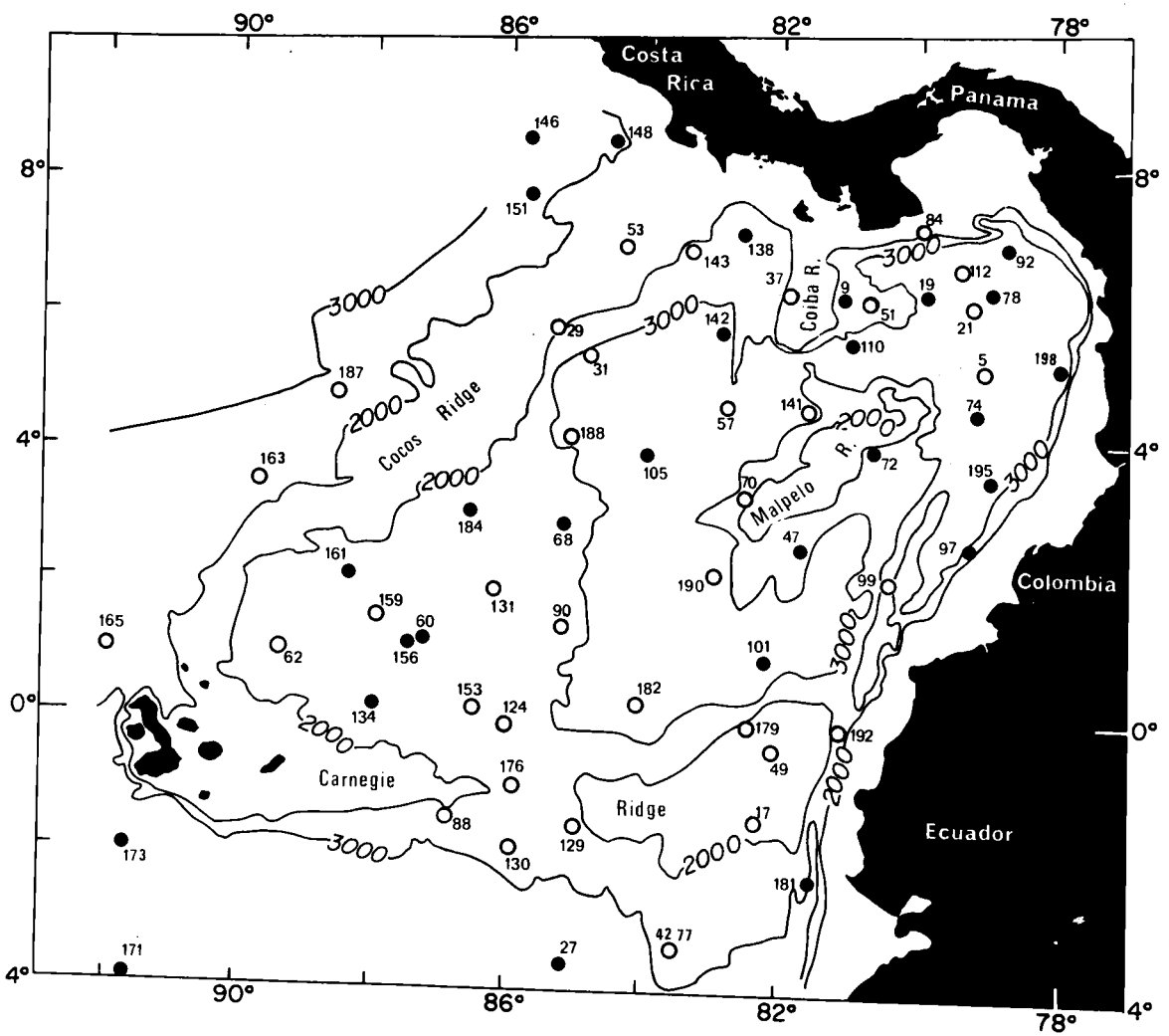

Figure 6. Bathymetry of the Panama Basin, contours in meters. Dots represent locations in surface samples. Open circles indicate samples containing reworked Tertiary and early Pleistocene radiolaria.

Character of the Radiolarian Assemblages

The surface sediment study shows that several processes had acted on the assemblages that modified the faunal composition to a considerable extent. The processes that alter the original composition of an assemblage can either be chemical, such as solution in the water column or in the sediment, or mechanical, such as lateral transport, reworking and winnowing. Solution of opaline silica in water depths shallower than 1500 meters is probably the most important factor in changing a planktonic fauna to the character of the final radiolarian assemblage in the sediment (Berger, 1968). However, subsequent solution on the bottom and in the sediment (Siever, 1957; Arrhenius, 1963) can further alter the original aspect of the assemblage depending on the degree of saturation of the interstitial and bottom water with respect to silica. Predation by other organisms pack skeletons into fecal pellets, which settle quickly onto the sea floor, thus partially bypassing solution effects of surface waters (Schrader, 1971). Solution can also modify the original morphology of certain species in such a way that species identification is affected (Caulet, 1972).

Lateral transport and winnowing will prolong exposure of the radiolarian skeletons to chemical solution in bottom water en route and at its secondary resting place. If these processes work long enough on an assemblage, only the heaviest and sturdiest forms will remain. If both chemical and mechanical processes have played a

major role in the shaping of the preserved radiolarian assemblage, as may be the case in the Panama Basin, it may be difficult to distinguish the effects of solution from those of lateral transport and winnowing.

In order to evaluate these effects, all samples examined were assigned a preservation code, which ranged from 1 (very poor) to 5 (very good). The recognition of variations in the preservation of an assemblage is always somewhat subjective and ambiguous. This is because, in general, the term preservation is used to describe the present physical condition of the fossil skeletons relative to their presumed pristine state. However, all skeletons have probably experienced some degree of solution at one time or another. This alteration is probably the most important single source of differing opinions among workers regarding species concepts and leads to subjectivity in the recognition of variation in preservation states.

Preservation of the radiolarian faunas in the Panama Basin samples varies from poor to moderate (1.5 - 3.5). Preservation is poorest mainly in the deeper parts of the western and eastern basins whereas moderately preserved faunas occur on the ridges (Figure 7).

Reworking of older sediment is evident over most of the basin (Figure 6). The presence of reworked material in the surface

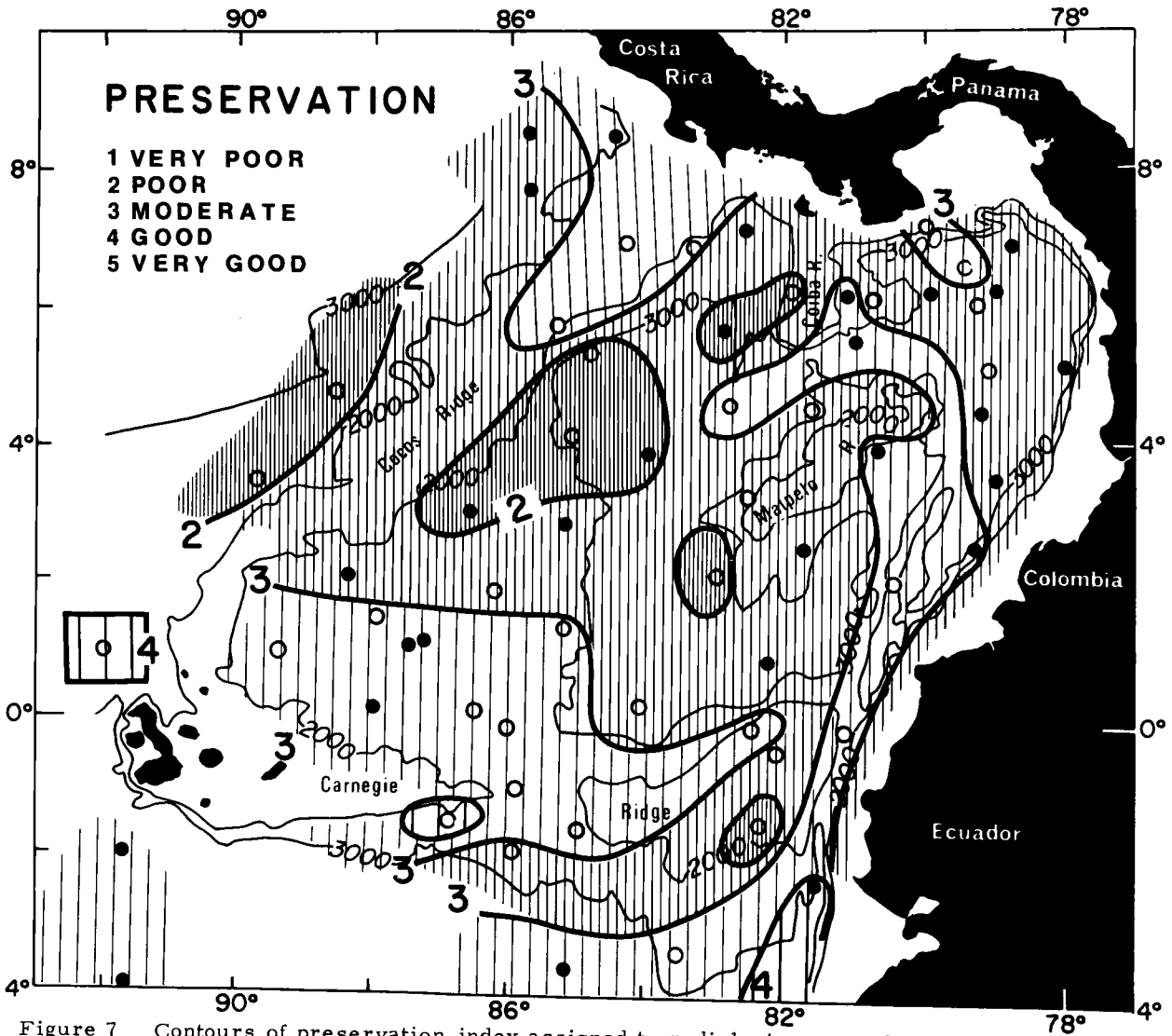

Figure 7 Contours of preservation-index assigned to radiolarian assemblages in the surface sediments of the Panama Basin.

sediments is inferred from the occurrence of known extinct species (most common: Stylatractus universus, Ommatartus penultimus, O. antepenultimus, O. hughesi, Stichocorys peregrina, S. delmontensis and Cannartus species) in these samples. The percentage of these reworked late Tertiary and early Quaternary species never is very high, usually less than 1% of the population. However, the source of this older admixed material may itself already be the result of reworking. At present, not enough information is available to recognize admixed material younger than 400,000 years B. P. (Stylatractus universus extinction plane) in sediment of Holocene age. Figure 6 shows that the occurrences of reworked samples form no clear pattern and it is possible that the reworking is the result mainly of localized bottom currents, slumping and benthic activity.

During the first phase of the study an abundance of fragments was observed in many samples. Thus, as category 132, fragments counts were included in the study. Admittedly, counting fragments can yield ambiguous results and no attempt was made to convert any given number of fragments into a number of whole specimens as Kowsmann (1973) did in his counts of Foraminifera. As a rule, those parts of radiolarian skeletons which represented between 60% and 25% of an individual were counted as fragments. Chaff and other very small fragments were not included. The ratio of fragments to whole specimens on a slide is a partial measure of the amount of

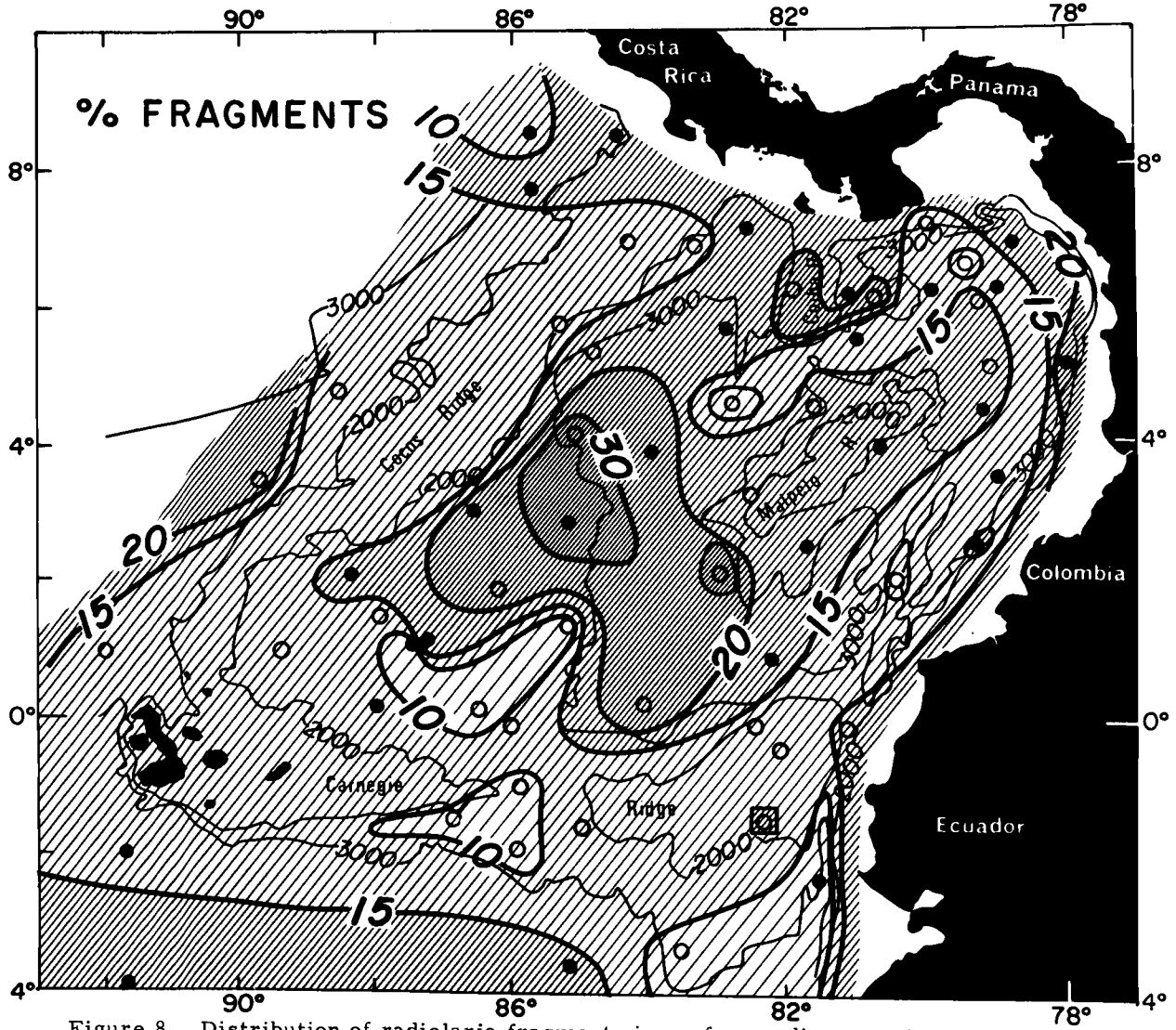

Figure 8 Distribution of radiolaria fragments in surface sediments (% of total whole radiolaria specimens).

winnowed material and might thus be indicative of the effect of mechanical and chemical processes on an assemblage. It may also be used as a partial check on the preservation state of a sample. It is apparent from Figure 8 that the center of the western basin is most enriched and the ridges are relatively low in fragments. Of particular interest is the very low concentration on the Carnegie Ridge saddle, which may indicate that sediment is swept away from this topographic depression and accumulates on both the lower northern and southern slopes. Evidence for large-scale erosion on the Carnegie Ridge saddle is given by Lonsdale et al. (1972) and B. T. Malfait (personal communication) who reported the presence of ripple marks and barchan dune-like features. The patch of low values at the foot of the Carnegie Ridge, below the saddle, is puzzling. If sediment is indeed swept away from the Ridge, one would expect that high fragment values would be observed in these. Local winnowing, however, might account for these low values.

Alternatively, if fragments are considered to be the result of test destruction through chemical solution, lack of fragments at a locality may indicate that such processes are not operating there and fragments are not produced. This explanation, however, is unlikely in view of the substantial evidence that exists in support of winnowing and lateral transport as the principle factors controlling the distribution of biogenic silica (Moore et al., 1973).

Test destruction through chemical solution will break the larger tests and grains into even finer particles. This stepwise fragmentation results in progressive removal by bottom currents of smaller grains, leaving a lag deposit of coarser particles.

In general, there is surprisingly good agreement between Figures 7 and 8, in spite of the amount of subjectivity in determining these two parameters. The higher preservation state on the ridges may result from removal of large amounts of fragments and lighter, corroded specimens. The relatively heavier, less corroded specimens are not removed and thus the assemblage will be assigned a higher preservation index.

The relationship between preservation state and percent of fragments can also be recognized in the eastern basin. The distribution patterns in Figures 7 and 8 resemble the flow pattern of bottom water, with a tongue reaching through the Coiba Gap into the eastern basin. Thus, the bottom current may carry the smaller and lighter fragments from the eastern into the western basin, decreasing the amount of fragmented material in the eastern basin and enriching the western basin.

The distribution of fragments shows that they are concentrated in the central, deeper part of the western basin, most probably as a result of winnowing at the crests and lateral transport down the flanks. This is confirmed by Kowsmann (1973) on the basis of

distribution patterns of Radiolaria in carbonate-free sediment, and of fine-grained carbonate, and by van Andel (1973) on the basis of the distribution of silt-size sediments.

Factor Analysis and Factor Mapping

As explained in the data evaluation section, factor analysis was used to evaluate the surface sediment data set. With an eigenvalue cutoff of 95%, the analysis yielded three factors which accounted for 97% of the variance among the surface samples.

The first factor (end-member is sample 47, south flank Malpelo Ridge) accounts for 65% of the variance and seems to represent primarily samples dominated by a tropical-equatorial fauna (Table 1). The most dominant species are those that belong to the Tetrapyle octacantha group, as well as Ommatartus tetrathalamus, Theoconus minythorax, Lithelius minor and Thecosphaera sp. Except for Theoconus minythorax, these species are all quite robust. Most samples that contain a large proportion of this factor are high in fragments and chaff. If this factor indeed represents the tropical fauna, it would be expected that its distribution conforms somewhat to the surface circulation patterns. However, a map of the factor 1 values shows quite a different pattern (Figure 9). The highest values occur in areas at the base of topographic highs and include most of the western basin. The

TABLE 1

Radiolarian assemblages and species abundances
in surface and core end member samples

species abundances in % of population

Code No.	Species Name	End member sample from *FAST Q-mode analysis				
		surface			core	
		PL00047	PL00105	PO00181	PO04180	PO04313
S 1	Actinomma antarcticum	0	.185	0	.092	0
S 2	Actinomma arcadophorum	.380	.463	.092	.092	.081
S 3	Actinomma medianum	.190	.833	.368	.369	.325
S 4	Actinomma sp.	0	.093	0	.554	0
S 5	Amphirhopalum ypsilon	.570	0	.184	.369	.162
S 7	Cenosphaera cristata	0	0	.184	.369	.325
S 8	Collosphaera tuberosa	.190	0	.092	.184	0
S 16	Euchitonia group	.950	.093	.368	0	0
S 17	Heliodiscus asteriscus	.285	.370	.184	.277	0
S 20	Hexacontium entacanthum	.190	.370	.276	.369	.732
S 21	Hymeniastrum euclides	.950	.185	.644	.554	.325
S 22	Larcospira quadrangula	1.045	.278	0	.369	.162
S 23	Lithelius minor	1.614	1.295	1.288	1.200	.651
S 29	Ommatartus tetrathalamus tetrathalamus	3.039	7.863	.920	2.954	.814
S 32	Stylochlamydium venustum	.380	0	.276	.184	.407
S 33	Phorticium pylonium	.285	.278	.368	.369	2.117
S 37	Polysolenia murrayana	.190	2.035	2.484	.092	.244
S 38	Polysolenia spinosa	.855	.278	.368	.092	0
S 42	Siphonosphaera polysiphonia	.285	0	0	0	0
S 43	Spirema sp.	.095	0	.184	.369	1.465
S 45	Spongaster tetras tetras	.285	0	.184	0	0
S 46	Spongocore puella	.190	0	.460	.369	.081
S 47	Spongopyle osculosa	0	.093	.552	.461	.895
S 50	Spongotrochus glacialis	.285	0	.368	.277	.570
S 52	Spongurus sp.	.285	.185	.276	1.292	.407
S 54	Stylodictya sp. A	1.235	0	.276	.184	.162
S 55	Stylodictya sp. B	.570	0	.184	0	.081
S 57	Tetrapyle octacantha group	17.664	7.401	2.116	3.139	.325
S 58	Octopyle stenozoa	.950	.833	.644	0	.162
S 59	Hexacontium sp.	.095	2.405	.184	.092	0
S 60	Thecosphaera sp.	1.899	10.638	.828	1.846	1.058
S 64	Larcopyle butschli	.285	.185	.092	.369	.244
S 65	Druppatractus irregularis	.285	.093	.184	.461	.244

Table 1 continued

N 69	Liriospyris cf. reticulata	.475	.278	.092	.277	0
N 72	Anthocyrtidium ophirense	.475	0	.184	.646	.081
N 73	Anthocyrtidium zanguebaricum	.285	0	1.012	.184	.651
N 76	Carpocanium sp. A	.855	.463	.460	1.015	.570
N 80	Conarachnium (?) sp. A	.665	0	1.288	2.123	2.280
N 82	Cornutella profunda	.095	0	.092	.184	0
N 84	Dictyocryphalus papillosus	.285	1.110	.184	.646	.081
N 86	Dictyophimus infabricatus	.190	0	1.196	1.292	.977
N 88	Eucyrtidium acuminatum	.285	0	.644	.831	.162
N 90	Eucyrtidium hexagonatum	.380	0	.736	1.108	.488
N 91	Siphocampe aquilonaris	.285	.555	.736	.646	.407
N 93	Lamprocyclas cf. L. haysi	.095	.093	.368	.369	.244
N 94	Lamprocyclas maritales maritales	.570	2.683	.276	1.385	.162
N 95	Lamprocyclas maritales polypora	.095	.555	.184	1.200	.162
N 96	Lamprocyclas maritales ventricosa	.190	.278	.092	.369	.244
N 97	Lithostrobus (?) seriatus	.285	0	.276	1.015	.732
N104	Pterocanium grandiporus	.095	0	.736	1.292	.814
N107	Pterocanium praetextum eucolpum	0	0	.368	.461	.732
N108	Pterocanium praetextum praetextum	.380	0	0	.738	0
N109	Pterocanium trilobum	.570	0	.460	.738	.488
N113	Stichopilium bicorne	0	0	.460	.461	.895
N115	Theocalyptra davisiana	.285	.093	3.404	1.385	4.723
N117	Theoconus minythorax	2.469	.185	2.208	6.648	2.442
N123	Giraffospyris angulata	1.045	.370	.276	0	.081
N124	Tholospyris scaphipes	0	0	.460	.554	.570
N125	Rhodospyris sp.	0	0	.460	.369	.407

pattern can be explained by the bottom transport processes that control the sediment distribution in the basin and produce a predominance of heavier, more robust Radiolaria in this end member. Thus, this end member seems to be the residual of an original tropical factor rather than a representative of the tropical fauna itself. Only the low values in the southeastern and northeastern parts of the Basin may be explained by the surface circulation pattern, since these areas are less under the influence of the tropical surface water.

The second factor (end member sample 105, center of western basin, west of Malpelo Ridge) represents a very impoverished fauna. Robust, heavy forms completely dominate and the assemblage is very rich in fragments and chaff. This factor could not be mapped convincingly. It is most prominent in the northern part of the western basin, represented by the white area in Figure 9. It is also important in sample 78 in the central eastern basin. The impoverished nature of the fauna strongly suggests that this factor is the result of lateral transport and solution. Several of the same robust species that are characteristic for factor 1 are enriched in this assemblage suggesting that further strong modification of the factor 1 assemblage will result in the apparently residual assemblage of factor 2. The areal incoherence of this factor, which accounts for 32.6% of the variance, is suggestive

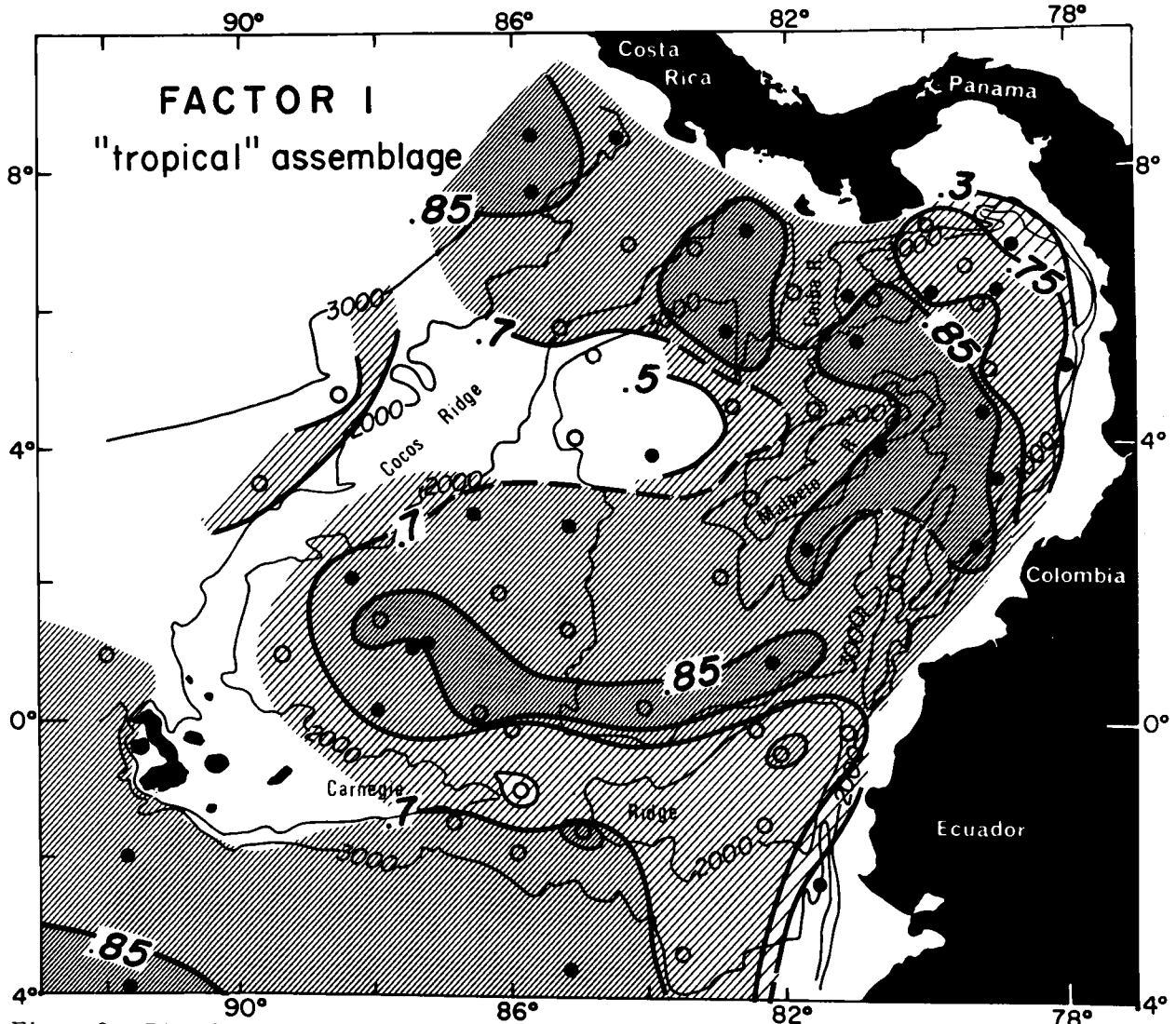

Figure 9 Distribution map of factor 1, "tropical" assemblage, in surface sediments of the Panama Basin.

of the localized pattern of solution and sediment redistribution.

Factor 3 (sample 181, northern end Peru Trench) accounts for only 2.4% of the variance in the surface sediments. In spite of this the factor could be mapped, although with very low values (Figure 10). Compositionally, this assemblage (Table 1) appears to be related to Peru Current assemblages, which the author observed in a few surface sediment samples from south of the Panama Basin. The distribution pattern for this factor suggests an association with water masses, influenced by the north flowing Peru Current. The low values can be explained by erosion on the Carnegie and Cocos Ridges and by solution and lateral transport in the eastern basin. The influence of the last process may be seen in the distributional tongue which reaches westward through the Coiba Gap. In part, the low values may be an artifact resulting from the comparison of an end member sample that has very good preservation and seems little affected by solution, dilution or winnowing processes, with samples that are generally poorly to moderately preserved.

The distribution of factor 3 in the sediments is also similar to the productivity map. Attempts that have been made to relate primary productivity within the basin to the distribution of radiolaria (Kowsmann, 1973) and opal (Moore et al., 1973) have shown no clear relationship. To clarify if a relationship exists between productivity and Peru Current water circulation, a 1:1

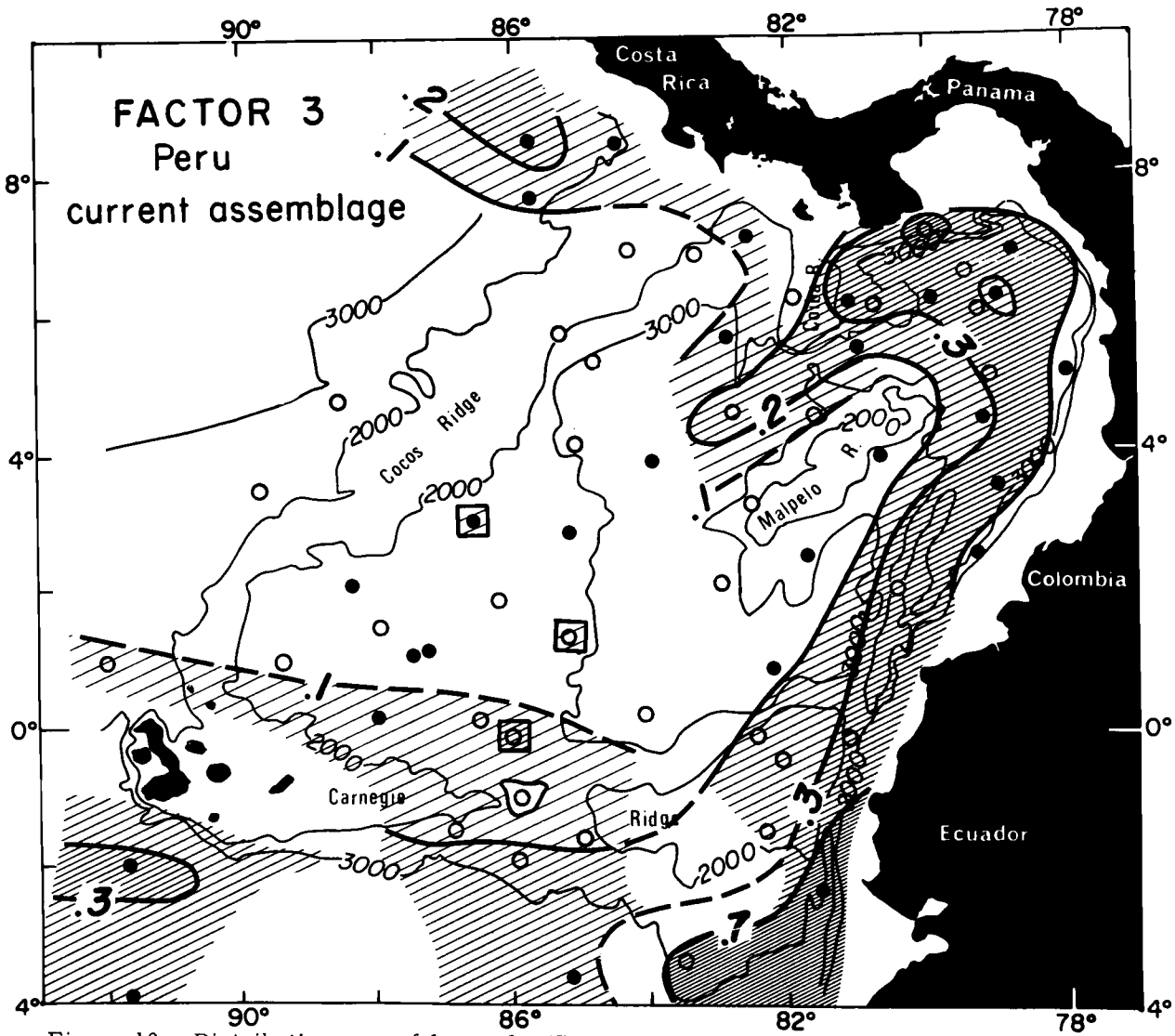

Figure 10 Distribution map of factor 3, "Peru Current" assemblage in surface sediments of the Panama Basin.

correlation between primary productivity and radiolarian assemblages in the plankton may be assumed. In Figure 11, factor 3 values are plotted against the surface productivity values for those sample locations where factor 3 had a value of 0.1 or more. A correlation coefficient of r = .39 shows this hypothesis to be unsubstantiated. This may be explained by the nature of the water associated with the zone of high productivity along the Colombian coast, which is the result of mixing of continental runoff, the Equatorial Countercurrent and the Peru Current, and thus is not Peru Current water proper. The low value of the correlation coefficient may be accounted for by the solution, dilution and reworking processes that play such an important role in the Panama Basin.

Summary of Surface Study

The radiolarian faunas of the surface sediments do not bear out the initial assumption that surface water conditions are reflected, without modifications, in the bottom sediments. On the contrary, processes at the sediment water interface, such as lateral tranpsort and winnowing, reworking and solution, strongly modify the original radiolarian assemblages. According to its fauna, factor 1, labeled "tropical", which accounts for 65% of the variance between samples, is a partial end product of these bottom

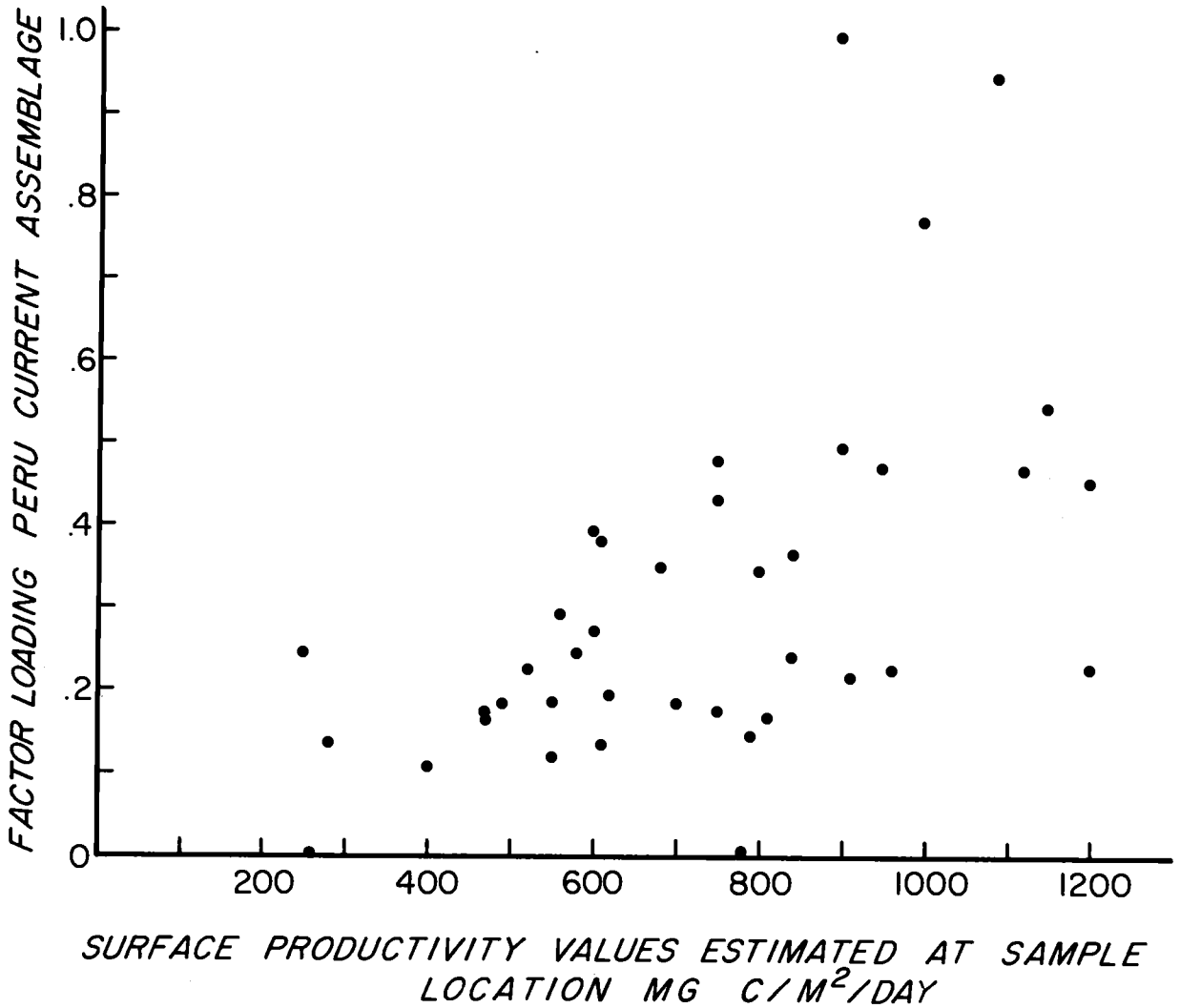

Figure 11. Factor loadings of the "Peru Current" samples v. surface productivity values estimated at sample location. Productivity values are measured in mg $C/m^2/day$.

current processes. Factor 3, the Peru Current influenced factor, on the other hand, reflects in a limited way surface oceanographic conditions, although its distribution may be partially forced by bottom topography. Since the Colombia Current is confined to a strip of water along the Colombia coast, the material that settles from these waters will be concentrated in the deep, enclosed eastern basin from which the only exit is through the Coiba Gap.

These observations place some severe restraints on the extraction of water mass information from the surface data. Sachs (1973b) demonstrated that the numerical factors which represent the radiolarian assemblages can be correlated with oceanographic parameters by means of a technique modified from Imbrie and Kipp's method (1971) for planktonic foraminifera. For a successful utilization of this method, several prerequisites have to be met by the data set. Samples that display evidence of:

a) reworking and consequently contamination with older microfossils,

b) significant dilution by terrigenous and volcanic components,

c) significant effects of solution,

have to be eliminated from the data set. Strict adherence to the first three prerequisites would reject the entire Panama Basin data set from the Imbrie and Kipp model.

STRATIGRAPHIC ANALYSIS

In view of the results of the surface sediment study, the emphasis in the investigation of several piston cores from the Panama Basin was changed. Originally it was the intention to try to relate changes of the faunal assemblages to changes in physical variables of the surface waters through the use of transfer functions as applied by Sachs (1973a, b) in his study of North Pacific sediments. Instead, the present study was focused on using the "Peru Current" end member to determine excursions of Peru Current water into the Panama Basin by means of Q-mode analysis of down-core sample data. For this purpose a number of piston and gravity cores were available from the YALOC-69 cruise of the R. V. Yaquina of Oregon State University.

The six cores selected (Figure 12), all located in the western basin, were selected because: 1) carbonate stratigraphies and twelve radiocarbon dates were available for four of them and 2) the western area, where there is a real (although diffuse) boundary, between "tropical" and "Peru Current" water, might have been more subject to change with time than the waters along the Colombian coast, which lay nearly continuously under influence of that Peru Current off-spring, the Colombia Current.

It was assumed that Arrhenius (1952) and Hays et al. (1969)

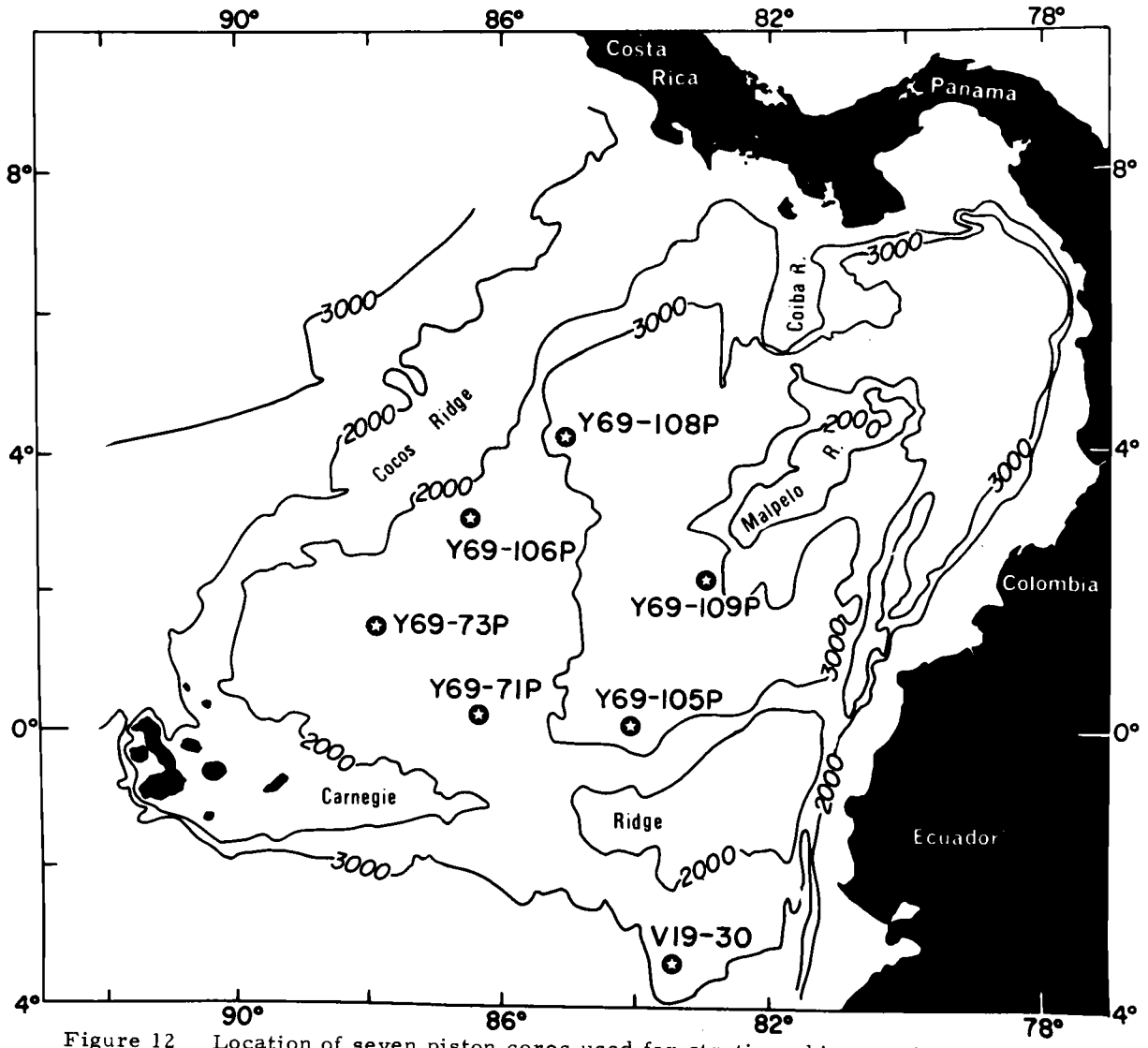

Figure 12 Location of seven piston cores used for stratigraphic examination.

were correct when they equated carbonate cycles with climatic fluctuation and that synoptic oceanographic information could be obtained. The cores were correlated on the basis of carbonate determinations made down each core. These carbonate stratigraphies were used to minimize the number of samples, while maintaining approximate synchroneity. The correlation was checked using radiocarbon dates on four of the cores.

The three cores on the north flank of the Carnegie Ridge (Y69-71P, Y69-73P and Y69-105P) have comparable sedimentation rates as calculated from the radiometric dates (Table 2). However, Y69-106P, with a rate of about 2 cm/1000 yrs. is lower by approximately a factor of five. The radiocarbon dates show that the tops of three cores (Y69-73P, Y69-105P and Y69-106P) are missing and extrapolation of the sedimentation rate for Y69-71P indicates that the age of the top sediment is approximately 2000 years B. P. In order to expand the areal extent of the datum planes for the latter part of the study, carbonate stratigraphies were determined subsequently for two additional cores. Unlike the other cores, these two (Y69-108P and Y69-109P) are low in carbonate and show little variation down the core. Correlation with the other cores is difficult to establish.

Analysis of the faunas in core Y69-108P showed that the siliceous microfossils were severely corroded (preservation code

TABLE 2

Radiocarbon age determinations and calculated sedimentation rates for Panama Basin cores

CORE	sample depth in cm.	Radiocarbon Age (yrs.)	Sedimentation rate
Y69-71P	30-40	6,630 ± 125	9.61 cm/1000 yrs.
	80-90	12,130 ± 180	
	160-170	17,170 ± 350	
Y69-73P	0-5	3,590 ± 100	<11,000 yrs. B.P., 9.3 cm/1000 yrs.
	48-53	8,900 ± 150	>11,000 yrs. B.P., 12.53 cm/1000 yrs.
	165-175	18,350 ± 320	
Y69-105P	0-13	3,050 ± 155	8.85 cm/1000 yrs.
	13-22	2,850 ± 180	
	58-70	9,540 ± 150	
Y69-106P	0-6	4,450 ± 110	1.97 cm/1000 yrs.
	10-15	9,030 ± 155	
	29-36	19,400 ± 800	
V 19-30	12-70	220,000*	5.77 cm/1000 yrs.

* Eastern equatorial Pacific ash layer, extrapolated age (Ninkovich, 1972, personal communication).

1-2 throughout the core), that the diversity of the fauna was consequently low and that reworked Tertiary radiolaria were present in all samples examined. Thus, it was decided to reject this core from the data set. Strong reworking was also evident throughout core Y69-109P and the carbonate stratigraphy indicates that this core penetrated several turbidites. In spite of this and of correlation problems with other cores, the faunal information was retained in the total data set. Late in the study a number of samples were requested from core V19-30, of which the carbonate stratigraphy was known. Unfortunately, the seven samples received were widely spaced throughout this 16 meter core, preventing correlation with others. However, because this core is located beneath present Peru Current waters, the information was useful in the sense that it provided a sample set of probably Peru Current "type" assemblages.

The carbonate curves of the cores from the Panama Basin are not easy to interpret, since they do not show the strong fluctuations observed by Arrhenius (1952) and Hays et al. (1969) farther west in the eastern equatorial Pacific. Variations are in general of low amplitude and the correlation presented in Figure 13 has been partially established with the aid of sedimentation rates calculated from radiocarbon dates and extrapolated downward. For Y69-106P this is consistent (N. G. Pisias, personal communication) with the

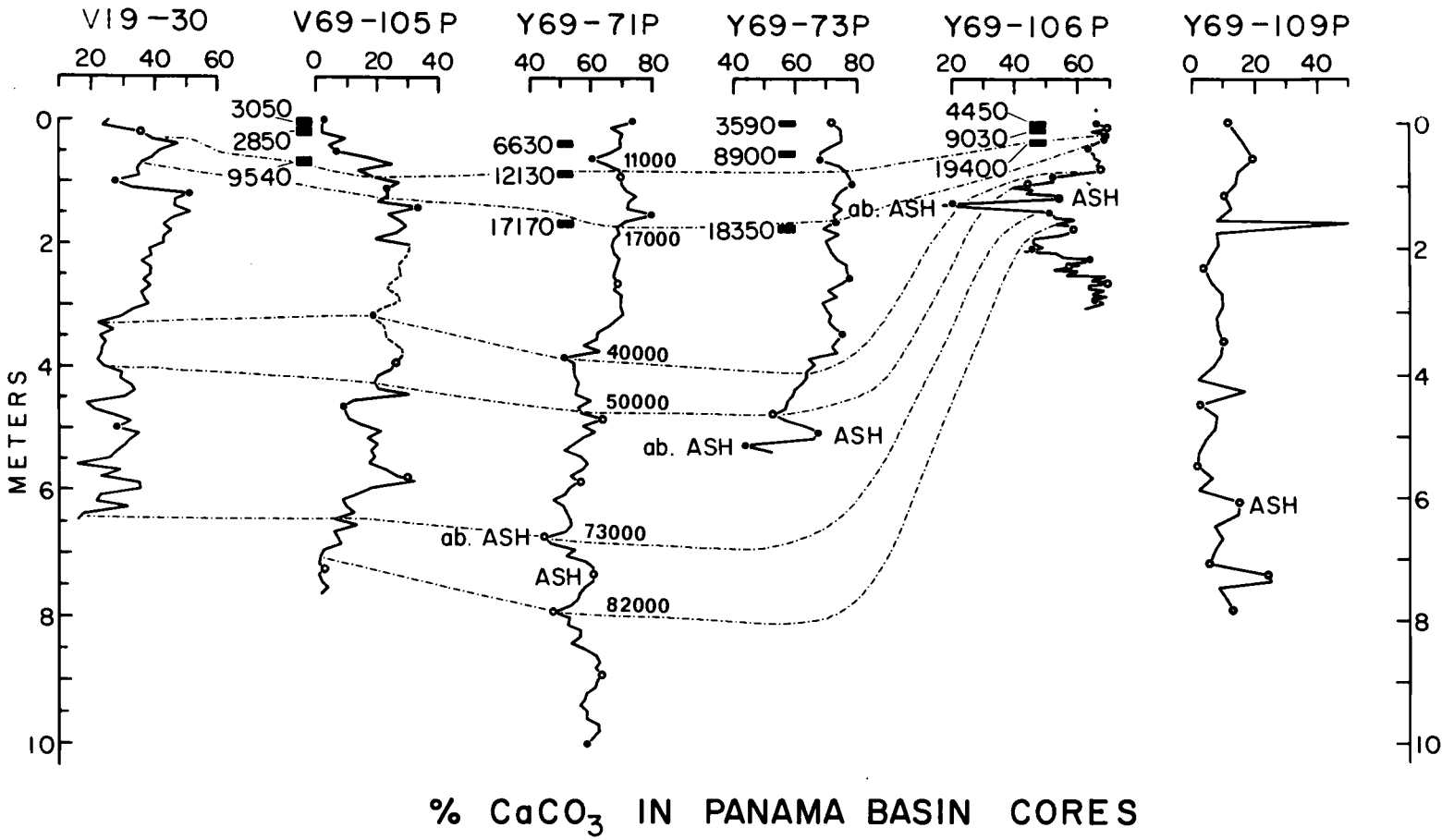

Figure 13 Carbonate stratigraphy for six cores from the Panama Basin. Location and age for radiocarbon dates shown to the left of each core where available. Dots on carbonate curves represent samples for stratigraphic studies. Open circles represent samples containing reworked Tertiary - early Pleistocene radiolaria. Correlation between cores indicated by dotted lines. Correlation based on shape of curves and on sedimentation rates obtained from radiocarbon dates (see Table 2). Ages in thousands of years.

level of extinction of Stylatractus universus (Hays, 1970).

The sediment in the cores consists mainly of silty clays of dusty yellow to olive brown color; a few foraminiferal sand layers occur. Foraminifera are common to abundant throughout the cores and mottling is common. Volcanic material is observed throughout and at several levels in the cores distinct ash layers are present (Figure 13).

Faunal Characteristics of Cores

The faunal assemblages of the cores are very similar to those of the surface sediment samples; high diversities are generally prevalent and the individual taxa show fluctuations in their frequencies. Preservation of the assemblages was more variable, but in general seemed to be better than in the surface sediments. Fragment counts do not differ significantly from those in the surface sediments.

In order to compare surface and subsurface assemblages, the three end members of the surface study were included in the down-core data set used for factor analysis. The result of this analysis (using the *FAST program) was a four factor model which accounted for 96.5% of the observed variance. Three of the end members of this data set (Table 3) correspond to the end members of the surface study. Only factor 2, which accounts for 32.8% of the variance,

cannot be easily compared to the surface factors. It resembles the Peru Current factor of the surface sediments, but contains elements of the tropical factor (Table 1).

The same data set was subjected next to Q-mode factor analysis through the *CABFAC program. This program does not express the factors in terms of end members (samples) but only as contributions from orthogonal vectors to each sample. It also yields a factor score matrix for each factor, which gives the proportional contribution of each species to the individual factors. The program also provides a measure of the adequacy of the model, called "communality" on a scale of 1.0 to 0. If a sample is completely explained by the set of factors, it has a communality index of 1.0 and when the sample is not explained at all, the communality will be 0. The communalities for the four-factor Q-mode analyses are high (from .775 to .978, see Appendix IV).

Because *CABFAC allows only 60 variables (categories) in the matrix, 71 of the 131 categories used in this study had to be eliminated from the data set. Sixty-eight species were rejected with a cutoff at 1%. One species was rejected because it did not occur in any of the end member samples from the previous two Q-mode factor analyses. Two more (Lithomitra arachnea and Artostrobus annulatus) occurred in high frequencies in only two samples of core Y69-71P. Although they probably reflect a real change in fauna,

TABLE 3

Q-mode analysis program	Factors from *FAST	Varimax Factor matrix / End Member Samples	Factor 1 "tropical"	Factor 2 "Peru C."	Factor 3 "Solution 1"	Factor 4 "Solution 2"
		% of variance	65.03	2.38	32.59	-
*FAST surface data	1	PL 00047	1.0	0	0	-
	2	PL 00105	0	0	1.0	-
	3	PO 00181	0	1.0	0	-
		% of variance	54.13	9.06	4.00	32.81
*FAST core data	1	PL 00047	1.0	0	0	0
	2	PO 04313	0	0	0	1.0
	3	PL 04180	0	1.0	0	0
	4	PL 00105	0	0	1.0	0
	end member samples expressed in terms of *CABFAC factors	% of variance	51.66	35.96	6.02	6.35
*CABFAC core data		PL 00047	<u>.969</u>	.152	.064	.006
		PL 04180	.052	<u>.911</u>	.133	.066
		PO 00181	.360	.846	.146	.051
		PL 00105	.565	.142	<u>.756</u>	-0.040
		PO 04313	.414	.697	.209	<u>-0.493</u>

Relationship of surface and sub-surface end members of Q-mode analysis, using the *FAST program, with the factors given by the *CABFAC Q-mode analysis. Highest sample contributions to the *CABFAC factor are underlined; The *CABFAC % of variance is normalized to 100% for better comparison with the variance within the *FAST analyses.

since there is little evidence of solution or bottom transport, they were not comparable to any of the other assemblages in the data set. A Q-mode analysis using the *CABFAC program was then performed on a matrix of 59 (variables) x 67 (samples), resulting in another 4-factor model, which accounted for 91.8% of the variance.

In Table 3 the relationship between the factors from the different Q-mode analyses are shown. The first three factors from the *CABFAC Q-mode analysis correspond to those of the surface study, as well as to factors 1, 3 and 4 of the *FAST Q-mode analysis of the core samples (compare Table 1 and Appendix V). It should be noted that the second end member of this last *FAST analysis also compares rather well with factor 2 of the *CABFAC analysis, which partially confirms the faunal affinity of this sample to the "Peru Current" assemblage. This sample also has the highest value for factor 4 in the *CABFAC analysis. The nature of this factor assemblage cannot be readily explained. It contains elements of both factor 1 and factor 2. Mixing of these two factor assemblages plus subsequent solution and winnowing might have played an important role in the final shaping of this assemblage.

The agreement in the result obtained by the two Q-mode factor analyses (Table 3) shows that reduction from 131 to 59 categories did not alter the results in any significant way. If

anything, it enhanced the Peru Current "signal". This means that the fluctuations in abundance of the rejected 72 categories or rare species do not contain information that is critical to the resolution of the data set.

The values for the four factors in each core (except V19-30) are plotted versus ages calculated from sedimentation rates in Figures 14 and 15. In all cores the values of the factors vary with time, although the magnitude of the changes is not always very large. Factors 1, 3 and 4 have approximately similar variations with time, possibly because factor 3 and perhaps also factor 4 may be solution and winnowing residues of factor 1. Factor 2 tends to vary in opposition. The relatively high "Peru Current" factor value of sample PO 04313 in the *CABFAC Q-mode analysis is difficult to explain since this sample also is very strongly representative of factor 4. Factor 4 is in negative space (Appendix IV) and its highest (absolute) values are negative. Thus, if there is any relationship between factors 2 and 4, this should demonstrate itself in Figures 14 and 15, and factor 4 should be roughly a mirror image of factor 2. From the figures it can be seen that this is only approximately true for cores Y69-105P and Y69-73P and considerably better for Y69-106P.

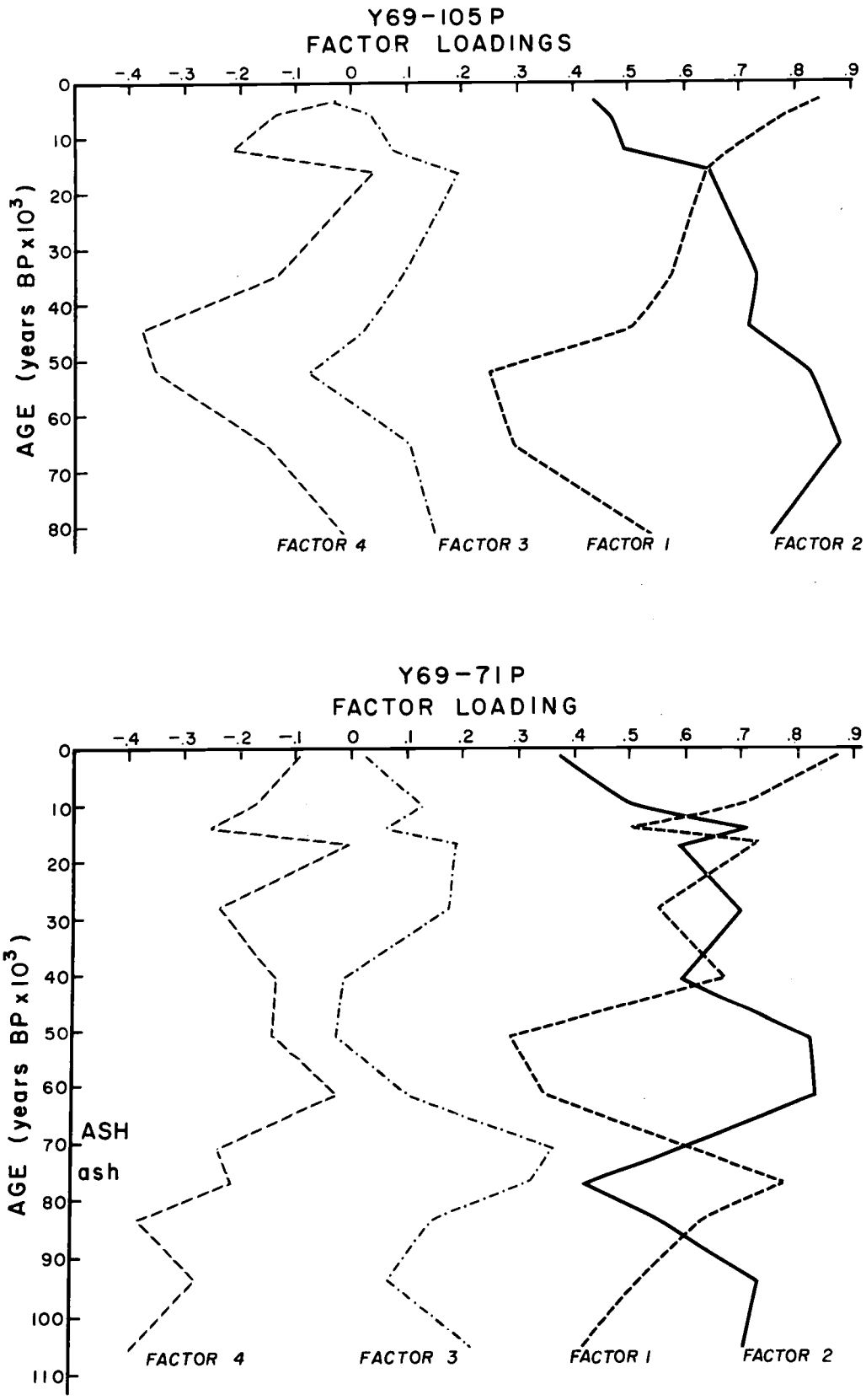

Figure 14 Plots of factor vs. age for cores Y69-105P and Y69-71P.

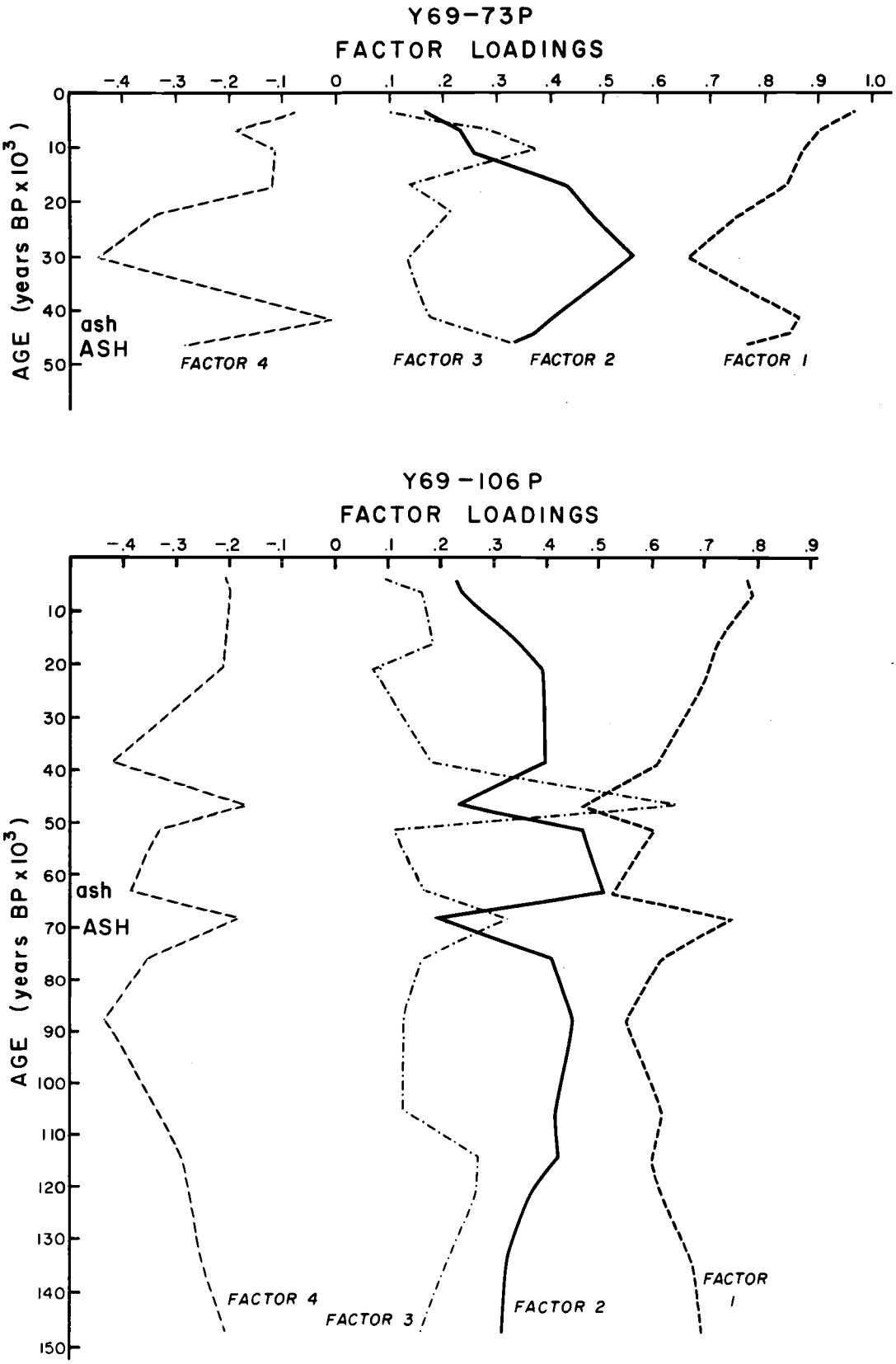

Figure 15 Plots of factor vs. age for cores Y69-73P and Y69-106P.

Correlation and Interpretation of faunal analysis

It has not been possible to express changes in the faunal assemblages with time quantitatively in terms of changes in environmental parameters, such as temperature. Nevertheless, they can be indirectly related to variations in oceanographic conditions and fluctuations in atmospheric circulation and climatic oscillations may be inferred from the observed faunal changes.

In the preceding chapter it was noted that the Peru Current assemblage is more important in pre-Recent sediments than in surface samples in the western basin. Therefore, factor 2 of the *CABFAC analysis, which is associated with the Peru Current, was chosen as a measure of oceanographic and climatic change in the eastern equatorial Pacific. In Figure 16, left column, the faunal indices of this factor are plotted against age for all cores except Y69-109P. Within the limitations imposed by the sample intervals, there is a reasonable correlation between times of higher and lower "Peru Current" faunal indices among the cores. The Peru Current assemblage was dominant from about 70,000 to 50,000 years B. P. From that point to about 40,000 years B. P. it was much reduced in favor of the tropical assemblage, but became the dominant factor again during the latest Pleistocene. It began to decrease slowly at about 20,000 to 15,000 years B. P. and decreased markedly across the Pleistocene-Holocene boundary at 11,000

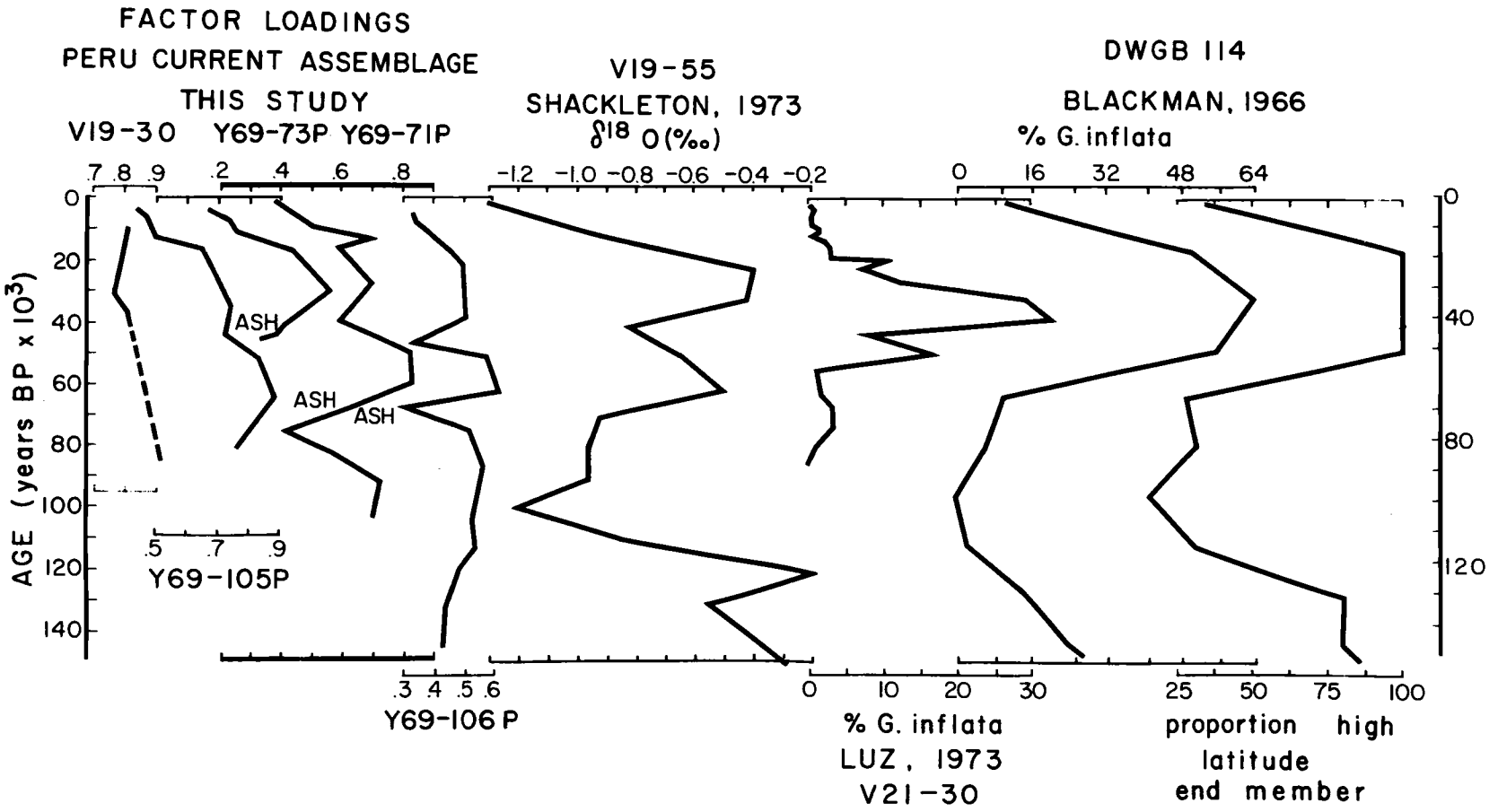

Figure 16 Correlation and chronology of faunal indices of eight eastern equatorial and southeast Pacific cores.

years B. P. Thus it appears that the Peru Current controlled the oceanic regime in the Panama Basin during most of the late Pleistocene, including the last interglacial. Only at the end of the last interglacial did conditions begin to approximate those of the Holocene.

The Panama Basin faunal data vary with time in a manner similar to the planktonic Foraminifera data in the southeast Pacific (Luz, 1973; Blackman, 1966) suggesting that the postulated variations of the Peru Current system in the Panama Basin are probably true. The timing of the changes is the same as that observed further to the south by Blackman. Both Luz and Blackman indicate a rather abrupt change to a cooler oceanographic regime around 65,000 years B. P. Luz also indicates a short reverse trend to warmer conditions between 40,000 and 50,000 years B. P.

On the basis of a factor analysis of foraminiferal data, Blackman and Somayajulu (1966) conclude that Pleistocene climatic changes were synchronous in both the Pacific and Atlantic Oceans. Ericson and Wollin (1970) on the other hand, postulate from an examination of frequency variations of Globorotalia menardii in samples from the tropical Pacific that Atlantic and Pacific climatic oscillations were out of phase during most of the Pleistocene. They surmised that the introduction into the Peru Current system of anomalously cold water from the nearby Antarctic ice sheet influenced the area of Blackman

and Somayajulu's study and deduced that the Pleistocene record in the Pacific varies from region to region. In questioning the validity of correlations between water masses based on a single species, Morin et al. (1970) concluded that the Pleistocene climatic history for both oceans was parallel. From a factor analysis of foraminiferal data in tropical southeast Pacific cores, Luz (1973) confirmed the parallelism of Pacific and Atlantic climatic cycles. On the basis of oxygen isotope analysis of Luz's samples, Shackleton (in Luz, 1973) confirmed the time scale on which Luz's conclusions are based. Neither Blackman's nor Luz's data substantiate the observations made in this study that the last interglacial in the eastern equatorial and southeast Pacific was cooler than the Holocene.

A warm period around 40,000 years B. P., corresponding to the one inferred in this study was recognized by Colinvaux (1972) in a study of the lake deposits in an old explosion crater on San Cristobal (Chatham) in the Galapagos Islands. In this locality a succession of red clay deposits and gyttja (a sapropelic black mud) occurs which can be interpreted in terms of climatic change. The red clays accumulated during glacial times when the Pacific dry zone was more persistent and was located more northerly than at present, so that no water collected in the lake basin. The gyttjas accumulated under more moist conditions. Radiocarbon dates on the two gyttja deposits gave an age of 10,170 years B. P. for the

lower boundary of the uppermost gyttja, and >34,300 and >48,000 years B. P. for the top and bottom of an older, deeper layer, respectively. Pollen analyses of the gyttja deposits substantiate the suggestion of alternating moist and dry climatic conditions for the Galapagos Islands for at least the past 50,000 years.

The climatic changes inferred from fluctuations in faunal indices in the Panama Basin are supported by the results of paleoclimatic research elsewhere. The Peru Current factor curve for core Y69-106P, the longest record among the Panama Basin cores, may be selected for correlation (Figure 17) with paleotemperature records from Colombia (van der Hammen, 1968) and the North Atlantic (Sancetta et al., 1973), and with the oxygen isotope curve for the Greenland ice cap (Imbrie, 1972). From about 80,000 years B. P. until the present, the general shape of the curves is similar. A rapid climatic deterioration is indicated at about 73,000 years B. P. and lasted until approximately 50,000 years B.P. After a warmer interval between 50,000 and 40,000 years B. P. cold conditions were dominant again until the onset of climatic warming which started around 11,000 years B. P. and continued through the Holocene. It should be noted that the warming trend beginning at 50,000 years B. P. is not as pronounced in the data from Colombia as in records from the North Atlantic and the Greenland ice cap. Also, it appears that the trend towards Holocene warming started earlier (between

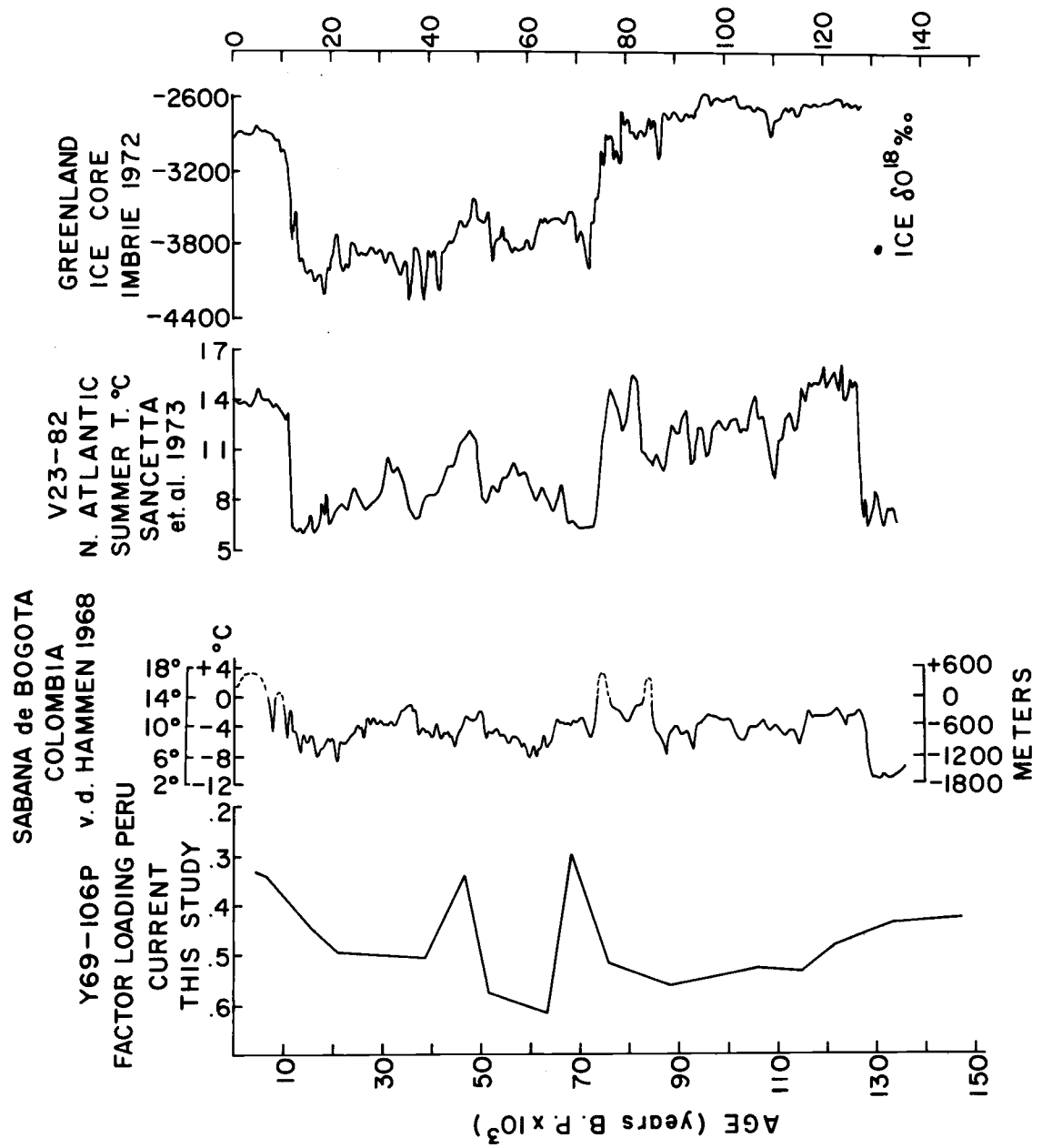

Figure 17 Comparison of temporal fluctuations of the Peru Current as indicated by the factor values of core Y69-106P with late Pleistocene - Holocene records elsewhere The record from Colombia shows the theoretical displacement of the forest limit as caused by temperature fluctuations only. This curve was adjusted to the present time-scale by linear expansion of the Holocene, Glacial, and Interglacial parts of the records, assuming a constant sedimentation rate within each of those intervals. In the North Atlantic record faunal indices, from a quantitative analysis of planktonic foraminifera, were caliberated to estimates of sea surface temperature. The ice-core chronology of Dansgaard et al. (1971) was adjusted to the absolute chronology independently obtained for the North Atlantic deep-sea core V23-82, at 53°N, 22° W.

20,000 and 15,000 years B. P. in the Panama Basin and Colombia) than in the northern hemisphere (the North Atlantic, Greenland and Europe).

The records of the last interglacial from the Panama Basin and Colombia also differ from those of the northern hemisphere. The Colombian data indicate a cooler, dryer climate for the last interglacial than is shown by either Sancetta or Imbrie. That colder conditions prevailed is also shown by the faunal record of the Panama Basin. There the faunal indices indicate an oceanographic regime closely approximating glacial conditions. In this respect it is interesting to consider again the suggestion made by Ericson and Wollin (1970). Although they may have been incorrect in their interpretation of the phase relationships of Atlantic and Pacific climatic oscillations, their observation that the Pleistocene record varies from place to place in the Pacific seems to be substantiated by the Panama Basin data.

The evidence presented in this study suggests that during the southern winter the present atmospheric and oceanic circulation resembles glacial conditions in the eastern equatorial and southeast Pacific. This implies that during a glacial interval the Intertropical Convergence Zone in the eastern equatorial Pacific lay consistently farther north than at present and throughout the year probably oscillated between 15° and 20°N. At present, the Peru Current

itself does not flow north of 3°S, but from the faunal data it can be inferred that during the late Pleistocene the northern boundary of the Peru Current shifted to the north, probably in response to the intensified oceanographic and atmospheric circulation as postulated by Johnson (1972). It has been generally held that fluctuations in the Peru Current and its related upwelling depend on the strength of the southeasterlies and southerlies along the South American coast as well as on the westerlies in the eastern South Pacific (Schott, 1931; Schweigger, 1940, 1959; Wooster, 1960, 1961). As a consequence of the stronger southeast trades during the latest Pleistocene, the ITC moved to the north out of the Panama Basin region, thus placing the basin under the influence of the equatorial dry zone.

Bigarella and Andrade (1965) report evidence of widespread desiccation during glacial times and suggest that the Pleistocene climate of eastern Brasil alternated between arid to semi-arid conditions during glacials and humid tropical conditions during inter-glacials. Van der Hammen (1972), from palynological data in the Amazon Basin, and Damuth and Fairbridge (1970), from a study of deep-sea arkosic sands in the equatorial Atlantic, inferred a cooler, dry climate in tropical South America during the late Pleistocene. Suzuki (1971) ascribes this ice-age aridity to expansion of the South Atlantic and Azores Highs towards the equator.

The atmospheric circulation during glacial times was thus

characterized by a displacement towards the equator of the boundary between tropical easterlies and temperate-latitude westerlies. A lowering of the Pleistocene snow line in the Colombian and Peruvian Andes by 1000 to 1500 m is deduced from a variety of geomorphic phenomena by Hastenrath (1971). He reasons that a northward extension of the westerly wind regime during the Pleistocene would result in increased precipitation along the tropical Andes and hence a depression of the snow line. A depression of about 800 m of the snow line on the volcanoes of the Mexican meseta during the Pleistocene (Hastenrath, 1963) can also be explained by a concurrent southward shift of the atmospheric boundaries in the northern hemisphere.

From a study of present-day rainfall patterns in South America, Suzuki (1973) tentatively deduced an 8° northward displacement of the ITC and the southern hemisphere middle latitude westerlies in the last Glacial Age. Hastenrath's (1963) observation of a Pleistocene snow line at 3500 m in the Cordillera de Talamanca in Costa Rica, (at present there is no permanent snow line on the mountains of Central America) can be explained by the northward shift of the ITC and its accompanying belt of rainfall. Evidence of northward displacement of the ITC during the Pleistocene is also reported from elsewhere. Büdel (1963) and Fairbridge (1965), from observations in Africa, both conclude that during glacial periods the westwind belts shifted equatorward and Büdel contends that the

northward shift of the ITC across Africa can be contributed to increased glaciation in Antarctica during late Pleistocene times. From a study of fossil and recent dune patterns and dune trends in Australia, Sprigg (1959) inferred that the "Roaring Forty" prevailing westerly belt lay 5° north of its present position during the Pleistocene southern winter. Van Andel et al. (1967) estimated, from a study of the morphology and sedimentary facies in the Timor Sea, a 5° to 10° northward displacement of the westwind belts. Thus, there is widespread evidence that both hemispheric climatic belts moved towards the equator during glacials and toward the poles during interglacials.

However, it appears that topographic differences between individual continents can give rise to conditions that modify the general pattern of climatic change and are unique to separate areas. Faunal data from the Panama Basin as well as palynological evidence presented by van der Hammen (1968) indicate that conditions during the last interglacial in this region do not conform with the climatic record as deduced from studies elsewhere. The apparently cooler, and possibly dryer climate between 120,000 and 80,000 years B. P. in the proximity of northwestern South America appears to indicate conditions more glacial than those of interglacial, which is generally assumed to be warm and moist. At present there are only a few studies that bear on this problem. Recently, Shackleton and

Opdyke (1973), from oxygen isotope studies on a core from the western equatorial Pacific, concluded that less ice was stored in the polar ice caps during the last interglacial than at present. Mercer (1968), from geomorphic evidence in Antarctica, concluded that during the last inter-glacial the West Antarctic ice sheet had completely disappeard. Shackleton and Opdyke's results seem to corroborate this conclusion. Deglaciation of West Antarctica during the last interglacial would have released large quantities of cold water which subsequently may have been carried northward by the Peru Current system. This may account adequately for the presence of Peru Current water assemblages in the Panama Basin, at least during the first part of the last interglacial. However, the deglaciation of the West Antarctic ice sheet would still not explain the apparent cool conditions in the Panama Basin during the latter part of the last interglacial.

CONCLUSIONS

A quantitative study of radiolarian assemblages in Panama Basin surface sediments has shown that the distributions of these assemblages do not reflect present-day oceanographic patterns of upwelling, primary productivity and surface water circulation. Chemical and mechanical processes, in the water column and post-depositional, are most effective agents in the final shaping of the assemblages. The effects of solution, winnowing and lateral transport in the basin are closely associated and are definitive in determining the final distribution of the radiolarian faunas. Only one assemblage, which is associated with the Peru Current fauna, shows in a limited way an association with surface oceanographic conditions. Thus this fauna was used in a quantitative analysis of subsurface samples from four piston cores from within the western basin. For these cores, carbonate stratigraphies as well as a number of radiocarbon dates were available. Also, the sediments of the western basin may contain a better record of changing surface oceanographic conditions since they underlie a region where at present there is a rather diffuse boundary between the "tropical" and "Peru Current" water. A set of oceanographic and atmospheric conditions different from today, may have resulted in either a weakening, strengthening or shift of this boundary which would be recorded in the sediments deposited below.

The results of this stratigraphic analysis showed that during most of the late Pleistocene, assemblages associated with the Peru Current fauna were deposited in the Panama Basin. Re-appearance of tropical assemblages in the basin occurred just before the onset of the last glacial (from approximately 85,000 to 70,000 years B. P.), during a warm interval from about 50,000 to 40,000 years B. P., and finally during the Holocene. The shift towards the present-day oceanographic regime began approximately 20,000 years B. P. Conditions approximating those of a glacial period for the last interglacial in the Panama Basin are indicated by the presence of the Peru Current fauna in two of the cores. Palynological evidence from nearby Colombia agrees well with this observation. The yield of large quantities of cold water, released in the melting of the West-Antarctic ice cap can adequately explain this anomalous cold water in the region.

The strong coupling that exists between the behavior of the Peru Current system and atmospheric circulation in the southeastern Pacific, allows one to infer climatic conditions over the region over the time interval investigated, i. e. the past 130,000 years.

A northward shift of current boundaries has the important climatologic implication that the major wind belts and the South Pacific high pressure cell also shifted northward to the equator. This means that the Intertropical Convergence Zone must have been

more stationary, with a smaller amplitude of seasonal movement, in its northerly position between 15° and 20°N. Supporting evidence for a northward shift of the major wind belts of the Southern Hemisphere during the late Pleistocene is found in studies, based on geomorphic and palynologic evidence, from Central and South America, and the Galapagos Islands. That this is a world-wide phenomena is corroborated by studies from Africa and Australia.

An important consequence of a northward shift of the Intertropical Convergence Zone in the eastern tropical Pacific is that atmospheric and oceanic gradients would be very steep at these low latitudes. Records of these gradients should be present in sea floor sediments and on land.

Only further studies of deep-sea sediments from the eastern equatorial Pacific as well as analysis of land-based sequences from Central America may shed more light on this problem.

BIBLIOGRAPHY

Arrhenius, G. O. 1952. Sediment cores from the East Pacific. Repts. Swedish Deep-Sea Exped. (1947-1948). Fasc. 1, 5, 277 p.

Arrhenius, G. O. 1963. Pelagic Sediments. In: The Sea, Ed. by M. N. Hill. Vol. 3 New York, Interscience. p. 655-727.

Bandy, O. L., R. E. Casey and R. C. Wright. 1971. Late Neogene planktonic zonation, magnetic reversals and radiometric dates, Antarctic to the tropics. In: Antarctic Oceanology I, ed. by J. L. Reid. Am. Geophys. Union, Antarctic Res. Ser., 15:1-26.

Benson, R. N. 1966. Recent Radiolaria from the Gulf of California. unpubl. Ph. D. thesis, University of Minnesota, 578 numb. leaves. (University Microfilms #66-12, 189).

Berger, W. H. 1968. Radiolarian skeletons: Solution at depths. Science. 159:1237-1238.

Bigarella, J. J. and G. G. Andrade. 1965. Contribution to the study of the Brazilian Quaternary. Geol. Soc. Am. Sp. Pap. 84: 433-451.

Blackman, A. 1966. Pleistocene stratigraphy of cores from the southeast Pacific Ocean. unpubl. Ph. D. thesis, University of California, San Diego, 200 numb. leaves.

Blackman, A. and B. L. K. Somayajulu. 1966. Pacific Pleistocene cores: faunal analysis and geochronology. Science. 154:886-889.

Büdel, J. 1963. Die Pliozän und quartären Pluvialzeiten der Sahara. Eisz. u. Geg. 14:161-187.

Caulet, J. 1972. Premières observations sur la dissolution progressive des squelettes de Sphaerellaires (Radiolaires) en voie de sedimentation dans les vases de la Méditerranee. Incidences sur la systématique de ces formes. C.R. Acad. Sc. Paris, 274:2759-2762.

Colinvaux, P. A. 1972. Climate and the Galapagos Islands. Nature.

240:17-20.

Correns, C. W. 1937. Die Sedimente des aquatorialen, Atlantischen Ozeans. Wiss. Ergebn. Deutsch. Atlant. Exped. METEOR, 1925-1927. 3:1.

Damuth, J. E. and R. W. Fairbridge. 1970. Equatorial Atlantic deep-sea arkonic sands and ice-age aridity in tropical South America. Geol. Soc. Am. Bull. 81:189-206.

Dansgaard, W., S. J. Johnson, H. B. Clausen and C. C. Langway. 1971. Climatic record revealed by the Camp Century ice core. In: Late Cenozoic Glacial Ages, ed. by K. K. Turekian, Yale University Press, New Haven, p. 37-56.

Ericson, D. B. and G. Wollin. 1970. Pleistocene climate in the Atlantic and Pacific Oceans: A comparison based on deep-sea sediments. Science. 167:1483-1485.

Fager, E. W. 1957. Determination and Analysis of Recurrent Groups. Ecology. 38(4):586-595.

Fager, E. W. and J. A. McGowan. 1963. Zooplankton species groups in the North Pacific. Science. 140:453-460.

Fairbridge, F. W. 1965. Eiszeitklima in Nordafrika. Geol. Rundschau 54(1):399-414.

Forsbergh, E. D. 1969. On the climatology, oceanography and fisheries of the Panama Bight. Inter-American Tropical Tuna Commission. Bull. 14(2):49-385.

Goll, R. M. and K. R. Bjørklund. 1971. Radiolaria in surface sediments of the North Atlantic Ocean. Micropaleontology. 17(4):434-454.

Harbaugh, J. W. and D. F. Merriam. 1968. Computer applications in Stratigraphic Analysis. J. Wiley and Son, Inc., New York, 282 p.

Hastenrath, S. 1963. Über den Einfluss der Massenerhebung auf den Verlauf der Klima - und Vegetationsstufen im Mittel amerika und im südlichen Mexico. Geogr. Annaler 45(1):76-83.

Hastenrath, S. L. 1971. On the Pleistocene snow-line depression

in the arid regions of the South American Andes. J. Glaciology. 10(59):255-267.

Hays, J.D. 1965. Radiolaria and late Tertiary and Quaternary history of Antarctic Seas. In: Biology of the Antarctic Seas II, Am. Geophys. Union, Antarctic Res. Ser. 5:125-184.

Hays, J.D. 1970. Stratigraphy and evolutionary trends of Radiolaria in North Pacific Deep-Sea sediments. Geol. Soc. Am. Memoir 126:185-218.

Hays, J.D., T. Saito, N.D. Opdyke and L.H. Burckle. 1969. Pliocene-Pleistocene sediments of the equatorial Pacific: Their paleomagnetic, biostratigraphic, and climatic record. Geol. Soc. Am. Bull. 80(8):1481-1514.

Imbrie, J. 1972. Correlation of the climatic record of the Camp Century ice core (Greenland) with foraminiferal paleotemperature curves from North Atlantic deep-sea cores. Geol. Soc. Am. Abstracts 4(7):550.

Imbrie, J. and N.G. Kipp. 1971. A new micropaleontological method for quantitative paleo-climatology: Application to a late Pleistocene Caribbean core. In: The Late Cenozoic Glacial Ages, ed. by K.K. Turekian. Yale University Press, New York. p. 71-181.

Imbrie, J. and Tj. H. van Andel. 1964. Vector analysis of heavy-mineral data. Geol. Soc. Am. Bull. 75:1131-1156.

Johnson, D.A. 1972. Ocean-floor erosion in the equatorial Pacific. Geol. Soc. Am. Bull. 83:3121-3144.

Kanaya, T. and K. Koizumi. 1966. Interpretation of diatom thanatocenoesis from the North Pacific applied to a study of core V19-30 (Studies of a deep-sea core V20-130). Scientific Rep. Tohoku University, Japan, Second Series (Geology) 37:89-130.

Klovan, J.E. and J. Imbrie. 1971. An Algorithm and Fortran-IV Program for Large-Scale Q-Mode Factor Analyses and Calculation of Factor Scores. Math. Geol. 3(1):61-77.

Kowsmann, R.O. 1973. Coarse components in surface sediments of the Panama Basin. J. Geology, in press.

Krumbein, W. C. and F. A. Graybill. 1965. An Introduction to Statistical Methods in Geology. McGraw-Hill, New York, 475 p.

Laird, N. P. 1971. Panama Basin deep water properties and circulation. J. Mar. Res. 29(3):226-234.

Lonsdale, P., B. T. Malfait and F. N. Spiess. 1972. Abyssal sand waves on the Carnegie Ridge. Geol. Soc. Am. Abstracts 4(7):579-580.

Love, C. M. 1970. Biological and nutrient chemistry data from principal participating ships, first and second monitor cruise, August-September, 1967. U. S. Dept. Commerce, EASTROPAC Atlas, 4.

Love, C. M. 1971. Biological and nutrient chemistry data from principal participating ships, first survey cruise, February-March, 1967. U. S. Dept. Commerce, EASTROPAC Atlas, 2.

Luz, B. 1973. Stratigraphic and paleoclimatic analysis of late Pleistocene tropical southeast Pacific cores. Quaternary Res. 3(1):56-72.

Lynts, G. W. 1971. Analysis of the planktonic foraminiferal fauna of core 6275, Tongue of the Ocean, Bahamas, Micropaleontology. 17(2):152-166.

Manson, V. and J. Imbrie. 1964. Fortran program for factor and vector analysis of geologic data using an IBM 7090 or 7094/1401 computer system. Kansas Geol. Survey, Spec. Distrib. Publ. 13:1-46.

Mercer, J. H. 1968. Antarctic ice and Sangamon sea level. Int. Assoc. Scient. Hydrology, Publ. 79:218-225.

Moore, T. C., Jr. 1973a. Late Pleistocene-Holocene oceanographic changes in the northeaster Pacific. Quaternary Res. 3(1):99-109.

Moore, T. C., Jr. 1973b. Method for randomly distributing grains for microscopic examination. J. Sed. Petr. (in press).

Moore, T. C., Jr., G. R. Heath and R. O. Kowsmann. 1973. Biogenic sediments of the Panama Basin. J. Geology (in press).

Morin, R. W., F. Theyer and E. Vincent. 1970. Pleistocene climates in the Atlantic and Pacific Oceans: A re-evaluated comparison based on deep-sea sediments. Science. 169:365-366.

Nigrini, C. A. 1967. Radiolaria in pelagic sediments from the Indian and Atlantic Oceans. Bull. Scripps Inst. Oceanog. 11:1-125.

Nigrini, C. A. 1968. Radiolaria from eastern tropical Pacific sediments. Micropaleontology 14(1):51-63.

Nigrini, C. A. 1970. Radiolarian assemblages in the North Pacific and their application to a study of Quaternary sediments in core V20-130. Geol. Soc. Am. Memoir 126:139-183.

Owen, R. W. and B. Zeitzschel. 1970. Phytoplankton production: seasonal change in the oceanic eastern tropical Pacific. Marine Biology. 7(1):32-36.

Pak, H. and J. R. V. Zaneveld. 1973. The Cromwell Current on the east side of the Galapagos Islands. J. Geophys. Res., (in press).

Parker, F. L. and W. H. Berger. 1971. Faunal and solution patterns of planktonic foraminifera in surface sediments of the South Pacific. Deep-Sea Res. 18:73-107.

Pratje, O. 1951. Die Kieselsäureorganismen des Südatlantischen Ozeans als Leitformen in den Bodenablagerungen. Deutsche Hydrogr. Zeitschr. 4(1-2):1-6.

Renz, G. W. 1973. The distribution and ecology of Radiolaria in the Central Pacific: plankton and surface sediments. unpubl. Ph. D. thesis, University of California, San Diego, 251 numb. leaves.

Riedel, W. R. 1958. Radiolaria in Antarctic sediments. B. A. N. Z. A. R. E. reports, ser. B. 6(10):217-255.

Sachs, H. M. 1973a. Quantitative Radiolarian-based paleo-oceanography in late Pleistocene subarctic Pacific sediment. unpubl. Ph. D. thesis, Brown University, 208 numb. leaves.

Sachs, H. M. 1973b. North Pacific Radiolarian assemblages and

their relationship to oceanographic parameters. Quaternary Res. 3(1):73-88.

Sachs, H. M. 1973c. Late Pleistocene history of the North Pacific: evidence from a quantitative study of radiolaria in core V21-73. Quaternary Res. 3(1):89-98.

Sancetta, C., J. Imbrie and N. G. Kipp. 1973. Climatic record of the past 130,000 years in North Atlantic deep-sea core V23-82: correlation with the terrestrial record. Quaternary Res. 3(1):110-116.

Schott, G. 1931. Der Peru Strom und seine nordlichen Nachbargebieten im normaler und abnormaler Ausbildung. Ann. Hydrograph. 59:161-257.

Schott, W. 1935. Die Foraminiferen in dem aquatorialen Teil des Atlantischen Ozeans. Wiss. Ergebn. Deutsch. Atlant. Exped. METEOR, 1925-1927. 3(3):43-134.

Schrader, H. J. 1971. Fecal pellets: Role in sedimentation of pelagic diatoms. Science. 174:55-57.

Schweigger, E. H. 1940. Studies of the Peru Coastal Current with reference to the extraordinary summer of 1939. Proc. Pacific Sci. Congr. Pacific Sci. Assoc., 6th, Berkeley, 3:177-195.

Schweigger, E. H. 1959. Die Westküste Südamerikas im Bereich des Peru-Stroms. Keyser Verlag, Heidelberg, 513 p.

Shackleton, N. J. and N. D. Opdyke. 1973. Oxygen isotope and paleomagnetic stratigraphy of equatorial Pacific core V28-238: Oxygen isotope temperatures and ice volumes on a 10^5 year and 10^6 year scale. Quaternary Res. 3(1):39-55.

Siever, R. 1957. The silica budget in the sedimentary cycle. Am. Mineralogist. 42:821-841.

Sprigg, R. C. 1959. Stranded sea beaches and associated sand accumulation of the upper Southeast. Roy. Soc. South Australia Trans. 82:183-193.

Steemann Nielsen, E. 1952. The use of radioactive carbon (^{14}C) for measuring organic production in the sea. J. Cons. Explor. Mer. 18:117-140.

Steemann Nielsen, E. and E.A. Jensen. 1957. Primary oceanic production, the autotrophic production of organic matter in the oceans. "Galathea" Repts. 1:49-120.

Stevenson, M. 1970. Circulation in the Panama Bight. J. Geophys. Res. 75(3):659-672.

Stevenson, M.R. and B.A. Taft. 1971. New evidence of the Equatorial Undercurrent east of the Galapagos Islands. J. Mar. Res. 29(2):103-115.

Suzuki, H. 1971. Climatic zones of the Würm glacial age. Bull. Dept. Geogr. Univ. Tokyo. 3:35-46.

Suzuki, H. 1973. Recent and Würm climates of the west coast of South America. Bull. Dept. Geogr. Univ. Tokyo. 5:1-32.

Valentine, J.W. and R.G. Peddicord. 1967. Evaluation of fossil assemblages by Cluster Analysis. J. Paleontology 41(2):502-507.

van Andel, Tj. H. 1973. Texture and dispersal of sediments in the Panama Basin. J. Geology (in press).

van Andel, Tj. H., G.R. Heath, T.C. Moore, Jr. and D.F.R. McGeary. 1967. Late Quaternary history, climate, and oceanography of the Timor Sea, northwestern Australia. Am. J. Sci. 265(11):737-758.

van Andel, Tj. H., G.R. Heath, B.T. Malfait, D.F. Heinrichs and J.I. Ewing. 1971. Tectonics of the Panama Basin, eastern equatorial Pacific. Geol. Soc. Am. Bull. 82:1489-1580.

van der Hammen, T. 1968. Climatic and vegetational succession in the equatorial Andes of Colombia. Colloq. Geogr. 9:187-194.

van der Hammen, T. 1972. Changes in vegatation and climate in the Amazon basin and surrounding areas during the Pleistocene. Geol. Mijnbouw 51(6):641-643.

Wooster, W.S. 1959. Oceanographic observations in the Panama Bight, "ASKOY" expedition, 1941. Bull. Am. Mus. Nat. History 118(3):119-151.

Wooster, W.S. 1960. El Nino. Calif. Coop. Fish. Invest. Rept. 7:43-45.

Wooster, W.S. 1961. Yearly changes in the Peru Current. Limnol. Oceanogr. 6:222-226.

Wooster, W.S. and T.C. Cromwell. 1958. An oceanographic description of the eastern tropical Pacific. Bull. Scripps Inst. Oceanog. 7(3):169-282.

Wooster, W.S. and M. Gilmartin. 1961. The Peru-Chile Undercurrent. J. Mar. Res. 19(3):97-122.

Wyrtki, K. 1965. Surface currents of the eastern tropical Pacific Ocean. Bull. Inter-American Tropical Tuna Commission. 9(5):271-304.

Wyrtki, K. 1966. Oceanography of the eastern equatorial Pacific Ocean. Oceanogr. Mar. Biol. Ann. Rev. 4:33-68.

APPENDICES

APPENDIX I. Surface Samples

PL: Lamont PS: Scripps PO: OSU

Core	Water Depth (corr. meters)	Sampler	Sample Top (cm)	Sample Bottom (cm)	Latitude (deg. min.)	Longitude (deg. min.)		Samples
IDEN V15-13	3116	PC	11	14	05.80	079.04		PL00005 5
IDEN V15-15	2659	PC	17	20	06.08	081.03		PL00009 4
IDEN V15-31	1417	PC	20	23	-01.30	082.19		PL00017 2
IDEN V17-40	3091	PC	13	17	06.08	079.54		PL00019 4
IDEN V17-41	3437	PC	13	16	05.58	079.15		PL00021 1
IDEN V17-44	3358	PC	15	18	-03.34	085.07		PL00027 2
IDEN V18-350	1838	PC	8	10	05.42	085.16		PL00029 4
IDEN V18-351	3007	PC	5	8	05.18	084.45		PL00031 1
IDEN V18-354	1348	PC	10	13	06.12	081.54		PL00037 2
IDEN V19-25	2404	PC	10	13	02.28	081.42		PL00047 2
IDEN V19-27	1373	PC	10	13	-00.28	082.04		PL00049 4
IDEN V20-14	3131	PC	9	12	06.04	080.39		PL00051 1
IDEN V20-15	1736	PC	26	28	06.57	084.17		PL00053 3
IDEN V21-25	3081	PC	19	22	04.36	082.44		PL00057 2
IDEN V21-28	2714	PC	11	14	01.05	087.17	FECONTAM	PL00060 5
IDEN V21-29	712	PC	12	14	00.57	089.21		PL00062 2
IDEN V21-212	3338	PC	9	12	02.50	085.08		PL00068 3
IDEN V21-214	2246	PC	13	16	03.50	080.38		PL00072 2
IDEN V21-215	3418	PC	12	15	04.24	079.10		PL00074 4
IDEN V21-217	1774	PC	13	16	06.11	078.57		PL00078 3
IDEN V24-35	2869	PC	10	13	07.06	079.58		PL00084 4
IDEN RC8-102	2180	PC	7	10	-01.25	086.51		PL00088 3
IDEN RC8-103	2937	PC	17	20	01.16	085.10		PL00090 5
IDEN RC9-62	3250	PC	17	20	06.50	078.44		PL00092 2
IDEN RC9-65	2074	PC	21	24	02.31	079.15		PL00097 2
IDEN RC9-66	4218	PC	21	24	01.58	080.27	D UNCERT	PL00099 4
IDEN RC9-67	3091	PC	15	18	00.49	082.09		PL00101 1
IDEN RC10-52	2243	PC	18	22	03.52	083.56		PL00105 5
IDEN RC10-252	3398	PC	10	13	05.28	080.58		PL00110 5
IDEN RC10-253	3219	PC	46	49	06.31	079.24		PL00112 2
IDEN RIS-32P	2770	PC	11	13	-00.09	085.59		PS00124 4
IDEN TRI-HF-2	2214	HF	0	10	-01.35	084.58		PS00129 4
IDEN TRI-HF-4	2580	HF	0	10	-01.55	085.55		PS00130 5
IDEN TRI-HF-5	2688	HF	0	10	01.50	086.11		PS00131 1
IDEN TRI-HF-10	2482	HF	0	10	00.08	087.58		PS00134 4
IDEN P-HF-7	3429	HF	0	10	07.06	082.32		PS00138 3
IDEN P-HF-14	3384	HF	0	10	04.28	081.36		PS00141 1
IDEN P-HF-17	3384	HF	0	10	05.38	082.51		PS00142 2
IDEN P-HF-18	2246	HF	0	10	06.51	083.17		PS00143 3
IDEN P-HF-21	2950	HF	0	10	08.32	085.45		PS00146 1
IDEN P-HF-23	2488	HF	0	10	08.27	084.27		PS00148 3
IDEN P-HF-27	2990	HF	0	10	07.42	085.43		PS00151 1
IDEN Y69-71P	2740	PC	14	20	00.06	086.29		PO00153 3
IDEN Y69-72P	2586	PC	40	47	01.01	087.27		PO00156 1
IDEN Y69-73P	2707	PC	26	32	01.27	087.56		PO00159 4
IDEN Y69-74P	2586	PC	26	33	02.02	088.19		PO00161 1
IDEN Y69-75M1	2198	MC	34	37	03.29	089.42		PO00163 3
IDEN Y69-76M1	2319	MC	19	22	01.00	092.01		PO00165 5
IDEN Y69-84M1	3748	MC	14	16	-03.59	091.40		PO00171 1
IDEN Y69-86M1	3245	MC	11	14	-01.59	091.40		PO00173 3
IDEN Y69-102P	2223	PC	10	17	-01.04	085.51		PO00176 1
IDEN Y69-103P	1808	PC	10	16	-00.05	082.26		PO00179 4
IDEN Y69-104M1	3892	MC	20	22	-02.18	081.31		PO00181 1
IDEN Y69-105P	3408	PC	10	12	00.09	084.03		PO00182 2
IDEN Y69-106P	2870	PC	18	24	02.59	086.33		PO00184 4
IDEN Y69-107M1	2716	MC	20	22	04.47	088.29		PO00187 2
IDEN Y69-108P	3390	PC	10	16	04.09	085.02		PO00188 3
IDEN Y69-109P	3721	PC	6	12	02.05	082.59		PO00190 5
IDEN Y69-110P	3083	PC	28	34	-00.13	081.06		PO00192 2
IDEN Y69-112P	3848	PC	16	16	03.30	078.57		PO00195 5
IDEN Y69-113M1	3816	MC	20	22	05.02	078.00		PO00198 3

APPENDIX II

Projected Factor Matrix - Oblique Projection
*FAST

Surface Sample	Factor 1 "tropical"	Factor 2 "solution"	Factor 3 "Peru Current"
PL 00005	.67225	.08382	.39461
PL 00009	.76793	.01085	.36564
PL 00019	.65618	.06086	.45674
PL 00021	.71148	.20134	.22490
PL 00027	.83963	.04078	.21922
PL 00029	.79146	.31026	-0.01080
PL 00047	1.00000	-0.00000	-0.00000
PL 00049	.83859	-0.02400	.29203
PL 00051	.36087	.35992	.46983
PL 00053	.77330	.26583	.04681
PL 00057	.66135	.26571	.24748
PL 00060	.91033	.07314	.08841
PL 00062	.55975	.57520	-0.07394
PL 00068	.82176	.24438	.02548
PL 00072	.87594	.10324	.08865
PL 00074	.86724	-0.01083	.24315
PL 00078	-0.07290	.75588	.48062
PL 00084	.54478	-0.29575	.77885
PL 00088	.75880	.19579	.14587
PL 00090	.71477	.24186	.16221
PL 00092	.41270	.36736	.43191
PL 00097	.86108	.19922	-0.00616
PL 00099	.82723	-0.06275	.34483
PL 00101	.91467	.10285	.04428
PL 00105	.00000	1.00000	-0.00000
PL 00110	.91615	-0.11268	.22669
PL 00112	.54206	.12009	.54986
PS 00124	.63129	.14904	.35085
PS 00129	.93585	-0.03811	.16987
PS 00130	.83819	.02197	.24127
PS 00131	.77364	.31606	.00546
PS 00134	.83994	.09010	.18376
PS 00138	.91361	-0.03180	.18568
PS 00141	.77155	.15185	.17681
PS 00142	.94486	-0.03174	.13721
PS 00143	.85259	.18107	.03486
PS 00146	.92187	-0.15767	.27041
PS 00148	.72449	.27912	.11800
PS 00151	.93577	-0.07460	.19437
PO 00153	.94901	-0.06918	.13298
PO 00156	.83719	.22909	-0.01265
PO 00159	.97066	.06767	-0.02323
PO 00161	.82194	.24552	.02144
PO 00163	.66625	.48024	-0.09171
PO 00165	.80442	.11005	.18332
PO 00171	.87011	.03225	.16813
PO 00173	.73973	-0.22872	.49683
PO 00176	.48073	.63667	.00189
PO 00179	.67251	.25415	.22603
PO 00181	.00000	.00000	1.00000
PO 00182	.96265	.01931	.05749
PO 00184	.83461	.15068	.10820
PO 00187	.26460	.75033	-0.00768
PO 00188	.11985	.88631	.06043
PO 00190	.82979	.18279	.08646
PO 00192	.51231	.22378	.47097
PO 00195	.78526	-0.04929	.39670

APPENDIX III

Projected Factor Matrix - Oblique Projection
Sub-surface *FAST

Core	Sample	Sample Depth (cm)	Preservation	FACTOR 1 "tropical"	FACTOR 2 "solution 2"	FACTOR 3 "Peru Current"	FACTOR 4 "solution 1"
V19-25	PL00047	10-13	2.5	1.00000	0	-0.00000	-0.00000
RC10-52	PL00105	18-22	1.5	0	.00000	0	1.00000
Y69-104M1	P000181	15-17	5.0	.30361	.00416	.88269	.00283
V19-30	PL04177	20-21	3.5	.30116	.28548	.64935	-0.11751
V19-30	PL04178	100-101	4.0	.47249	.29795	.57430	-0.16891
V19-30	PL04179	120-121	3.5	.10337	.26144	.66721	.04014
V19-30	PL04180	500-501	4.0	.00000	.00000	1.00000	.00000
V19-30	PL04181	720-721	3.0	-0.02744	.30361	.58476	.34726
V19-30	PL04182	1040-1041	3.0	-0.28966	.57683	.48547	.23203
V19-30	PL04183	1680-1681	3.5	.15175	.02583	.77052	.30449
Y69-71P	P004302	0-1	3.5	.81668	.41433	-0.01957	-0.15105
Y69-71P	P004303	60-61	4.0	.48063	.58290	.04283	-0.03505
Y69-71P	P004304	90-91	4.0	.29019	.75862	.17837	-0.17840
Y69-71P	P004305	150-151	4.0	.56718	.27102	.34753	.06395
Y69-71P	P004306	260-261	4.0	.26729	.71379	.17749	-0.01376
Y69-71P	P004307	380-381	3.0	.56732	.56285	.15538	-0.22960
Y69-71P	P004308	480-481	4.0	.17396	.57756	.44204	-0.27564
Y69-71P	P004345	580-581	4.0	.22552	.34305	.61801	-0.07808
Y69-71P	P004309	670-671	3.0	.15802	.68792	.04876	.27273
Y69-71P	P004310	730-731	3.0	.37297	.64072	-0.13546	.25471
Y69-71P	P004311	790-791	3.5	.27775	.98024	-0.19012	-0.06533
Y69-71P	P004312	890-891	4.0	.29187	.74966	.20135	-0.17747
Y69-71P	P004313	1000-1001	3.5	.00000	1.00000	.00000	.00000
Y69-73P	P004293	0-1	2.5	.92630	.15691	-0.09949	.02116
Y69-73P	P004294	60-61	3.5	.62826	.37628	-0.19092	.25402
Y69-73P	P004295	100-101	3.0	.56831	.20464	-0.03685	.41511
Y69-73P	P004296	160-161	3.0	.70685	.28505	.13666	.01105
Y69-73P	P004297	250-251	3.5	.44263	.70641	-0.11027	.07643
Y69-73P	P004298	340-341	4.0	.32546	.94343	-0.15736	-0.08294
Y69-73P	P004299	470-471	2.5	.78364	.05121	.27148	.11498
Y69-73P	P004300	500-501	2.5	.60500	.35140	.01731	.20205
Y69-73P	P004301	520-521	2.0	.37377	.59408	-0.19864	.28991
Y69-105P	P004156	0-1	2.0	.91490	.13440	.27654	-0.21263
Y69-105P	P004157	49-50	2.0	.73256	.35125	.15394	-0.14168
Y69-105P	P004158	109-110	2.5	.54494	.48803	.09462	-0.09814
Y69-105P	P004159	140-141	3.0	.54741	.01725	.59397	.09849
Y69-105P	P004160	309-310	3.0	.47683	.35146	.47685	-0.10039
Y69-105P	P004161	389-390	3.5	.30464	.83400	.13234	-0.24468
Y69-105P	P004162	461-462	3.5	.13281	.78507	.34545	-0.39215
Y69-105P	P004163	578-579	3.5	.14450	.39986	.64902	-0.08686
Y69-105P	P004164	719-720	3.5	.45938	.11923	.67035	.00052
Y69-106P	P004165	2-3	1.5	.76087	.43183	-0.09143	-0.04061
Y69-106P	P004166	9-10	1.5	.70508	.41685	-0.07957	.06461
Y69-106P	P004167	31-32	2.0	.60878	.45078	.03151	.07092
Y69-106P	P004168	41-42	2.0	.68862	.47752	.07641	-0.10931
Y69-106P	P004169	76-77	2.5	.36071	.88119	-0.18698	.00886
Y69-106P	P004170	92-93	2.0	.02611	.26116	.05145	.77404
Y69-106P	P004171	101-102	2.5	.46907	.71209	.01909	-0.08705
Y69-106P	P004172	124-125	2.5	.31630	.80289	.01691	-0.02551
Y69-106P	P004173	134-135	1.0	.55414	.33095	-0.07693	.32783
Y69-106P	P004174	149-150	2.5	.43632	.73590	-0.07529	-0.00044
Y69-106P	P004175	173-174	2.5	.35028	.90569	-0.12922	-0.08326
Y69-106P	P004176	208-210	2.0	.48373	.69168	-0.02376	-0.04537
Y69-106P	P004346	226-227	2.5	.37231	.58567	.04253	.18026
Y69-106P	P004347	239-240	3.5	.40903	.55234	.00159	.18858
Y69-106P	P004348	262-263	2.5	.53868	.49887	-0.01510	.11907
Y69-106P	P004349	290-291	2.5	.63235	.40555	.03813	.05598
Y69-109P	P004235	0-1	2.5	.84168	.35215	-0.06109	-0.07282
Y69-109P	P004238	60-61	1.5	.50753	.06453	.15713	.49960
Y69-109P	P004241	120-121	3.0	.63593	.26528	.06675	.23026
Y69-109P	P004248	240-24.	2.0	.50392	.46149	.01115	.20232
Y69-109P	P004254	360-361	3.0	.32676	.52944	-0.11168	.33479
Y69-109P	P004259	460-461	3.5	.63161	.08932	.44208	.10367
Y69-109P	P004264	560-561	3.5	.63051	-0.05100	.72979	-0.01454
Y69-109P	P004267	620-621	3.0	.60202	.19661	.29746	.15808
Y69-109P	P004272	720-721	3.5	.80438	.12668	.45497	-0.16773
Y69-109P	P004277	800-801	4.0	.36285	.60659	.07486	.09673

APPENDIX IV

Varimax Factor Matrix

sub-surface *CABFAC

	Sample	Communality	Factor 1 'tropical'	Factor 2 'Peru Current'	Factor 3 'solution 1'	Factor 4 'solution 2'
1	3947	.9661	.9689	.1521	.0638	.0056
2	3105	.9126	.5647	.1425	.7562	-0.0405
3	3181	.8691	.3598	.8460	.1458	.0512
4	4177	.8201	.3839	.8106	.0786	-0.0974
5	4178	.8750	.5238	.7672	.0428	-0.1007
6	4179	.7815	.2821	.8098	.1956	-0.0887
7	4180	.8548	.0516	.9111	.1328	.0658
8	4181	.8972	.3295	.7762	.4085	-0.1385
9	4182	.9039	.1065	.8307	.3546	-0.2771
10	4183	.8642	.3723	.7756	.3519	.0125
11	4302	.9441	.8755	.3747	.0252	-0.1912
12	4303	.8522	.7085	.5090	.1293	-0.2727
13	4304	.8926	.5097	.7081	.0633	-0.3568
14	4305	.9252	.7275	.5912	.1864	-0.1081
15	4306	.9364	.5558	.6956	.1741	-0.3367
16	4307	.8622	.6743	.5924	-0.0139	-0.2375
17	4308	.8100	.2845	.8185	-0.0287	-0.2414
18	4345	.8363	.3504	.8280	.1012	-0.1331
19	4309	.9506	.5989	.5899	.3594	-0.3387
20	4310	.9690	.7698	.4184	.3185	-0.3163
21	4311	.9501	.6290	.5478	.1476	-0.4822
22	4312	.9123	.5109	.7233	.0642	-0.3521
23	4313	.9444	.4144	.6969	.2092	-0.4932
24	4293	.9800	.9682	.1674	.0922	-0.0773
25	4294	.9735	.9008	.2279	.2725	-0.1891
26	4295	.9776	.8710	.2586	.3737	-0.1108
27	4296	.9317	.8424	.4369	.1312	-0.1177
28	4297	.9649	.7603	.4779	.2117	-0.3372
29	4298	.9574	.6554	.5569	.1330	-0.4471
30	4299	.9509	.8672	.4103	.1744	-0.0069
31	4300	.9652	.8512	.3812	.2574	-0.1703
32	4301	.8970	.7694	.3373	.3292	-0.2879
33	4156	.9138	.8479	.4397	-0.0322	-0.0253
34	4157	.8664	.7915	.4685	.0365	-0.1384
35	4158	.7749	.6894	.4982	.0794	-0.2125
36	4159	.8611	.6413	.6412	.1915	.0443
37	4160	.8999	.5817	.7316	.0929	-0.1331
38	4161	.9232	.5118	.7189	.0266	-0.3792
39	4162	.8813	.2516	.8285	-0.0783	-0.3543
40	4163	.8946	.2946	.8795	.1091	-0.1496
41	4164	.8877	.5417	.7561	.1490	-0.0194
42	4165	.9411	.8829	.3318	.0961	-0.2056
43	4166	.9703	.8876	.3409	.1649	-0.1979
44	4167	.9537	.8236	.4453	.1874	-0.2047
45	4168	.9476	.8100	.4900	.0738	-0.2144
46	4169	.9755	.7125	.5049	.1872	-0.4218
47	4170	.8959	.5745	.3404	.6502	-0.1649
48	4171	.9510	.7071	.5732	.1164	-0.3301
49	4172	.9539	.6320	.6146	.1733	-0.3831
50	4173	.9613	.8563	.2987	.3314	-0.1706
51	4174	.9423	.7237	.5151	.1730	-0.3511
52	4175	.9537	.6590	.5605	.1337	-0.4330
53	4176	.9397	.7297	.5280	.1377	-0.3308
54	4346	.9456	.7064	.5341	.2798	-0.2861
55	4347	.9163	.7281	.4817	.2730	-0.2822
56	4348	.9242	.7883	.4371	.2216	-0.2505
57	4349	.9020	.8068	.4246	.1720	-0.2030
58	4235	.9681	.9184	.3095	.0637	-0.1576
59	4238	.9563	.8144	.3347	.4238	-0.0369
60	4241	.9717	.8622	.3791	.2621	-0.1259
61	4248	.9477	.7982	.4392	.2692	-0.2123
62	4254	.9457	.7584	.3760	.3982	-0.2657
63	4259	.9060	.7466	.5598	.1875	-0.0144
64	4264	.9157	.6286	.7104	.1084	.0651
65	4267	.9342	.7832	.5121	.2310	-0.0722
66	4272	.9449	.7746	.5868	.0076	-0.0194
67	4277	.8869	.6712	.5561	.2218	-0.2790

APPENDIX V

*CABFAC Scaled Varimax Factor Scores

Code No.	Species	FACTOR 1 "tropical"	FACTOR 2 "Peru Current"	FACTOR 3 "solution 1"	FACTOR 4 "solution 2"
S 1	Actinomma antarcticum	.135	.227	-0.167	.280
S 2	Actinomma arcadophorum	.218	.024	.050	.025
S 3	Actinomma medianum	.172	.360	.221	.309
S 4	Actinomma sp.	.233	.132	-0.145	-0.214
S 5	Amphirhopalum ypsilon	.126	.261	.020	.070
S 7	Cenosphaera cristata	-0.080	.372	.208	.156
S 8	Collosphaera tuberosa	.205	.019	-0.167	-0.117
S 16	Euchitonia group	.558	.231	-0.213	.056
S 17	Heliodiscus asteriscus	.134	.062	.014	-0.095
S 20	Hexacontium entacanthum	.317	.987	-0.769	.099
S 21	Hymeniastrum euclides	.186	.496	.233	-0.117
S 22	Larcospira quadrangula	.335	.347	-0.468	-0.175
S 23	Lithelius minor	.454	1.149	.064	-0.120
S 29	Ommatartus tetrathalamus	1.901	-0.034	3.664	-2.886
S 32	Stylochlamydium venustum	.138	.565	-0.074	-0.100
S 33	Phorticium pylonium	.185	.799	-0.425	.184
S 37	Polysolenia murrayana	.002	1.121	.467	.950
S 38	Polysolenia spinosa	.217	.057	-0.014	.163
S 42	Siphonosphaera polysiphonia	.062	.323	-0.089	.138
S 43	Spirema sp.	-0.145	.555	.287	.261
S 45	Spongaster tetras	.208	.028	-0.179	-0.123
S 46	Spongocore puella	.017	.509	-0.242	-0.208
S 47	Spongopyle osculosa	-0.158	.727	.423	.215
S 50	Spongotrochus glacialis	.124	.562	.338	.624
S 52	Spongurus sp.	.097	.715	.149	.118
S 54	Stylodictya sp. A	.447	.454	-0.463	.186
S 55	Stylodictya sp. B	.145	.288	-0.224	.050
S 57	Tetrapyle octacantha group	7.224	.027	-0.575	1.244
S 58	Octopyle stenozoa	.121	.183	.210	.015
S 59	Hexacontium sp.	.006	.053	.600	.145
S 60	Thecosphaera sp.	-0.176	.820	5.898	.727
S 64	Larcopyle butschli	-0.048	.249	.124	.037
S 65	Druppatractus irregularis	.116	.174	.123	-0.278
N 69	Liriospyris cf. reticulata	.241	.047	-0.199	-0.151
N 72	Anthocyrtidium ophirense	.428	.115	-0.117	-0.353
N 73	Anthocyrtidium zanguebaricum	.344	.797	-0.313	-0.173
N 76	Carpocanium sp.	.225	.320	.315	-0.951
N 80	Conarachnium sp. A	-0.092	2.558	.281	1.028
N 82	Cornutella profunda	-0.080	.567	-0.776	-0.594
N 84	Dictyocephalus papillosus	-0.065	.254	.540	-0.177
N 86	Dictyophimus infabricatus	-0.350	1.863	.361	.232
N 88	Eucyrtidium acuminatum	.062	.710	-0.474	-0.385
N 90	Eucyrtidium hexagonatum	.186	1.187	-0.680	.129
N 91	Siphocampe aquilonaris	-0.029	.756	.602	.222
N 93	Lamprocyclas cf. L. havsi	-0.007	.399	.392	-0.248
N 94	Lamprocyclas maritales	.277	.411	.532	-0.084
N 95	Lamprocyclas polypora	-0.096	.364	.665	-0.053
N 96	Lamprocyclas ventricosa	.014	.185	.447	-0.332
N 97	Lithostrobus (?) seriatus	-0.026	1.802	-1.788	-0.366
N104	Pterocanium grandiporus	-0.076	.959	.063	-0.060
N107	Pterocanium eucolpum	-0.173	.755	-0.013	.140
N108	Pterocanium praetextum	.213	.073	-0.140	-0.462
N109	Pterocanium trilobum	.341	.440	-0.099	-0.228
N113	Stichopilium bicorne	-0.032	.658	-0.305	.157
N115	Theocalyptra davisiana	-0.495	4.360	.199	3.261
N117	Theoconus minythorax	.183	3.259	-0.766	-5.686
N123	Giraffospyris angulata	.728	-0.016	-0.372	-0.034
N124	Pholospyris scaphipes	-0.055	.640	-0.366	-0.195
N125	Rhodospyris sp.	.134	1.000	-0.258	.347

APPENDIX VI

Systematics Section

Most of the radiolarian species used in this study have been previously described elsewhere. It was attempted to reference the latest, most complete, species description and/or illustration available in the English language. Thus almost all the synonemies that are given in this section are incomplete. More extensive synonemies are presented in the species references cited. For each species a code number is given, preceded by an S or N, for spumellarian or nassellarian. This is the designation used for each species during the counting process and computer processing.

TAXONOMY

Order Polycystina Ehrenberg

Polycystina Ehrenberg, 1838, emend. Riedel, 1967, p. 291-298.

Suborder Spumellaria Ehrenberg, 1875

Family Collosphaeridae Müller, 1858 emend. Riedel 1971

Genus Collosphaera Müller 1855

Collosphaera tuberosa Haeckel 1887
S8

Collosphaera tuberosa Haeckel; Nigrini 1971, pl. 34. 1, fig. 1

Genus Disolenia Ehrenberg 1860

Disolenia quadrata (Ehrenberg)
S12

Disolenia quadrata (Ehrenberg); Nigrini, 1967, p. 19, pl. 1, fig. 5

Disolenia zanguebarica (Ehrenberg)
S13

Disolenia zanguebarica (Ehrenberg); Nigrini, 1967, p. 20, pl. 1, fig. 6

Genus Polysolenia Ehrenberg 1872

Polysolenia sp.
S34 Plate 1, fig. 1

Polysolenia (?); Riedel and Sanfilippo, 1971, p. 1608, pl. 1B, fig. 7-11

Polysolenia flammabunda (Haeckel)
S35

Polysolinia flammabunda (Haeckel); Nigrini, 1967, p. 15, pl. 1, fig. 2.

Polysolenia lappacea (Haeckel)
S36

Polysolenia lappacea (Haeckel); Nigrini, 1967, p. 16, pl. 1, fig. 3

Polysolenia murrayana (Haeckel)
S37

Polysolinia murrayana (Haeckel); Nigrini, 1968, pl. 1, figs. 1a, b

Polysolenia spinosa (Haeckel)
S38

Genus Siphonosphaera Müller 1858

Siphonosphaera polysiphonia Haeckel
S42

Siphonosphaera polysiphonia Haeckel; Nigrini, 1967, p. 18, pl. 1, figs. 4a, b

Otosphaera auriculata Haeckel
S30

Otosphaera auriculata Haeckel; Nigrini, 1967, p. 22, pl. 1, fig. 7

Otosphaera polymorpha Haeckel
S31

Otosphaera polymorpha Haeckel; Nigrini, 1967, p. 23, pl. 1, fig. 8

Genus Buccinosphaera Haeckel 1887

Buccinosphaera invaginata Haeckel
S6

Bucinosphaera invaginata Haeckel; Nigrini, 1971, pl. 34. 1, fig. 2

Family Actinommidae Haeckel 1862
emend. Riedel, 1967, p. 294

Genus Cenosphaera Ehrenberg 1854

Cenosphaera cristata Haeckel ?
S7 Plate 1, fig. 5

Cenosphaera cristata Haeckel ?; Riedel, 1958, p. 223, pl. 1, figs. 1, and 2

Genus Actinomma Haeckel 1862

Actinomma arcadophorum Haeckel
S2

Actinomma arcadophorum Haeckel; Nigrini, 1967, p. 29, pl. 2, fig. 3

Actinomma antarcticum (Haeckel)
S1

Actinomma antarcticum (Haeckel); Nigrini, 1967, p. 26, pl. 2, fig. 1

Actinomma medianum Nigrini
S3

Actinomma medianum Nigrini, 1967, p. 27, pl. 2, fig. 2

Actinomma sp.
S4 Plate 1, fig. 2

Actinomma sp. Benson, 1966, p. 164, pl. 5, fig. 6

Actinomma sp. Sachs, 1973, p. 137, pl. 2.1, fig. g

Genus Anomalacantha Loeblich and Tappan, 1961

Heteracantha dentata Mast
S19 Plate 1, fig. 9

Anomalacantha dentata (Mast); Benson, 1966, p. 170, pl. 5, figs. 10, 11

Genus Cladococcus Müller 1856

Cladococcus stalactites Haeckel
S66 Plate 1, fig. 3

Cladococcos stalactites Haeckel; Benson, 1966, p. 173, pl. 6, figs. 2, 3

Genus Cromyechinus Haeckel 1881

Cromyechinus antarctica (Dryer)
S9 Plate 1, fig. 4, a, b, c

Cromyechinus antarctica (Dryer); Petrushevskaya, 1968, p. 22, fig. 13 (I-VI), fig. 14 (I-VII)

Genus Druppatractus Haeckel 1887

Druppatractus irregularis Popofsky
S65 Plate 1, fig. 11a, b

Druppatractus irregularis Popofsky; Benson, 1966, p. 180, pl. 7, fig. 9-11

Genus Echinomma Haeckel 1881

Echinomma leptodermum Jörgensen
S14 Plate 1, fig. 7

Echinomma leptodermum Jörgensen; Hays, 1965, p. 169, pl. 1, fig. 2

Echinomma delicatulum (Dogiel)
S15 Plate 1, fig. 6

Echinomma delicatulum (Dogiel); Riedel, 1958, p. 225, pl. 1, fig. 6

Echinomma delicatulum (Dogiel); Petrushevskaya, 1968, p. 22, fig. 11, I-III

Echinomma delicatulum (Dogiel); Ling et al., 1971, p. 710, pl. 1, fig. 4

NOTE: In the course of this study it was observed that this species may be the same as Thecosphaera sp., and that because of a generally better preservation state of some specimens, the species was separated into two groups early in the study.

Genus Hexacontium Haeckel, 1882

Hexacontium entacanthum Jörgensen
S20 Plate 1, fig. 8

Hexacontium entacanthum Jörgensen; Benson, 1966, p. 149, pl. 3, figs. 13, 14

Hexacontium sp.
S59 Plate 2, fig. 2a, b

Hexacontium cf. heteracantha (Popofsky); Benson, 1966, p. 156, pl. 4, figs. 6-7

Actinomma sp. aff. Hexacontium arachnoidale Hollande et Enjumet; Petrushevskaya and Kozlova, 1972, p. 515, pl. 9, figs. 4-7.

Genus Stylatractus Haeckel

Stylatractus sp.
S53 Plate 1, fig. 10

Xiphatractus pluto (Haeckel), Benson, 1966, p. 184, pl. 7, figs. 14-17

Stylatractus sp. Petrushevskaya, p. 27, fig. 15, I-IV

Genus Styptosphaera

Styptosphaera ? spumacea Haeckel
S56

Styptosphaera ? spumacea Haeckel, Nigrini, 1970, p. 167, pl. 1, figs. 7, 8

Genus Thecosphaera Haeckel

Thecosphaera sp. ?
S60 Plate 2, fig. 1, a, b, c

Thecosphaera sp., Benson, 1966, p. 132, pl. 2, figs. 11-13

NOTE: In this category all spherical forms, with or without spines, with 1-3 concentric spherical shells, and generally strong pore bars were grouped together. As noted above, this grouping may have resulted in counting corroded specimens of E. delicatulum with this category.

Genus Haliomma Ehrenberg 1838

Haliomma sp. ?
S61

Haliomma erinaceum Haeckel; Popofsky, 1912, p. 102, pl. 4, fig. 1

Haliomma erinaceum Haeckel; Renz, 1973, pl. 2, fig. 4a, b

Genus Spongurus Haeckel 1861

Spongurus pylomaticus Riedel
S51 Plate 2, fig. 3

Spongurus pylomaticus Riedel, 1958, p. 226, pl. 1, fig. 10, 11

Spongurus pylomaticus Riedel; Petrushevskaya, 1968, p. 29, fig. 16, I, II

Spongurus pylomaticus Riedel; Ling et al., 1971, p. 711, pl. 1, fig. 5

Spongurus sp.
S52 Plate 2, fig. 4

Spongurus sp. Petrushevskaya, 1968, p. 30, fig. 16, III, fig. 26, I

Genus Astrosphaera Haeckel, 1887

Rhizoplegma ? boreale (Cleve)
S40

Rhizoplegma ? boreale (Cleve); Petrushevskaya, 1968, p. 12, fig. 8

Rhizoplegma ? boreale (Cleve); Ling et al., 1971, p. 710, pl. 1, fig. 2, 3

Subfamily Saturnalinae Deflandre 1953

Genus Saturnalis Haeckel, 1881,
emend Nigrini 1967

Saturnalis circularis Haeckel
S41

Saturnalis circularis Haeckel, Nigrini, 1967, p. 25, pl. 1, fig. 9

Subfamily Artiscinae Haeckel, 1881, emend Riedel, 1967

Genus Ommatartus Haeckel
emend Riedel, 1971

Ommatartus tetrathalamus coronatus (Haeckel)
S28

Panartus tetrathalamus coronatus Haeckel, Nigrini, 1970, p. 168, pl. 7, figs. 13-14

Ommatartus tetrathalamus tetrathalamus (Haeckel)
S29

Panartus tetrathalamus Haeckel, Nigrini, 1967, p. 30, pl. 2, fig. 4

Articiscinae incertae sedis, Riedel, 1971

Genus Cypassis Haeckel, 1887

Cypassis irregularis Nigrini
S11 Plate 2, fig. 5

Cypassis irregularis Nigrini, 1968, p. 53, pl. 1, fig. 2

Family Phacodiscidae Haeckel, 1881

Genus Heliodiscus Haeckel, 1862

Heliodiscus asteriscus Haeckel
S17

Heliodiscus asteriscus Haeckel; Nigrini, 1967, p. 32, pl. 3, figs. 1a, b

Heliodiscus echiniscus Haeckel
S18

Heliodiscus echiniscus Haeckel, Nigrini, 1967, p. 34, pl. 3, figs. 2a, b

Genus Hymeniastrum Ehrenberg 1847

Hymeniastrum euclides Haeckel
S21

Hymeniastrum euclides Haeckel; Benson, 1966, p. 222, pl. 12, figs. 1-3

Hymeniastrum euclides Haeckel; Ling and Anikouchine, 1967, p. 1488, pls. 191, 192, fig. 3

Family Spongodiscidae Haeckel, 1862, emend Riedel, 1967

Genus Amphirhopalum Haeckel
emend Nigrini, 1967

Amphirhopalum ypsilon Haeckel
S5

Amphirhopalum ypsilon Haeckel; Nigrini, 1967, p. 35, pl. 3, fig. 3 a, d

Amphirhopalum ypsilon Haeckel; Nigrini, 1971, p. 447, pl. 34. 1, fig. 7a, c

Genus Euchitonia Ehrenberg 1860

Euchitonia group
S16

NOTE: This group includes E. mülleri Haeckel and E. elegans (Ehrenberg) as discussed by Nigrini (1967) and Ling and Anikonchine (1967); a patagium may or may not be present.

Genus Ommatodiscus Stöhr, 1880

Ommatodiscus pantanellii Carnevale
S67 Plate 2, fig. 7

Ommatodiscus pantanellii Carnevale; Benson, 1966, p. 207, pl. 9, figs. 7-8, pl. 10, fig. 1, text fig. 12

Genus Spongaster Ehrenberg 1860

Spongaster tetras irregularis Nigrini
S44

Spongaster tetras irregularis Nigrini, 1967, p. 43, pl. 5, fig. 2

Spongaster tetras tetras Ehrenberg
S45

Spongaster tetras tetras Ehrenberg; Nigrini, 1967, p. 41, pl. 5, fig. 1a, b

Genus Spongocore Haeckel, 1887

Spongocore puella Haeckel
S46 Plate 2, fig. 6

Spongocore puella Haeckel; Nigrini, 1970, p. 168, pl. 2, fig. 2

Genus Spongotrochus Haeckel 1861

Spongotrochus glacialis Popofsky
S50 Plate 2, fig. 9

Spongotrochus ? glacialis Popofsky; Riedel, 1958, p. 227, pl. 2, figs. 1, 2, text fig. 1

Spongotrochus glacialis Popofsky, Petrushevskaya, 1968, p. 40, figs. 21, 22, 26 II

Genus Stylochlamydium Haeckel 1887

Stylochlamydium venustum (Bailey)
S32 Plate 2, fig. 8

Stylochlamydium venustum (Bailey); Petrushevskaya, 1968, p. 34, fig. 19, I-VI
Stylochlamydium venustum (Bailey); Ling et al., 1971, p. 711, pl. 1, figs. 7, 8

Genus Stylodictya Ehrenberg 1847

Stylodictya sp. A
S54 Plate 3, fig. 1

Stylodictya validispina Jörgensen; Petrushevskaya, 1968, p. 30, fig. 17, IV-V

Stylodictya aculeata Jörgensen; Petrushevskaya, 1968, p. 32, fig. 17, I-III

NOTE: Because of generally poor preservation, it was usually difficult to determine which of the two species above was present. However, they could always be distinguished from Stylodictya sp. B. (S55).

Stylodictya sp. B.
S55 Plate 3, fig. 2

Stylodictya sp. Petrushevskaya, 1968, p. 32, fig. 18, I-IV

Genus Stylotrochus Haeckel, 1862

Stylotrochus sp. A
S48 Plate 3, fig. 4, 5

NOTE: Disc-shaped, inner part of spongy framework has irregular concentric rings or possibly spiral convolutions, center thickened. Up to 30 smooth, pyramidal spines of variable size. These spines are outer prolongation of inner radial beams which may arise from the various inner concentric rings. From the edge of a V-shaped notch in the margin of the disc arise two strong spines, bladed at the base. This species is very rare.

Stylotrochus sp. B.
S49 Plate 3, fig. 3

NOTE: This species is similar to Stylotrochus sp. A, but the inner concentric rings are more clearly visible, and the spongy margin is much reduced. Three strong, bladed spines arise from the edge of a V-shaped notch in the margin. Rare.

Genus Spongopyle Dreyer, 1889

Spongopyle osculosa Dreyer
S47

Spongopyle osculosa Dreyer; Riedel, 1958, p. 225, pl. 1, fig. 12

Spongodiscus ? osculosus (Dreyer); Petrushevskaya, 1968, p. 39, fig. 20, I, II

Family Tholoniidae Haeckel, 1887

Genus Amphitholus Haeckel, 1887

Amphitholus sp. cf. acanthometra Haeckel
S27

Amphitholus acanthometra Haeckel; Benson, 1966, p. 258, pl. 17, figs. 4-7

NOTE: This species is very rare and the poor preservation made a definite determination of this species difficult.

Genus Cubotholus Haeckel, 1887

Cubotholus sp.
S10 Plate 3, fig. 6

Cubotholus cf. octoceras Haeckel; Benson, 1966, p. 260, pl. 17, fig. 8.

Family Pyloniidae Haeckel, 1882

Genus Tetrapyle Müller 1882

Tetrapyle octacantha Müller
S57 Plate 3, fig. 10a, b

Tetrapyle octacantha Müller; Benson, 1966, p. 245, pl. 15, fig. 3-10 pl. 16, fig. 1, text fig. 18

Genus Pylonium Haeckel, 1882

Pylonium sp.
S39 Plate 3, fig. 7

Pylonium sp., Benson, 1966, p. 250, pl. 16, fig. 2

NOTE: Because this species has two complete systems of dimensive girdles, it is considered to belong to the genus Pylonium. Benson (1966) gives a detailed description of this species and thinks it may be a variant of Tetrapyle octantha. Very rare.

Genus Octopyle Haeckel, 1882

Octopyle stenozoa Haeckel
S58 Plate 3, fig. 8

Octopyle stenozoa Haeckel; Benson, 1966, p. 251, pl. 16, figs. 3,4

Genus Phorticium Haeckel, 1882

Phorticium pylonium (Haeckel)
S33 Plate 3, fig. 9a, b

Phorticium pylonium (Haeckel) Cleve; Benson, 1966, p. 252, pl. 6, figs. 5-9, pl. 17, figs. 1-3.

Family Litheliidae Haeckel, 1861

Genus Lithelius Haeckel, 1861

Lithelius minor Jörgenson
S23 Plate 4, fig. 4

Lithelius minor Jörgensen; Benson, 1966, p. 262, pl. 17, figs. 9-10, pl. 18, figs. 1-4.

Lithelius nautiloides Popofsky
S24 Plate 4, fig. 1

Lithelius nautiloides Popofsky; Riedel, 1958, p. 228, pl. 2, figs. 3, 4, text fig. 2

Lithelius ? nautiloides Popofsky; Petrushevskaya, 1968, p. 50, figs. 27, 28, I; 29, I.

Lithelius ? riedeli Petrushevskaya
S25

Lithelius ? riedeli Petrushevskaya, 1968, p. 53, fig. 28, II; fig. 29, II.

Genus Larcospira Haeckel, 1887

Larcospira quadrangula Haeckel
S22 Plate 4, fig. 2

Larcospira quadrangula Haeckel; Benson, 1966, p. 266, pl. 18, figs. 7-8

Genus Spirema Haeckel, 1882

Spirema sp.
S43 Plate 4, fig. 3

Spirema sp., Benson, 1966, p. 268, pl. 18, figs. 9-10.

Family Pylodiscidae Haeckel, 1887

Genus Hexapyle Haeckel 1881

Hexapyle dodecantha Haeckel
S26 Plate 4, fig. 6

Hexapyle dodecantha Haeckel; Benson, 1966, p. 275, pl. 18, figs. 14-16, text fig. 20.

Family Larcopylidae Dreyer, 1889

Genus Larcopyle Dreyer, 1889

Larcopyle bütschlii Dreyer
S64 Plate 4, fig. 5

Larcopyle bütschli Dreyer; Benson, 1966, p. 280, pl. 19, figs. 3-5

Larcopyle sp. ?
S63

Larcopyle ? sp; Benson, 1966, p. 279, pl. 19, figs. 1-2

NOTE: The very rare occurrence and poor preservation precluded positive identification of this species.

Suborder Nassellaria Ehrenberg 1875

Family Plagoniidae Haeckel, 1881, emend. Riedel, 1967

Genus Helotholus Jörgensen, 1905

Helotholus histricosa Jörgensen
N92 Plate 4, fig. 8

Helotholus histricosa Jorgensen; Benson, 1966, p. 459, pl. 31, figs. 4-8.

Genus Antarctissa Petrushevskaya, 1968

Antarctissa denticulata (Ehrenberg)
N71 Plate 4, fig. 13

Antarctissa denticulata (Ehrenberg); Petrushevskaya, 1968, p. 84, fig. 49, I - IV.

Genus Lithomelissa Ehrenberg, 1847

Lithomelissa spp.
N102

NOTE: Both Benson (1966) and Petrushevskaya (1968) give a thorough treatment of this group. In the Panama Basin the genus is rare and for counting purposes all Lithomelissa species were grouped together in one category.

Genus Plectacantha Jorgensen, 1905

Plectacantha cremastoplegma Nigrini
N79

Plectacantha cremastoplegma Nigrini, 1968, p. 55, pl. 1, fig. 3

Family Acanthodesmiidae Haeckel, 1862
emend Riedel, 1971

Genus Dendrospyris Haeckel, 1881
emend. Goll, 1969

Dendrospyris (?) damaecornis (Haeckel)
N120

Triceraspyris damaecornis Haeckel; Nigrini, 1967, p. 46, pl. 5, fig. 5

Dendrospyris damaecornis (Haeckel): Goll, 1968, p. 1420, pl. 173, figs. 1-4.

Genus Dorcadospyris Haeckel, 1881
emend. Goll, 1968

Dorcadospyris sp.
N78

Ceratospyris sp., Nigrini, 1967, p. 48, pl. 5, fig. 6

Genus Giraffospyris Haeckel, 1881
emend. Goll, 1968

Giraffospyris angulata (Haeckel)
N123 Plate 4, fig. 7

Giraffospyris angulata (Haeckel); Goll, 1969, p. 331, pl. 59, figs. 4, 6, 7, 9

Genus Liriospyris Haeckel, 1881
emend. Goll, 1968

Liriospyris cf. reticulata (Ehrenberg)
N69

Amphispyris reticulata (Ehrenberg); Nigrini, 1967, p. 44, pl. 5, fig. 3

Amphispyris costata (Haeckel); Nigrini, 1967, p. 45, pl. 5, fig. 4

Liriospyris reticulata (Ehrenberg); Goll, 1968, p. 1429, pl. 176, figs. 9, 11, 13

NOTE: Because A. costata is basically similar to L. reticulata, and considering the generally poor preservation of Radiolaria in the Panama Basin, these two species could not always be easily separated. Thus, to facilitate counting, these two species were grouped together in one category.

Genus Tholospyris Haeckel, 1881
emend. Goll, 1968

Tholospyris scaphipes (Haeckel)
N124

Tholospyris scaphipes (Haeckel); Goll, 1969, p. 328, pl. 58, figs. 1-8, 13, 14

Triceraspyris sp. cf. T. antarctica (Haeckel)
N121 Plate 4, fig. 9

Triceraspyris antarctica (Haeckel); Riedel, 1958, p. 230, pl. 2, fig. 6, 7

Triceraspyris (?) antarctica (Haeckel); Petrushevskaya, 1968, p. 62, fig. 37, I-III

NOTE: This species is very rare and the poor preservation of the few observed specimens, precluded definite identification as T. antarctica.

Dendrospyris cf D. anthocyrtoides (Bütschli)
N126 Plate 4, fig. 14

Desmospyris anthocyrtoides (Bütschli); Benson, 1966, p. 332, pl. 23, figs. 6-8

Dendrospyris stabilis Goll, 1968, p. 1422, pl. 173, figs. 16-18, 20

NOTE: This species is very similar to those illustrated by Benson and Goll. D. stabilis, illustrated by Goll, appears to have identical morphology with D. anthocyrtoides illustrated by Benson. Because this species is rare, no conscious effort was made to further investigate this species.

Genus Rhodospyris Haeckel, 1882

Rhodospyris sp.
N125 Plate 4, fig. 12a, b

Rhodospyris sp.; Benson, 1966, p. 329, pl. 23, fig. 3-5

Genus Nephrodictyum Haeckel, 1882

Nephrospyris renilla Haeckel
N129 Plate 4, fig. 1

Nephrodictyum renilla Haeckel; Benson, 1966, p. 302, pl. 21, fig. 5

Family Carpocaniidae Haeckel, 1881
emend. Riedel, 1967

Genus Carpocanium Ehrenberg, 1847

Carpocanium sp. A.
N76

Carpocanium sp. A.; Nigrini, 1968, p. 55, pl. 1, fig. 4

Family Theoperidae Haeckel, 1881
emend. Riedel, 1967

Genus Cyrtopera Haeckel, 1881

Cyrtopera languncula Haeckel
N83

Cyrtopera languncula Haeckel, 1887, p. 1451, pl. 75, fig. 10

Genus Dictyophimus Ehrenberg, 1847
emend. Nigrini, 1967, 1968

Dictyophimus crisiae Ehrenberg
N85

Dictyophimus crisiae Ehrenberg; Nigrini, 1967, p. 66, pl. 6, fig. 7

Dictyophimus infabricatus Nigrini
N86 Plate 4, fig. 11

Dictyophimus infabricatus Nigrini, 1968, p. 56, pl. 7, fig. 6

Dictyophimus mawsoni Riedel
N87

Dictyophimus mawsoni Riedel, 1958, p. 234, pl. 3, figs. 6, 7

Dictyophimus gracilipes Bailey
N106 Plate 4, fig. 2

Dictyophimus gracilipes Bailey; Benson, 1966, p. 382, pl. 25, figs. 4-6

NOTE: This is a small species, which is very rare in the Panama Basin sediments. At the beginning of this study, the description given by Benson was followed to recognize this species. Petrushevskaya (1968) has given a more elaborate treatment to the genus Dictyophimus and it is likely that other Dictyophimus species were counted with this species.

Genus Eucyrtidium Ehrenberg, 1847
emend. Nigrini, 1967

Eucyrtidium acuminatum (Ehrenberg)
N88

Eucyrtidium acuminatum (Ehrenberg); Nigrini, 1967, p. 81, pl. 8, fig. 3

Eucyrtidium anomalum Haeckel
N89 Plate 4, fig. 16

Eucyrtidium anomalum Haeckel; Benson, 1966, p. 496, pl. 34, figs. 4, 5

Eucyrtidium hexagonatum Haeckel
N90

Eucyrtidium hexagonatum Haeckel; Nigrini, 1967, p. 83, pl. 8, fig. 4

Genus Eucecryphalus Haeckel, 1861

Eucecryphalus sp.
N122 Plate 4, fig. 10

Eucecryphalus sp., Benson, 1966, p. 450, pl. 30, fig. 6, 7

Genus Lithopera Ehrenberg, 1847

Lithopera bacca Ehrenberg
N100

Lithopera bacca Ehrenberg; Nigrini, 1967, p. 54, pl. 6, fig. 2

Genus Lithostrobus Butschli, 1882

Lithostrobus sp. cf. L. hexagonalis Haeckel
N101

Lithostrobus sp. cf. L. hexagonalis Haeckel; Nigrini, 1968, p. 58, pl. 1, fig. 10

Lithostrobus (?) seriatus Haeckel
N97 Plate 4, fig. 15 a, b

Siphocampium cf. seriatus Haeckel; Benson, 1966, p. 521, pl. 35, figs. 12, 13

Lithostrobus (?) seriatus Haeckel; Petrushevskaya, 1968, p. 143, fig. 82, I-IV.

Genus Lithocampe Ehrenberg, 1838

Lithocampe sp.
N99

Lithocampe sp., Nigrini, 1967, p. 87, pl. 8, fig. 6

Genus Pterocanium Ehrenberg, 1847

Pterocanium grandiporus Nigrini
N104

Pterocanium grandiporus Nigrini, 1968, p. 57, pl. 1, fig. 7

Pterocanium praetextum praetextum (Ehrenberg);
N108

Pterocanium praetextum praetextum (Ehrenberg); Nigrini, 1967, p. 68, pl. 7, fig. 1

Pterocanium praetextum eucolpum Haeckel
N107

Pterocanium praetextum eucolpum Haeckel; Nigrini, 1967, p. 70, pl. 7, fig. 2

Pterocanium trilobum (Haeckel)
N109

Pterocanium trilobum (Haeckel); Nigrini, 1967, p. 71, pl. 7, fig. 3

Pterocanium sp. A
N127 Plate 5, fig. 3

NOTE: Cephalis subspherical with few, subcircular, well separated pores, bearing a conical horn of approximately twice the length. Thorax subglobular, rough, with large rounded pores. Peristome constricted. Feet approximately same length

as thorax or longer, triangular pyramidal, curving outward in the proximal portion, almost straight distally, slightly divergent. Traces of the abdomen are preserved on lower edge of the thorax. This is a rather large and robust species. Rare.

Genus Stichopilium Haeckel, 1881

Stichopilium bicorne Haeckel
N113 Plate 5, fig. 8

Stichopilium bicorne Haeckel; Benson, 1966, p. 422, pl. 29, figs. 1, 2

Genus Theocalyptra Haeckel, 1887

Theocalyptra bicornis (Popofsky)
N114 Plate 5, fig. 4a, b

Theocalyptra (?) bicornis (Popofsky); Petrushevskaya, 1968, p. 124, fig. 71, II-VII
fig. 72, I-IV

Theocalyptra bicornis (Popofsky); Sachs, 1973, p. 174, pl. 2.5, figs. n, o

Theocalyptra davisiana (Ehrenberg)
N115 Plate 5, fig. 5a, b

Theocalyptra davisiana (Ehrenberg); Riedel, 1958, p. 239, pl. 4, figs. 2-3, text fig. 10

Cycladophora davisiana Ehrenberg; Petrushevskaya, 1968, p. 120, fig. 69, I-VII

Family Pterocoryidae Haeckel, 1881
emend. Riedel, 1967

Genus Anthocrytidium Haeckel, 1881

Anthocyrtidium ophirense (Ehrenberg)
N72

Anthocyrtidium ophirense (Ehrenberg); Nigrini, 1967, p. 56, pl. 6, fig. 3

Anthocyrtidium zanguebaricum (Ehrenberg)
N73

Anthocyrtidium zanguebaricum (Ehrenberg); Nigrini, 1967, p. 58, pl. 6, fig. 4

Genus Conarachnium Haeckel, 1881

Conarachnium (?) sp. A
N80 Plate 5, fig. 7

Conarachnium (?) sp. A,; Nigrini, 1968, p. 56, pl. 1, fig. 5

Conarachnium (?) sp. B
N81 Plate 5, fig. 6

NOTE: This species is very similar to Conarachnium sp. A. A is different in having a much larger thorax with >10 pores in a vertical series and >8 on a half equator. This species was observed in assemblages further to the south of the Panama Basin off the coast of Peru, and thought to be characteristic to the Peru Current fauna. In the Panama Basin it is very rare, which may be due to its susceptability to solution. Because of its rarity in the surface samples, it was grouped together with Conarachnium sp. A in category N80 for the surface and stratigraphic analysis.

Genus Lamprocyclas Haeckel, 1881
sens. emend. Nigrini, 1967

Lamprocyclas maritales maritales Haeckel
N94

Lamprocyclas maritales maritales Haeckel; Nigrini, 1967, p. 74, pl. 7, fig. 5

Lamprocyclas maritales polypora Nigrini
N95

Lamprocyclas maritales polypora Nigrini, 1967, p. 76, pl. 7, fig. 6

Lamprocyclas maritalis ventricosa Nigrini
N96

Lamprocyclas maritales ventricosa Nigrini, 1968, p. 57, pl. 1, fig. 9

Lamprocyclas cf. L. haysi Kling
N93

Lamprocyrtis haysi Kling, 1973, pl. 5, figs. 15-16; pl. 15, figs. 1-3

NOTE: When Kling (1973) created the new genus Lamprocyrtis he remarked that the genus was difficult to characterize because of rather marked differences between initial and latest members of the lineage which were accomodated by this genus. Considering these difficulties, it was decided to retain this species within the genus Lamprocyclas.

Genus Pterocorys Haeckel, 1881

Pterocorys hirundo Haeckel
N105

Pterocorys hirundo Haeckel; Riedel, 1958, p. 238, pl. 3, fig. 11, pl. 4, fig. 1, text fig. 9

Pterocorys hirundo Haeckel; Ling et al., 1971, p. 715, pl. 2, figs. 8-10

Genus Theoconus Haeckel, 1887

Theoconus hertwigii (Haeckel)
N116

Theoconus hertwigii (Haeckel): Nigrini, 1967, p. 73, pl. 6, fig. 4

Theoconus minythorax Nigrini
N117 Plate 5, fig. 9

Theoconus zancleus (Müller); Benson, p. 482, pl. 33, fig. 5

Theoconus minythorax Nigrini, 1968, p. 57, pl. 1, fig. 8

Genus Theocorythium Haeckel, 1887

Theocorythium trachelium trachelium (Ehrenberg)
N119

Theocorythium trachelium trachelium (Ehrenberg); Nigrini, 1967, p. 79, pl. 8, fig. 2, pl. 9, fig. 2

Theocorythium trachelium dianae (Haeckel)
N118

Theocorythium trachelium dianae (Haeckel); Nigrini, 1967, p. 77, pl. 8, fig. 1a, b, pl. 9, fig. 1a, b

Family Artostrobiidae Riedel, 1967

Genus Artostrobus Haeckel, 1887

Artostrobus annulatus (Bailey)
N70

Artostrobus annulatus (Bailey); Riedel, 1958, p. 241, pl. 4, fig. 6

Artostrobus annulatus (Bailey); Petrushevskaya, 1968, p. 98, fig. 56, I-V

Artostrobus annulatus (Bailey); Ling et al., 1971, p. 715, pl. 2, fig. 11

Genus Dictyocryphalus Haeckel, 1881

Dictyocryphalus papillosus (Ehrenberg)
N84

Dictyocryphalus papillosus (Ehrenberg); Nigrini, 1967, p. 63, pl. 6, fig. 6

Genus Lithomitra Butschli, 1882

Lithomitra arachnea (Ehrenberg)
N98

Lithomitra arachnea (Ehrenberg); Riedel, 1958, p. 242, pl. 4, figs. 7, 8

Lithomitra arachnea (Ehrenberg); Ling et al., 1971, p. 716, pl. 2, figs. 13, 14

Lithomitra sp.
N128

Lithomitra infundibulum Haeckel; Benson, 1966, p. 502, pl. 34, figs. 10-12

NOTE: This species is very similar to L. infundibulum as illustrated by Benson. The first abdominal joint is larger than illustrated by Benson, and conical only in its upper part towards the thorax.

Genus Siphocampe Haeckel, 1881

Siphocampe aquilonaris (Bailey)
N91

Lithocampe (?) aquilonaris (Bailey); Petrushevskaya, 1968, p. 138, fig. 79, I-III

Siphocampe aquilonaris (Bailey): Ling et al., 1971, p. 716, pl. 2, fig. 12

Siphocampe corbula (Harting)
N111

Siphocampe corbula (Harting); Nigrini, 1967, p. 85, pl. 8, fig. 5, pl. 9, fig. 3

Genus Spirocyrtis Haeckel, 1881

Spirocyrtis scalaris Haeckel
N112

Spirocyrtis scalaris Haeckel; Nigrini, 1967, p. 88, pl. 8, fig. 7; pl. 9, fig. 4

Genus Cornutella Ehrenberg, 1838
emend. Nigrini, 1967

Cornutella profunda Ehrenberg
N82

Cornutella profunda Ehrenberg; Nigrini, 1967, p. 60, pl. 6, figs. 5a, b, c

Genus Peripyramis Haeckel, emend. Riedel, 1958

Peripyramis circumtexta Haeckel
N103

Peripyramis circumtexta Haeckel; Riedel, 1958, p. 231, pl. 2, figs. 8, 9

Family Cannobotryidae Haeckel, 1881 emend. Riedel, 1967

Genus Botryocyrtis Ehrenberg, 1860

Botryocyrtis scutum (Harting)
N75

Botryocyrtis scutum (Harting); Nigrini, 1967, p. 52, pl. 6, figs. 1a, b, c

Genus Centrobotrys Petrushevskaya, 1965

Centrobotrys thermophila Petrushevskaya
N77

Centrobotrys thermophila Petrushevskaya; Nigrini, 1967, p. 49, pl. 5, fig. 7; text fig. 26

Genus Saccospyris Haecker, 1907 emend. Petrushevskaya, 1968

Saccospyris antarctica Haecker
N74 Plate 4, fig. 17

Saccospyris antarctica Haecker; Petrushevskaya, 1968, p. 149, fig. 85, II

Saccospyris conithorax Petrushevskaya
N110

Saccospyris conithorax Petrushevskaya, Petrushevskaya, 1965, p. 150, fig. 85, I

REFERENCES TO TAXONOMY

Benson, R.N. 1966. Recent Radiolaria from the Gulf of California. unpubl. Ph. D. thesis, University of Minnesota, 578 numb. leaves. (University Microfilms #66-12, 189).

Goll, R.M. 1968. Classification and phylogeny of Cenozoic Trissocyclidae (Radiolaria) in the Pacific and Caribbean basins, Part I. J. Paleontology 42(6):1409-1432.

Goll, R.M. 1969. Classification and phylogeny of Cenozoic Trissocyclidae (Radiolaria) in the Pacific and Caribbean basins, Part II. J. Paleontology 43(2):322-339.

Haeckel, E. 1887. Report on the Radiolaria collected by H.M.S. Challenger during the years 1873-1876. Rept. Voyage Challenger, Zool. 18, Pt. I, II. Edinburgh. 1803 p.

Hays, J.D. 1965. Radiolaria and late Tertiary and Quaternary history of Antarctic Seas. In: Biology of the Antarctic Seas. II, Am. Geophys. Union, Antarctic Res. Ser. 5:125-184.

Ling, H.Y., C.J. Stadum and M.L. Welch. 1971. Polycystine Radiolaria from Bering Sea surface sediments. Proc. II planktonic conference, Rome 1970, A. Farinacci, ed., p. 705-729.

Ling, Hsin-Yi and W.A. Anikouchine. 1967. Some spumellarian Radiolaria from the Java, Philippine, and Mariana Trenches. J. Paleontology 41(6):1481-1491.

Nigrini, C.A. 1971. Radiolarian zones in the Quaternary of the equatorial Pacific Ocean. In: "Micropaleontology of Oceans", B.M. Funnell and W.R. Riedel, eds., Cambridge University Press. p. 443-461.

Nigrini, C.A. 1970. Radiolarian assemblages in the North Pacific and their application to a study of Quaternary sediments in core V20-130. Geol. Soc. Am. Memoir 126:139-183.

Nigrini, C.A. 1968. Radiolaria from eastern tropical Pacific sediments. Micropaleontology 14(1):51-63.

Nigrini, C.A. 1967. Radiolaria in pelagic sediments from the Indian and Atlantic Oceans. Bull. Scripps Inst. Oceanog. 11:1-125.

Petrushevskaya, M.G. 1968. Radiolarians of orders Spumellaria and Nanellaria of the Antarctic region (from material of the Soviet Antarctic Expedition). In: "Biological reports of the Soviet Antarctic Expedition (1955-1958), Vol. 3, A.P. Andriyashev and P.V. Ushakov, eds., translated from Russian, Israel Program for Scientific Translations, Jerusalem, 1968; p. 2-186.

Petrushevskaya, M.G. and G.E. Kozlova. 1972. Radiolaria: Leg 14, Deep Sea Drilling Project. In: Hayes, D.E., Pimm, A.C. et al., 1972, Initial Reports of the Deep Sea Drilling Project, Vol. XIV, Washington (U.S. Govt. Printing Office); p. 495-648.

Popofsky, A. 1912. Die Sphaerellarien des Warm wassergebietes, 1. Deutsche Südpolar-Expedition 1901-1903, Vol. 13 (Zool., Vol. 5) (2):73-159.

Renz, G.W. 1973. The distribution and ecology of Radiolaria in the Central Pacific plankton and surface sediments. unpubl. Ph.D. thesis, University of California, San Diego, 251 numb. leaves.

Riedel, W.R. 1971. Systematic classification of polycystine Radiolaria. In: "The Micropaleontology of Oceans", B.M. Funnell and W.R. Riedel, eds., Cambridge University Press; p. 649-661.

Riedel, W.R. 1958. Radiolaria in Antarctic sediments. B.A.N.Z.A.R.E. reports, ser. B., 6(10):217-255.

Riedel, W.R. 1967. Class Actinopoda, Protozoa. In: "The Fossil Record", a symposium with documentation, Geol. Soc. London; p. 291-298.

Riedel, W.R. and A. Sanfilippo. 1971. Cenozoic Radiolaria from the western tropical Pacific, Leg 7, Deep Sea Drilling Project. In: Winterer, E.L., Riedel, W.R. et al., 1971. Initial Reports of the Deep Sea Drilling Project, Vol. VII, Washington (U.S. Govt. Printing Office); p. 1529-1672.

Sachs, H.M. 1973. Quantitative Radiolaria-based paleo-oceanography in late Pleistocene subarctic Pacific sediments. unpubl. Ph.D. thesis, Brown University, 208 numb. leaves.

Plate 1

Figure		Magnification
1	Polysolenia sp; Y69-71P, 14-20 cm	128X
2	Actinomma sp; Y69-73P, 470-471 cm	128X
3	Cladococcus stalactites Haeckel; Y69-104 M1, 15-17 cm	128X
4a	Cromyechinus antarctica (Dryer); Y69-104 M1, 15-17 cm	128X
4b, c	Cromyechinus antarctica (Dryer); Y69-105P, 309-310 cm	128X
5	Cenosphaera cristata Haeckel ?; Y69-104 M1, 15-17 cm	150X
6	Echinomma delicatulum (Dogiel); RC10-252, 10-13 cm	150X
7	Echinomma leptodermum Jörgensen; V19-30, 1680-1681 cm	128X
8	Hexacontium entacanthum Jörgensen; Y69-116P, 18-24 cm	128X
9	Heteracantha dentata Mast; Y69-104 M1, 15-17 cm	128X
10	Stylatractus sp.; RC10-52, 18-22 cm	128X
11	Druppatractus irregularis Popofsky, V24-35, 10-13 cm	150X

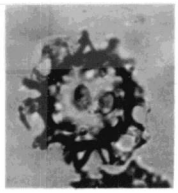

1

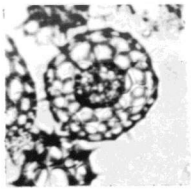

2

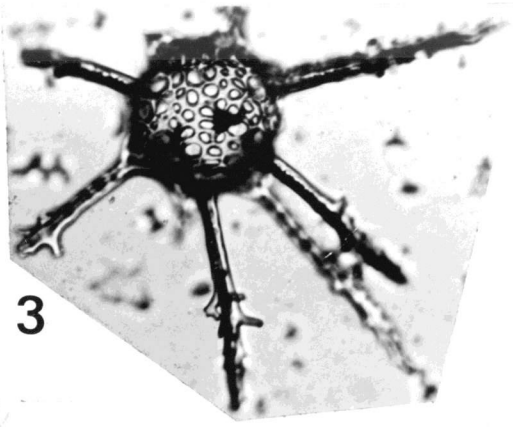

3

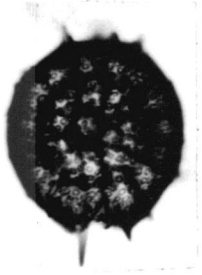

4a

4b

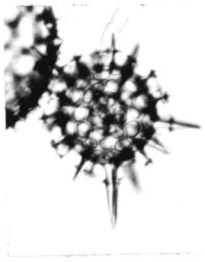

4c

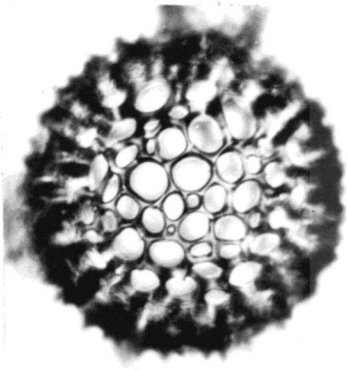

5

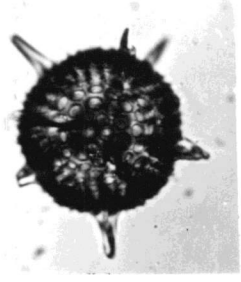

6

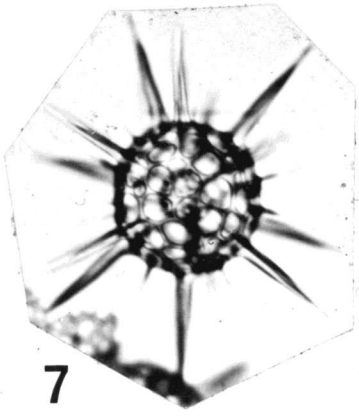

7

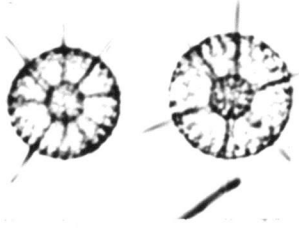

8

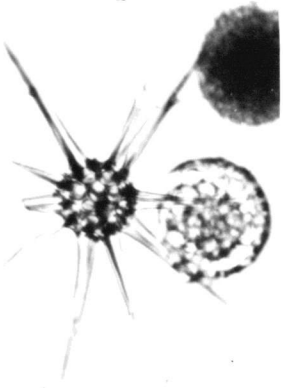

9

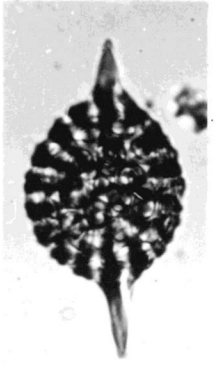

10

11a

11b

Plate 2

Figure		Magnification
1a, b, c	Thecosphaera sp.; RC10-52, 18-22 cm	128X
2a	Hexacontium sp.; RC10-52, 18-22 cm	150X
2b	Hexacontium sp.; V21-217, 13-16 cm	128X
3	Spongurus pylomaticus Riedel; V19-30, 720-721 cm	150X
4	Spongurus sp.; RC10-252, 10-13 cm	150X
5	Cypassis irregularis Nigrini; Y69-104 M1, 15-17 cm	150X
6	Spongocore puella Haeckel; RC10-252, 10-13 cm	150X
7	Ommatodiscus pantanellii Carnevale; V24-35, 10-13 cm	150X
8	Stylochlamydium venustum (Bailey); Y69-104 M1, 15-17 cm	212X
9	Spongotrochus glacialis Popofsky; V19-30, 720-721 cm	212X

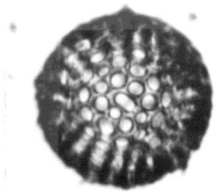

1a

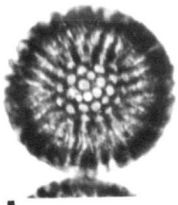

1b

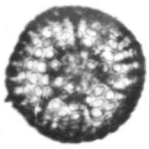

1c

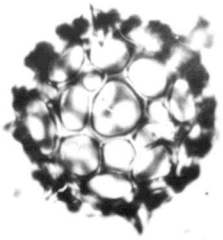

2a

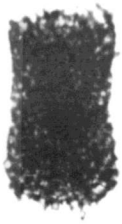

3

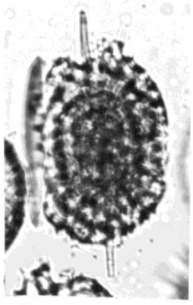

4

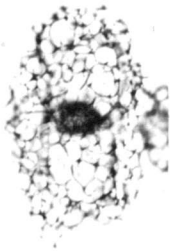

5

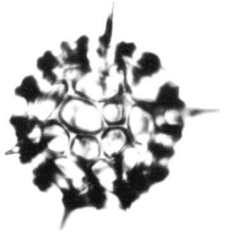

2b

6

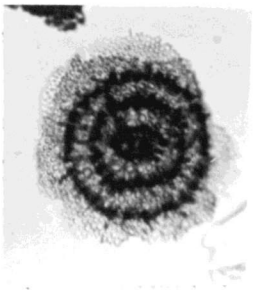

7

9

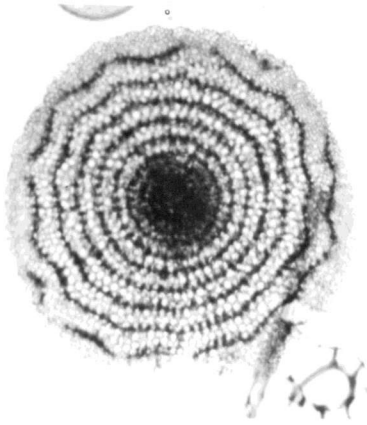

8

Plate 3

Figure		Magnification
1	Stylodictya sp. A; V24-35, 10-13cm	212X
2	Stylodictya sp. B; V19-25, 10-13 cm	212X
3	Stylotrochus sp. B; V24-35, 10-13 cm	212X
4	Stylotrochus sp. A; V15-13, 11-14 cm	212X
5	Stylotrochus sp. A; V19-30, 20-21 cm	150X
6	Cubotholus sp.; Y69-107 M1, 20-22 cm	128X
7	Pylonium sp.; Y69-71P, 14-20 cm	128X
8	Octopyle stenozoa Haeckel; RC8-102, 7-10 cm	150X
9a,b	Phorticium pylonium (Haeckel); V19-30, 500-501 cm	150X
10a,b	Tetrapyle octacantha Müller; RC8-102, 7-10 cm	150X

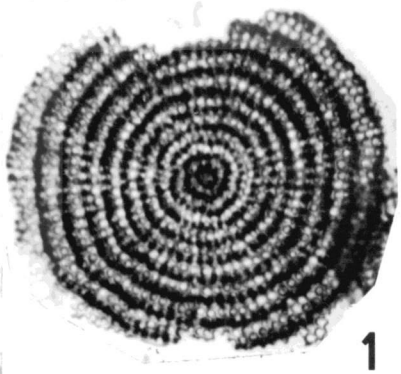

1

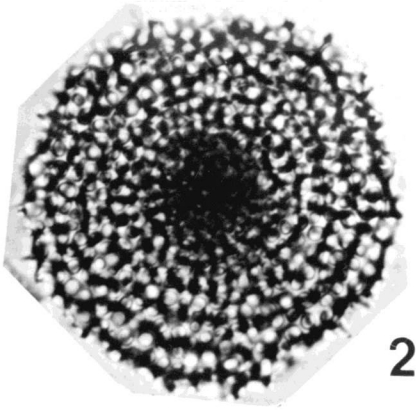

2

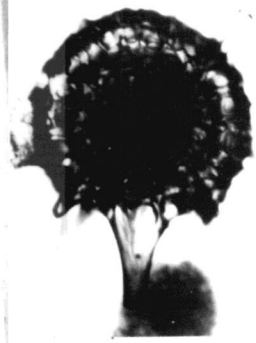

3

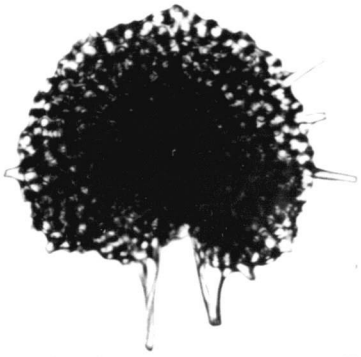

4

5

6

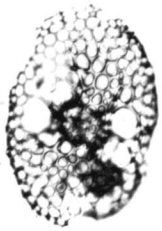

7

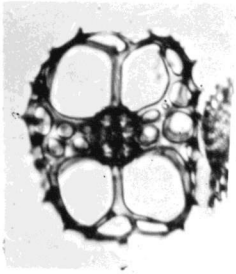

8

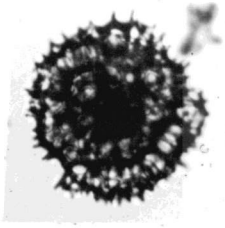

9 a

10 b

10 a

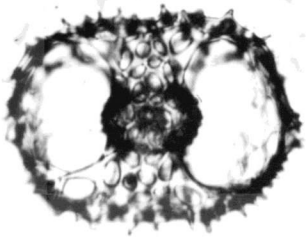

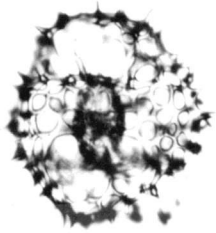

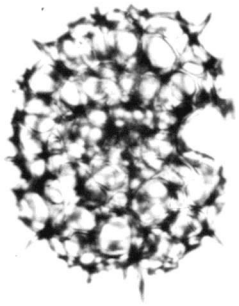

9 b

Plate 4

Figure		Magnification
1	Lithelius nautiloides Popofsky; V19-30, 500-501 cm	212X
2	Larcopyle quadrangula Haeckel; RC8-102, 7-10 cm	150X
3	Spirema sp.; Y69-104 M1, 15-17 cm	212X
4	Lithelius minor Jörgensen; Y69-104 M1, 15-17 cm	212X
5	Larcopyle bütschli Dreyer; V24-35, 10-13 cm	212X
6	Hexapyle dodecantha Haeckel; V24-35, 10-13 cm	150X
7	Giraffospyris angulata (Haeckel); RC8-102, 7-10 cm	212X
8	Helotholus histricosa Jörgensen; Y69-104 M1, 15-17 cm	150X
9	Triceraspyris sp. cf. T. antarctica (Haeckel); V19-30, 1680-1681 cm	150X
10	Eucecryphalus sp.; Y69-104 M1, 15-17 cm	212X
11	Dictyophimus infabricatus Nigrini; Y69-104 M1, 15-17 cm	212X
12a	Rhodospyris sp.; V19-30, 20-21 cm	212X
12b	Rhodospyris sp.; V19-30, 500-501 cm	212X
13	Antarctissa denticulata (Ehrenberg) V19-30, 500-501 cm	150X

Plate 4 (continued)

Figure		Magnification
14	Dendrospyris cf. D. anthocyrtoides (Bütschli); RC8-102, 7-10 cm	150X
15a, b	Lithostrobus (?) seriatus Haeckel, Y69-86 M1, 11-14 cm	150X
16	Eucyrtidium anomalum Haeckel, Y69-86 M1, 11-14 cm	128X
18	Saccospyris antarcticum Haeckel, V19-30, 500-501 cm	150X

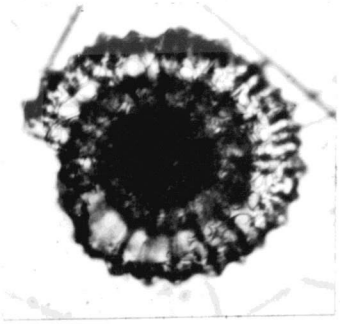
1

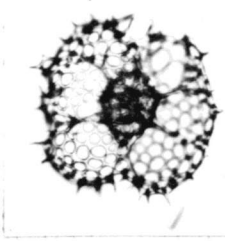
2

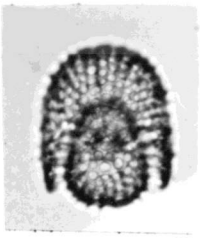
3


4

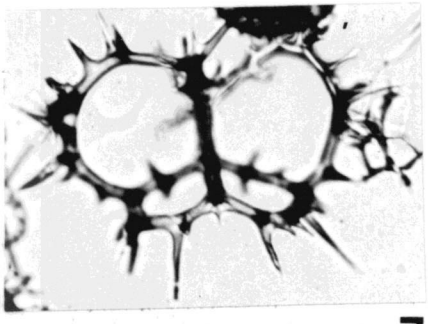
7

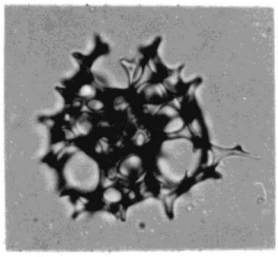
6

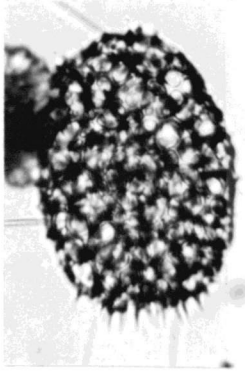
5

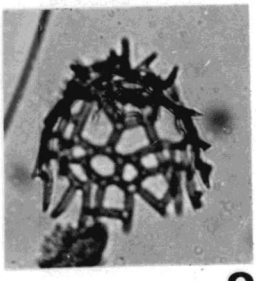
8


9

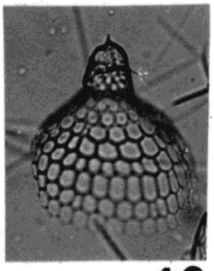
10

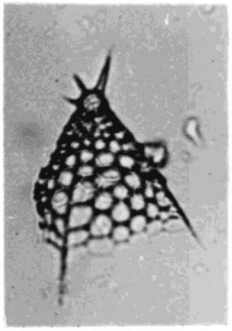
11

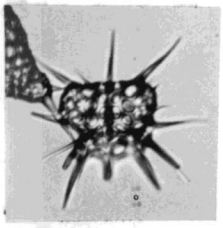
12 a


13

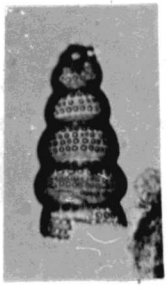
15 a

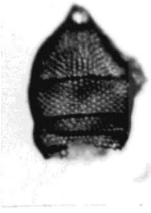
16

17

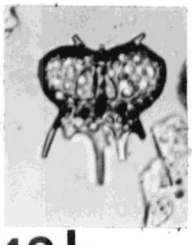
12 b

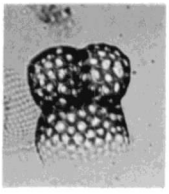
14


15 b

Plate 5

Figure		Magnification
1	Nephrospyris renilla Haeckel; Y69-104 M1, 15-17 cm	150X
2	Dictyophimus gracilipes Bailey; Y69-104 M1, 15-17 cm	150X
3	Pterocanium sp. A; Y69-71P, 0-1 cm	212X
4	Theocalyptra bicornis (Popofsky); V19-30, 500-501 cm	150X
5	Theocalyptra davisiana (Ehrenberg); V21-29, 12-14 cm	150X
6	Conarachnium sp. B.; V19-30, 500-501 cm	212X
7	Conarachnium sp. A.; Y69-104 M1, 15-17 cm	212X
8	Stichopilium bicorne Haeckel; Y69-104 M1, 15-17 cm	150X
9	Theoconus minythorax Nigrini; RC8-102, 7-10 cm	212X
10	Lithomitra sp.; V24-35, 10-13 cm	150X

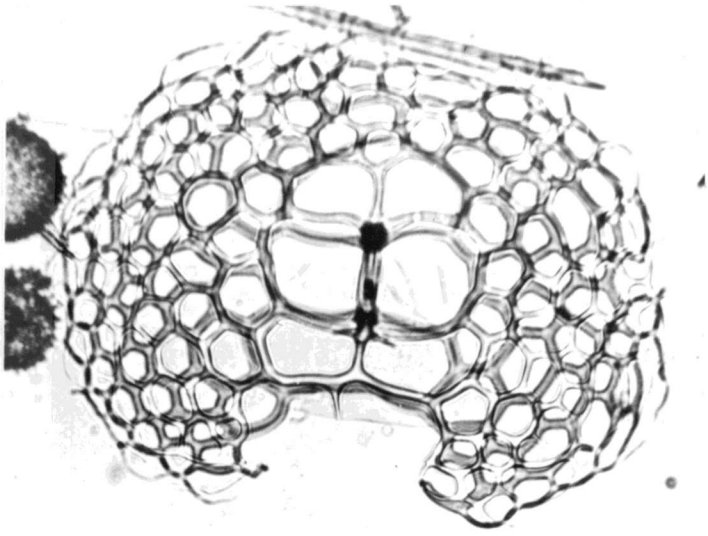

1

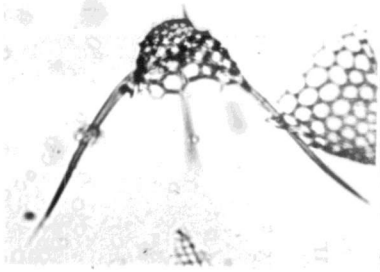

2

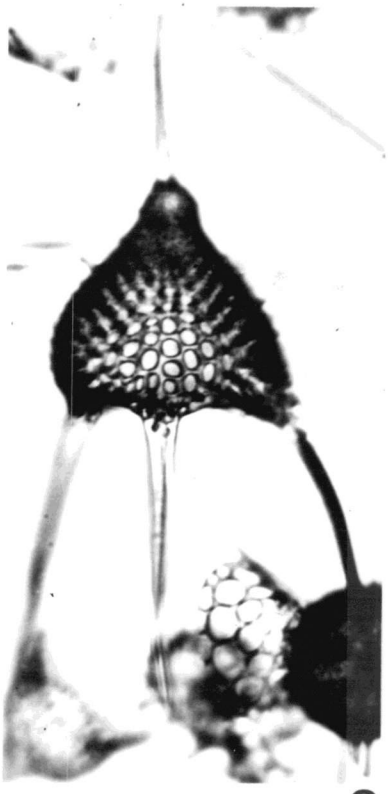

3

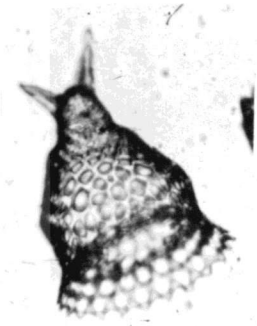

4a

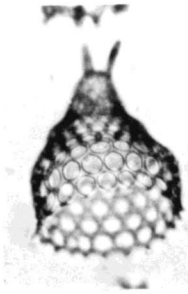

4b

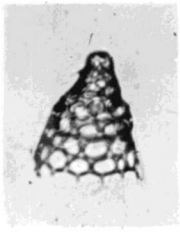

5a

5b

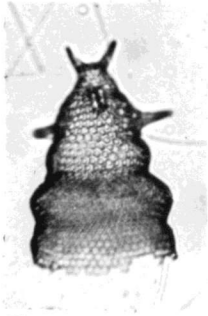

8

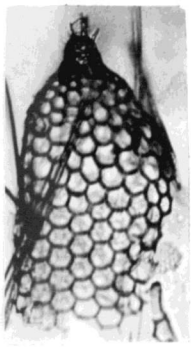

6

7

9

10a

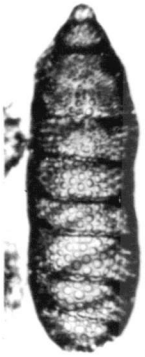

10b

APPENDIX VII

Numerical listing of species used in this study. The numbering system on the % of population data output, corresponds to this listing.

S 1 Actinomma antarcticum (Haeckel)
S 2 Actinomma arcadophorum Haeckel
S 3 Actinomma medianum Nigrini
S 4 Actinomma sp.
S 5 Amphirhopalum ypsilon Haeckel
S 6 Buccinosphaera invaginata Haeckel
S 7 Cenosphaera cristata Haeckel ?
S 8 Collosphaera tuberosa Haeckel
S 9 Cromyechinus antarctica (Dryer)
S10 Cubotholus sp.
S11 Cypassis irregularis Nigrini
S12 Disolenia quadrata (Ehrenberg)
S13 Disolenia zanguebarica (Ehrenberg)
S14 Echinomma leptodermum Jörgensen
S15 Echinomma delicatulum (Dogiel)
S16 Euchitonia group
S17 Heliodiscus asteriscus Haeckel
S18 Heliodiscus echiniscus Haeckel
S19 Heteracantha dentata Mast
S20 Hexacontium entacanthum Jörgensen
S21 Hymeniastrum euclides Haeckel
S22 Larcospira quadrangula Haeckel
S23 Lithelius minor Jörgensen
S24 Lithelius nautiloides Popofsky
S25 Lithelius (?) riedeli Petrushevskaya
S26 Hexapyle dodecantha Haeckel
S27 Amphitholus sp. cf acanthometra Haeckel
S28 Ommatartus tetrathalamus coronatus (Haeckel)
S29 Ommatartus tetrathalamus tetrathalamus Haeckel
S30 Otosphaera auriculata Haeckel
S31 Otosphaera polymorpha Haeckel
S32 Stylochlamydium venustum (Bailey)
S33 Phorticium pylonium (Haeckel)
S34 Polysolenia sp.
S35 Polysolenia flammabunda (Haeckel)
S36 Polysolenia lappacea (Haeckel)
S37 Polysolenia murrayana (Haeckel)

S38 Polysolenia spinosa (Haeckel)
S39 Pylonium sp.
S40 Rhizoplegma (?) boreale (Cleve)
S41 Saturnalis circularis Haeckel
S42 Siphonosphaera polysiphonia Haeckel
S43 Spirema sp.
S44 Spongaster tetras irregularis Nigrini
S45 Spongaster tetras tetras Ehrenberg
S46 Spongocore puella Haeckel
S47 Spongopyle osculosa Dreyer
S48 Stylotrochus sp. A
S49 Stylotrochus sp. B
S50 Spongotrochus glacialis Popofsky
S51 Spongurus pylomaticus Riedel
S52 Spongurus sp.
S53 Stylatractus sp.
S54 Stylodictya sp. A
S55 Stylodictya sp. B
S56 Styptosphaera (?) spumacea Haeckel
S57 Tetrapyle octacantha Müller
S58 Octopyle stenozoa Haeckel
S59 Hexacontium sp.
S60 Thecosphaera sp.
S61 Haliomma sp. (?)
S62 --- No species labeled this code.
S63 Larcopyle sp.
S64 Larcopyle bütschli Dreyer
S65 Druppatractus irregularis Popofsky
S66 Cladococcus stalactites Haeckel
S67 Ommatodiscus pantanelli Carnevale
S68 --- No species labeled this code.
N69 Liriospyris cf. reticulata (Ehrenberg)
N70 Artostrobus annulatus (Bailey)
N71 Antarctissa denticulata (Ehrenberg)
N72 Anthocyrtidium ophirense (Ehrenberg)
N73 Anthocyrtidium zanguebaricum (Ehrenberg)
N74 Saccospyris antarctica Haeckel
N75 Botryocyrtis scutum Harting
N76 Carpocanium sp. A
N77 Centrobotrys thermophila Petrushevskaya
N78 Dorcadospyris sp.
N79 Plectacantha cremastoplegma Nigrini
N80 Conarachnium (?) sp. A
N81 Conarachnium (?) sp. B
N82 Cornutella profunda Ehrenberg

N 83	Cyrtopera languncula Haeckel
N 84	Dictyocryphalus papillosus (Ehrenberg)
N 85	Dictyophimus crisiae Ehrenberg
N 86	Dictyophimus infabricatus Nigrini
N 87	Dictyophimus mawsoni Riedel
N 88	Eucyrtidium acuminatum (Ehrenberg)
N 89	Eucyrtidium anomalum Haeckel
N 90	Eucyrtidium hexagonatum Haeckel
N 91	Siphocampe aquilonaris (Bailey)
N 92	Helotholus histricosa Jörgensen
N 93	Lamprocyclas cf. L. haysi Kling
N 94	Lamprocyclas maritales maritales Haeckel
N 95	Lamprocyclas maritales polypora Nigrini
N 96	Lamprocyclas maritales ventricosa Nigrini
N 97	Lithostrobus (?) seriatus Haeckel
N 98	Lithomitra arachnea (Ehrenberg)
N 99	Lithocampe sp.
N100	Lithopera bacca Ehrenberg
N101	Lithostrobus sp. cf. L. hexagonalis Haeckel
N102	Lithomelissa spp.
N103	Peripyramis circumtexta Haeckel
N104	Pterocanium grandiporus Nigrini
N105	Pterocanium hirundo Haeckel
N106	Dicyophimus gracilipes Bailey
N107	Pterocanium praetextum eucolpum Haeckel
N108	Pterocanium praetextum praetextum (Ehrenberg)
N109	Pterocanium trilobum (Haeckel)
N110	Saccospyris conithorax Petrushevskaya
N111	Siphocampe corbula (Harting)
N112	Spirocyrtis scalaris Haeckel
N113	Stichopilium bicorne Haeckel
N114	Theocalyptra bicornis (Popofsky)
N115	Theocalyptra davisiana (Ehrenberg)
N116	Theoconus hertwigii (Haeckel)
N117	Theoconus minythorax Nigrini
N118	Theoconus trachelium dianae (Haeckel)
N119	Theocorythium trachelium trachelium (Ehrenberg)
N120	Dendrospyris (?) damaecornis (Haeckel)
N121	Triceraspyris sp. cf. T. antarctica (Haeckel)
N122	Eucecrephalus sp.
N123	Giraffospyris angulata (Haeckel)
N124	Tholospyris scaphipes (Haeckel)
N125	Rhodospyris sp.

N126	Dendrospyris cf. D. anthocyrtoides (Bütschli)
N127	Pterocanium sp. A
N128	Lithomitra sp.
N129	Nephrospyris renilla (Haeckel)